Centro de Tecnologia e Urbanismo
Departamento de Engenharia Elétrica

Aislan Gabriel Hernandes

Rádio Cognitivo: Sensoriamento Espectral baseado em Consenso e Compromisso Tempo de Sensoriamento *versus* Vazão

Dissertação apresentada ao Programa de Pós-Graduação em Engenharia Elétrica da Universidade Estadual de Londrina para obtenção do Título de Mestre em Engenharia Elétrica.

Londrina, PR
2018

Aislan Gabriel Hernandes

Rádio Cognitivo: Sensoriamento Espectral baseado em Consenso e Compromisso Tempo de Sensoriamento *versus* Vazão

Dissertação apresentada ao Programa de Pós-Graduação em Engenharia Elétrica da Universidade Estadual de Londrina para obtenção do Título de Mestre em Engenharia Elétrica.

Área de concentração: Sistemas Eletrônicos
Especialidade: Sistemas de Telecomunicações

Orientador:
Prof. Dr. Taufik Abrão

Londrina, PR
2018

Ficha Catalográfica

Gabriel Hernandes, Aislan

Rádio Cognitivo: Sensoriamento Espectral baseado em Consenso e Compromisso Tempo de Sensoriamento *versus* Vazão. Londrina, PR, 2018. 105 p.

Dissertação (Mestrado) – Universidade Estadual de Londrina, PR. Departamento de Engenharia Elétrica .

1. Sistemas de Telecomunicações. 2. Rádio Cognitivo. 3. Sensoriamento Espectral. 4. Compromisso Tempo de Sensoriamento *versus* Vazão. I. Universidade Estadual de Londrina. Departamento de Engenharia Elétrica. Departamento de Engenharia Elétrica . II. Título.

Aislan Gabriel Hernandes

Rádio Cognitivo: Sensoriamento Espectral baseado em Consenso e Compromisso Tempo de Sensoriamento *versus* Vazão

Dissertação apresentada ao Programa de Pós-Graduação em Engenharia Elétrica da Universidade Estadual de Londrina para obtenção do Título de Mestre em Engenharia Elétrica.

Área de concentração: Sistemas Eletrônicos
Especialidade: Sistemas de Telecomunicações

Comissão Examinadora

Prof. Dr. Taufik Abrão
Depto. de Engenharia Elétrica - UEL
Universidade Estadual de Londrina
Orientador

Prof. Dr. Elieser Botelho Manhas Jr.
Depto. de Computação
Universidade Estadual de Londrina

Prof. Dr. Lucas Dias Hiera Sampaio
Depto. Acadêmico de Computação
Universidade Tecnológica Federal do Paraná
Campus Cornélio Procópio

5 de fevereiro de 2018

"O homem não é nada além daquilo que a educação faz dele."

Immanuel Kant

Agradecimentos

Agradeço primeiramente a Deus pelas oportunidades e desafios e a minha família pelo apoio durante todo esse tempo. Gostaria de agradecer também aos colegas e professores do Departamento de Engenharia Elétrica da Universidade Estadual de Londrina, principalmente ao meu orientador Prof. Dr. Taufik Abrão pela orientação e paciência e também aos meus colegas Ricardo Tadashi Kobayashi pela ajuda inicial em meus trabalhos, João Lucas Negrão, Lucas Claudino, Edno Gentilho Junior e Jaime Laelson Jacob.

Resumo

A primeira parte desta Dissertação consiste da análise de várias técnicas de sensoriamento espectral (SS, *spectrum sensing*), tais como, detector de energia (ED, *energy detector*), filtro casado (MF, *matched filter*), detector cicloestacionário, detector de autovalores e detector baseado na covariância, todos aplicáveis ao SS em banda única (SB, *single-band*). Resultados numéricos permitem uma comparação justa entre os detectores analisados considerando aplicações de sensoriamento espectral monobanda. Para SS em sistemas multibanda (MB, *multi-band*), há diversas técnicas que vêm sendo desenvolvidas nos últimos anos, tais como, sensoriamento de borda (*edge*) baseado em *wavelets* (WSS, *wavelet spectrum sensing*), *compressed sensing* (CS) e *direction of arrival* (DoA). Finalmente, para lidar com a agressividade do canal sem fio móvel, esquemas cooperativos podem ser utilizados em conjunto com rádio cognitivo (CR, *cognitive radio*). Os mais conhecidos protocolos para comunicação assistida por retransmissores (*relays*) são o protocolo AF (*amplify-and-forward*) e o protocolo DF (*decode-and-forward*) empregados no *relay* e também aqueles que empregam combinações de sinais, tais como, *soft combining*, que podem ser MRC (*maximal ratio combining*) e EGC (*equal gain combining*) empregados no receptor e *hard combining* baseados em regras de escolha, tais como, AND, OR e *majority*.

Na segunda parte deste trabalho é desenvolvida a solução de um problema de otimização que permite reduzir o tempo de sensoriamento (STO, *sensing time optimization*) e como resultado aumentar a vazão de um usuário secundário (SU, *secundary user*). O problema de otimização resultante é um problema côncavo e não linear (NLP, *nonlinear program*), que pode ser resolvido analiticamente e de forma direta. Resultados numéricos permitiram corroborar o tratamento de otimização analítico proposto.

Na terceira parte deste trabalho, uma técnica de sensoriamento espectral cooperativo (CSS, *cooperative spectrum sensing*), chamada regra de consenso com pesos melhorada (IWAC, *improved weighted average consensus*) foi proposta sob a forma de regras de consenso, que permite o desenvolvimento de soluções distribuídas em vez de soluções centralizadas (utilizando regra de combinação *hard* ou *soft*), sendo que a última abordagem requer uma central de fusão (FC, *fusion center*). A técnica de consenso IWAC permite que o CSS local troque informações entre os SUs vizinhos e também leva em consideração a própria condição de canal do SU, obtendo-se assim vantagens sobre o CSS centralizado, e performance parecida com os demais CSS decentralizados baseados em regras de consenso existentes na literatura, tais como, consenso médio (AC, *average consensus*), consenso médio com pesos (WAC, *weighted average consensus*) e o consenso médio com pesos acurado (WAC-AE, *weighted average consensus - accuracy exchange*), boa velocidade de convergência para o mesmo custo computacional entre as regras com peso, porém com perda marginal de desempenho em alguns cenários específicos.

Palavras-Chave: sensoriamento espectral, rede de rádio cognitivo, usuário primário, usuário secundário, tempo de sensoriamento, maximização da vazão,

sensoriamento espectral cooperativo distribuído, consenso.

Abstract

The first part of this work consists of analyzing of various spectrum sensing (SS) techniques, such as energy detector (ED), matched filter (MF), cyclostationary detector, eigenvalue detector and covariance detector, all applied to single band spectrum sensing (SB-SS) systems. Numerical results allow the comparison between SB detectors. For SS in multiband systems (MB-SS), there are several techniques that have been developed in recent years, such as edge sensing based on wavelets (WSS), compressed sensing (CS) and direction of arrival (DoA). Finally, to deal with the aggressiveness of the wireless channel, cooperative SS schemes can be used in combination with cognitive radio (CR). The well-established cooperative protocols are those that use one or more relays with one hop, namely AF protocol and DF protocol and also those that employ combinations of signals, such as soft combining (MRC and EGC) and hard combining (AND, OR and majority).
In the second part, it is presented the formulation and solution of a concave optimization problem that allows to reduce the sensing time (STO); as a result the proposed algorithm is able to increase the throughput of a secondary user (SU). Indeed, the formulated problem is a concave nonlinear optimization program (NLP). Numeric results allow one to check the solutions presented.
In the third part of this paper, a Cooperative Spectral Sensing (CSS) technique called improved weighted average consensus (IWAC) was developed in the form of consensus rules, which allows the development of distributed solutions rather than centralized solutions (using the hard or soft combining rule), the latter approach requires a central of decisions (FC, fusion center). The IWAC consensus technique allows the local CSS to exchange information between neighboring SUs and also takes into account the SU channel condition itself, thus gaining advantages over the centralized CSS and similar performance to consensus-based decentralized CSS in the literature, such as, average consensus (AC), weighted average consensus (WAC) and weighted average consensus - accuracy exchange (WAC-AE), such as good convergence velocity for same computational cost among the rules with weight, but with a marginal performance loss under specific scenarios.

Keywords: spectrum sensing, cognitive radio networks, primary user, secondary user, sensing time, throughput maximization, distributed cooperative spectrum sensing, consensus .

Sumário

Lista de Figuras

Lista de Tabelas

Lista de Abreviaturas

5G Quinta Geração de Telefonia Móvel (*Fifth Generation*)

AC Consenso Médio (*Average Consensus*)

AF Amplifica e Transmite (*Amplify-and-Foward*)

AWGN Ruído Aditivo Gaussiano Branco (*Adictive White Gaussian Noise*)

CF Comprime e Transmite (*Compressed-and-Forward*)

CLT Teorema do Limite Central (*Central Limit Theorem*)

CS Subamostragem (*Compressed Sensing*)

CSS Sensoriamento Espectral Cooperativo (*Cooperative Spectrum Sensing*)

CRNs Redes de Rádio Cognitivo (*Cognitive Radio Networks*)

DF Decodifica e Transmite (*Decode-and-Forward*)

DoA Direção de Chegada (*Direction of Arrival*)

ED Detector de Energia (*Energy Detector*)

EGC Combinação de Ganhos Iguais (*Equal Gain Combining*)

ESPRIT Estimativa de Parâmetros de Sinais através de Técnicas de Invariância Rotacional (*Estimation of Signal Parameters via Rotational Invariance Techniques*)

FC Central de Decisões (*Fusion Center*)

FCC Comissão Federal de Comunicações (*Federal Comission Communication*)

IWAC Consenso Médio com Pesos Melhorado (*Improved Weighted Average Consensus*)

MAC Camada de Multiplo Acesso (*Medium Access Control*)

MB Multibanda (*Multiband*)

MCS Simulação Monte Carlo (*Monte Carlo Simulation*)

MF Filtro Casado (*Matched Filter*)

MRC Combinação de Máxima Razão (*Maximal Ratio Combining*)

MUSIC Classificação de Múltiplos Sinais (*MUltiple SIgnal Classification*)

NLP Programação Não-Linear (*Nonlinear Programming*)

QoS Qualidade de Serviço (*Quality of Service*)

PU Usuário Primário (*Primary User*)

ROC Características Operacionais do Receptor (*Receiver Operating Characteristics*)

SB Banda Única (*Single Band*)

SE Eficiência Espectral (*Spectral Efficiency*)

SH Mudança de Espectro (*Spectrum Handoff*)

SNR Relação Sinal-Ruído (*Signal-to-Noise Ratio*)

SS Sensoriamento Espectral (*Spectrum Sensing*)

STO Otimização do Tempo de Sensoriamento *versus* Vazão (*Sensing-Throughput Optimization*)

SU Usuário Secundário (*Secondary User*)

WAC Consenso Médio com Pesos (*Weighted Average Consensus*)

WAC-AE Consenso Médio com Pesos Acurado (*Weighted Average Consensus - Accuracy Exchange*)

WSS Sensoriamento Espectral baseado em *Wavelet* (*Wavelet Spectrum Sensing*)

Nota: Os acrônimos que não estão presentes nesta seção podem ser consultados diretamente nos trabalhos publicados ou submetidos, a partir do Apêndice A.

Convenções e Lista de Símbolos

Na notação das fórmulas, as seguintes convenções foram utilizadas:

- letras maiúsculas em negrito expressam matrizes, exemplo: $\mathbf{R_x}$ e $\mathbf{R_y}$;
- letras minúsculas em negrito representam vetores, exemplo: $\mathbf{x}$ e $\mathbf{y}$;
- letras em itálico indicam escalares, exemplo: λ e τ;
- $(\cdot)^H$ é o operador conjugado transposto (hermitiano);
- $\mathcal{N}(m, \sigma^2)$ é um processo aleatório gaussiano (ou normal) de média m e variância σ^2;
- $\mathbb{E}(\cdot)$ é o operador esperança estatística;
- $Q(\cdot)$ é a função cauda da gaussiana (função Q);
- $\Gamma(\cdot)$ é a função gama de Euler;
- $\max(\cdot)$ é o operador máximo do argumento;
- $\mathrm{P_r}(\cdot)$ é a probabilidade do argumento;

Principais símbolos utilizados ao longo deste trabalho:

símbolo	descrição
α	frequência cíclica e passo de iteração
B	largura de banda
C	capacidade
f	frequência
f_s	frequência de amostragem
γ	relação sinal-ruído (SNR)
R	vazão
λ	*threshold*
N	número de amostras

continua...

símbolo	descrição
σ_n^2	potência de ruído
P	potência de sinal
$\mathrm{P_d}$	probabilidade de detecção
$\mathrm{P_f}$	probabilidade de falso alarme
$\rho_{\max}$	máximo autovalor
$\rho_{\min}$	mínimo autovalor
S	sinal
$T(\cdot)$	teste estatístico
τ	tempo de sensoriamento
T	tempo total para sensoriamento espectral e transmissão de um SU

- Palavras em *itálico* são usadas para designar expressões em língua inglesa que não foram traduzidas.
- Os símbolos e notações que não estão presentes nesta seção podem ser consultados diretamente nos trabalhos publicados ou submetidos, a partir do Apêndice A.

1 Introdução

Devido ao crescimento dos serviços de comunicações sem fio, tais como, redes sociais, armazenamento em nuvem, *streaming* de áudio, *e-books*, serviços de *streaming* de vídeo (que utilizam 70% do tráfego de rede sem fio) dentre outros o espectro de frequências de interesse disponíveis vem se tornando cada vez mais escasso. As medições efetuadas pela *Federal Communications Commission* (FCC) (FCC Spectrum Policy Task Force, 2002), têm demonstrado que a maior parte do espectro licenciado não é utilizado de forma eficiente. O período de tempo de ocupação do espectro por um usuário licenciado varia de milissegundos até horas. Isto motiva a utilização do rádio cognitivo (CR, *cognitive radio*)(MITOLA; MAGUIRE G.Q., 1999), o qual é capaz de aumentar a eficiência espectral (SE, *spectrum efficiency*) dos sistemas de comunicações consideravelmente. Em uma rede do tipo IEEE 802.22 WRANs (*Wireless Regional Area Networks*), o objetivo principal em se utilizar o CR é maximizar a utilização do espectro dos canais de TV, que não são utilizados de forma contínua pelos usuários, tendo momentos em que a faixa de espectro permanece sem uso.

Pode-se dizer que o CR permite aos usuários primários (PUs, *primary users*), que detêm o direito de uso do espectro e aos usuários secundários (SUs, *secondary users*), que irão utilizar o espectro de forma oportunista, compartilhar a mesma banda de frequências, se e somente se, as políticas de acesso forem cumpridas por ambos os usuários. Neste esquema, o SU acessa o espectro do usuário licenciado (PU), sem causar danos à operação do PU; isto é chamado de esquema de acesso *underlay*. Em alternativa ao esquema de acesso *underlay*, o SU pode ocupar o espectro autorizado quando o PU é ausente; Neste contexto, o SU é visto como um usuário oportunista e chamado de esquema de acesso *overlay* (WYGLINSKI MAZIAR NEKOVEE, 2009), (ZHANG; ZHENG; CHEN, 2010) e (IBNKAHLA, 2014).

Formalmente, o CR é qualquer dispositivo de comunicação que possui características que remetem ao aprendizado e à inteligência (HAYKIN, 2005), e a partir disto consiga tomar decisões, tais como, transmitir, decodificar, etc. As principais tarefas realizadas por um CR são: sensoriamento espectral (SS, *spec-*

trum sensing) e o compartilhamento do espectro sem causar interferência ao PU (*spectrum sharing*)(IBNKAHLA, 2014), (HOSSAIN DUSIT NIYATO, 2009).

Outra tarefa importante que deve ser realizada pelo CR é a mudança de espectro devido à mobilidade ou padrão de atividade do usuário primário (SH, *spectrum handoff*) (IBNKAHLA, 2014). Sempre que um PU retorna para a sua banda licenciada, o SU que está utilizando a banda do PU tem de mudar sua banda atual para outra parte do espectro eletromagnético que esteja livre, a fim de evitar interferência ao PU. Este procedimento deve ser realizado com cuidado, a fim de evitar danos à comunicação do SU, o que afeta consideravelmente a qualidade de serviço (QoS, *quality of service*). Há duas opções para o SH: modo reativo e modo proativo. No modo reativo, o SU realiza o SS de outros canais disponíveis assim que o PU retorna a sua banda de uso. Neste tipo de SH, o SU consome algum tempo sensoriando o espectro novamente. Por outro lado, no modo proativo o SU possui de forma prévia uma lista de canais candidatos ao acesso uma vez que aconteça o retorno do PU, isto é, o SU constrói registros de dados sobre o comportamento de PUs, a fim de prever quais os canais vão estar disponíveis para acesso futuro.

1.1 Motivação

A próxima geração de sistemas de comunicação sem fio (5G) que está prevista para entrar em funcionamento a partir de 2020, exige grande eficiência espectral uma vez que há pouco espectro disponível e uma alta taxa de dados será exigida por estes sistemas. Neste sentido, o rádio cognitivo apresenta-se como uma alternativa viável para atender a estas demandas, uma vez que é capaz de otimizar o uso do espectro, aumentando a eficiência espectral. Porém, um procedimento inerente ao rádio cognitivo e que apresenta grandes desafios é o sensoriamento espectral pois necessita de diversos estudos para viabilizar futuras aplicações.
Desta forma, o estudo de novas técnicas de sensoriamento espectral é de fundamental importância e apresenta oportunidades e desafios de pesquisas na atualidade.

1.2 Temas em Sensoriamento Espectral Desenvolvidos

Neste trabalho de Dissertação de Mestrado três aspectos da temática sensoriamento espectral em rádio cognitivo são abordados:

- ◇ Ampla análise dos fundamentos e desenvolvimentos relativos ao Sensoriamento Espectral em Redes de Rádio Cognitivo;
- ◇ Compromisso Tempo de Sensoriamento *versus* Vazão em Redes de Rádio Cognitivo;
- ◇ Sensoriamento Espectral Cooperativo Distribuído em Redes de Rádio Cognitivo.

Assim, neste trabalho, diversas técnicas de SS foram analisadas, tanto em sistemas de comunicação de única banda (SB, *single-band*) quanto em sistemas multibanda (MB, *multi-band*), bem como tem sido abordado até aqui de forma introdutória o sensoriamento espectral CR no contexto cooperativo. Também foi estudada a relação entre o tempo de sensoriamento e a vazão de um SU; e como pode ser otimizado o compromisso tempo de sensoriamento *versus* vazão. Finalmente, na terceira parte deste trabalho foi proposta e caracterizada uma nova técnica para o sensoriamento espectral cooperativo na forma distribuída utilizando-se de técnicas de consenso.

Nos próximos capítulos serão abordados de forma mais detalhada os princípios básicos do problema do SS, o compromisso tempo de sensoriamento *versus* vazão e finalmente o sensoriamento espectral cooperativo distribuído. O texto de dissertação está divido em:

- **Capítulo 2**: Trata de forma geral os princípios básicos das principais técnicas de SS em redes de rádio cognitivo em diversos tipos de sistemas: única banda, múltiplas bandas e SS cooperativo;

- **Capítulo 3**: Discussão do problema de tempo de sensoriamento *versus* vazão em uma rede de rádio cognitivo a partir da solução de uma problema de otimização convexa. Este problema é de fundamental importância em Rádio Cognitivo pois impacta profundamente na capacidade de transmissão do SU bem como na confiabilidade do sensoriamento espectral;

- **Capítulo 4**: Extensiva análise e comparação de técnicas de SS cooperativo distribuído baseado em técnicas de consenso médio. Métodos distribuídos possuem vantagens em relação aos métodos centralizados, porque aproveitam melhor os recursos disponíveis da rede com mesma performance dos

métodos centralizados;

2 Sensoriamento Espectral em Redes de Rádio Cognitivo

O SS é a tarefa na qual o CR avalia uma porção do espectro, e estima se está ocupado ou não por um PU (YUCEK; ARSLAN, 2009) e (IBNKAHLA, 2014).

No SS, o CR deve detectar com confiabilidade a presença do PU sem causar qualquer interferência durante a execução do sensoriamento do espectro. Há muitas maneiras de detectar a presença ou ausência de um PU em uma faixa específica do espectro; a mais usual é começando por uma hipótese da presença ou ausência do PU, a construção de um teste estatístico $T(\cdot)$ e com base na comparação do sinal recebido pelo CR com um *threshold* específico λ toma-se a decisão, isto é, presença ou ausência do PU (IBNKAHLA, 2014). De forma simplificada, a figura (2.1) mostra como funciona a etapa do SS em um sistema de CR.

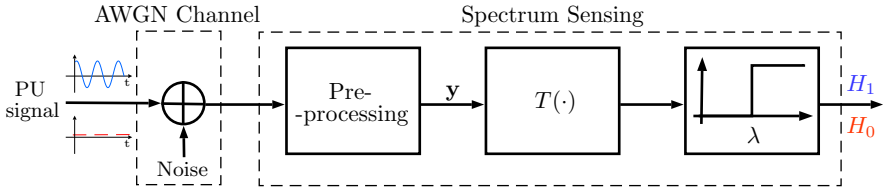

Figura 2.1: Esquema geral do SS em redes de rádio cognitivo (CRNs, *Cognitive Radio Networks*).
Fonte: Próprio autor.

2.1 Sensoriamento Espectral em Sistemas Mono-banda

A maneira mais simples e de menor complexidade computacional de realizar o SS é o detector de energia (ED, *energy detector*), que nada mais faz do que avaliar a energia contida em uma faixa espectral (YUCEK; ARSLAN, 2009), (BHARGAVI; MURTHY, 2010) e (IBNKAHLA, 2014). Caso esta energia for maior do que o *threshold* escolhido a decisão é tomada a favor da presença do PU, caso contrário

a decisão é pela ausência do PU. A principal desvantagem do ED é a sua elevada sensibilidade (baixa robustez) às incertezas do ruído aditivo gaussiano branco (AWGN, *Additive White Gaussian Noise*).

Existem muitos outros tipos de detectores descritos na literatura, por exemplo, filtro casado (MF, *matched filter*)(YUCEK; ARSLAN, 2009), (BHARGAVI; MURTHY, 2010) e (IBNKAHLA, 2014); detector cicloestacionário (SUTTON; NOLAN; DOYLE, 2008), (BHARGAVI; MURTHY, 2010) e (IBNKAHLA, 2014); detector de covariância (ZENG; LIANG, 2009b) e (IBNKAHLA, 2014) e o detector baseado em autovalores (ZENG; LIANG, 2009a) e (IBNKAHLA, 2014). Cada um deles, possuem características próprias conforme mostra a Tabela 2.1.

Tabela 2.1: Comparação entre os detectores aplicados ao SS em CRNs para sistemas SB.
Fonte: Adaptado de (IBNKAHLA, 2014).

Detector	Pot. Ruído	Requer Sinal PU	Diferencia Ruído	Sinal PU de: Sinais	Características
ED	✓				Simples
MF		✓	✓	✓	Ótimo em AWGN
CS		✓	✓	✓	Alta Complexidade
Covariância			✓	✓	Estimativas matriz de cov.
Autocorrel.			✓	✓	Similar ao Cov.

2.2 Sensoriamento Espectral em Sistemas Multibanda

Pode-se expandir o conceito de SS em SB para sistemas MB (HATTAB; IBNKAHLA, 2014). Sistemas MB têm recebido muita atenção, uma vez que os sistemas MB podem melhorar significativamente a QoS do SU. Usando sistemas MB, o SU não só tem um conjunto de canais candidatos para poder ocupar, mas também pode reduzir o SH e a interferência de dados devido ao retorno do PU (IBNKAHLA, 2014).

O SS em sistemas MB pode ser realizado através de técnicas de SS em série ou por meio de técnicas de SS em paralelo (IBNKAHLA, 2014). No SS em série, um detector SB utilizando um filtro passa-faixa reconfigurável (FBP) ou um

oscilador sintonizável varre todas as frequências do espectro. No SS em paralelo, uma estrutura na forma de banco de filtro e um detector a trabalhar em paralelo permite detectar todo o espectro mais rapidamente do que o SS em série.

Neste trabalho de Dissertação, é dado foco nas seguintes técnicas de SS em MB: detecção de borda (*edge*) utilizando *wavelets* (WSS, *wavelet spectrum sensing*) (TIAN; GIANNAKIS, 2006) e (IBNKAHLA, 2014), *compressed sensing* (CS) (TIAN; GIANNAKIS, 2007) e (IBNKAHLA, 2014), *direction of arrival* (DoA) (DHOPE; SIMUNIC, 2012), principalmente os estimadores *MUltiple SIgnal Classification* (MUSIC) (SCHMIDT, 1986) e *Estimation of Signal Parameters via Rotational Invariance Technique* (ESPRIT) (ROY; PAULRAJ; KAILATH, 1986) foram as que demonstraram mais importância nos últimos anos. De forma sucinta, a Tabela 2.2 resume as principais propriedades dos detectores MB.

Tabela 2.2: Comparação entre os principais detectores para sistemas MB. Fonte: Próprio Autor.

Detector	Vantagens	Desvantagens
WSS	Limites entre bandas desconhecidos	Falsas bordas (*edges*)
CS	Redução da taxa de amostragem	Conhecimento das matrizes de medidas e base esparsa
DoA	Nova dimensão a ser explorada	Uso específico em sistemas MIMO

2.3 Sensoriamento Espectral Cooperativo

Sistemas híbridos que podem ser utilizados em conjunto com CRNs são os *relays* de cooperação (DOHLER; LI, 2010) e os SUs cooperativos (IBNKAHLA, 2014), chamados de técnicas de sensoriamento espectral cooperativo (CSS,*cooperative spectrum sensing*) que proporcionam diversidade espacial ao sistema de comunicação quando inserido em canal com desvanecimento (*fading*) e sombreamento (*shadowing*) (IBNKAHLA, 2014).

Há basicamente três protocolos de comunicação cooperativos por *relays*, que são os protocolos AF (*amplify-and-forward*), DF (*decode-and-forward*) e CF (*compress-and-forward*). Há também esquemas de combinação *soft* e combinação *hard* quando emprega-se a cooperação por SUs. O protocolo AF é o esquema mais

simples e recebe uma versão do sinal do nó de origem (*source*) em um primeiro *slot* de tempo, ao passo que num segundo *slot* de tempo uma versão amplificada é enviada pelo *relay* para o nó de destino (*sink*). Em contraste, o protocolo DF decodifica o sinal recebido pelo *relay* a partir do *source* e, em seguida, reecodifica e reetransmite para o *sink*. A vantagem do protocolo AF é a sua simplicidade, mas tem a desvantagem de amplificar o ruído de entrada com o sinal do *source*. O protocolo DF tem a vantagem de decodificação; por conseguinte, o ruído não é amplificado. A desvantagem do protocolo DF é se o sinal recebido pelo *source* contém erros, o sinal não poderá ser decodificado corretamente e a comunicação pelo *relay* ficará comprometida. Se isso acontecer, a comunicação cooperativa deve ser imediatamente interrompida (DOHLER; LI, 2010).

No esquema em que se utilizam SUs cooperativos, o combinador *hard* é simplesmente a soma de decisão de todos SUs na rede; os SUs enviam suas decisões finais para uma central de decisões. Já para o combinador *soft*, os SUs compartilham suas informações com a central de decisões que faz a decisão pela ponderação, por um fator (pesos) que leva em consideração a importância da decisão de cada SU (IBNKAHLA, 2014). A tabela (2.3) sintetiza as principais características de cada esquema CSS.

Tabela 2.3: Comparação entre as técnicas de CSS.
Fonte: Próprio Autor.

Esquema CSS	**Vantagens**	**Desvantagens**
Hard	Combinação simples de cada usuário	Sujeito a erros de propagação
Soft	Pesos determinam a melhor performance	Maior complexidade
AF	Sinal melhora com ganho e menos complexo que outros protocolos	Propaga ruído com ganho
DF	Reduz propagação de ruído	Se a decodificação falha, a reentrasmissão falha (baixa SNR)

Finalmente, no contexto de CRNs, vale a pena notar que, por um lado, os PUs colocam exigências rigorosas sobre o uso do canal e limites de interferência pelo SUs; enquanto que, por outro lado, os SUs esperam elevados QoS a um baixo custo; o que caracteriza um problema do alta complexidade, abrindo espaço para muitos temas de pesquisas.

2.4 Resultados Numéricos

Nesta seção são apresentadas as principais contribuições e resultados desenvolvidos no trabalho do Apêndice A.1 em relação à primeira parte do trabalho de dissertação relacionado ao tema de SS em CRNs.

2.4.1 Contribuições

As principais contribuições do primeiro trabalho que é o capítulo de livro intitulado *Spectrum Sensing in Cognitive Radio Networks: Achievements and Challenges* escrito por Aislan Gabriel Hernandes, Ricardo Tadashi Kobayashi e Taufik Abrão e anexado no Apêndice A.1 são:

1. Análise sistemática das principais técnicas de SS-SB em termos do desempenho via ROC;
2. Comparação das principais técnicas SS-SB;
3. Comparação das principais técnicas SS-MB;
4. Comparação dos principais esquemas cooperativos.

Resultados numéricos relacionados com SS para sistemas SB em CRNs incluem as seguintes figuras de mérito:

a) características operacionais do receptor (ROC, *receiver operating characteristics*), sintetizada pela curva que relaciona a probabilidade de detecção (*detection probability*) com a probabilidade de falso alarme (*false alarm probability*);

b) probabilidade de detecção em função da SNR;

c) probabilidade de detecção em função do número de amostras do sinal recebido.

Todas estas figuras de mérito foram analisadas para os seguintes detectores SS monobanda: ED, MF, cicloestacionário, autovalores e de covariância. O desempenho do ED sob valores de SNR $\in [-30; -15]$[dB] é mostrado na Figura 2.2. Pode-se observar que para 1000 amostras, a curva da ROC em (a), está longe do valor ideal, isto é, probabilidade de detecção de 0.9 para probabilidade de falso alarme de 0.1 para SNR $= -15$[dB]. Conclui-se que o ED deve operar em altos valores de SNR, para evitar interferências aos PUs. Na Figura 2.2.(b), pode-se observar que altos valores de probabilidade de detecção são obtidos para valores de SNR superiores a -10[dB]; como consequência, mais amostras são necessárias para que o detector opere em baixos valores de SNR. Finalmente, na Figura 2.2.(c) tomando o valor de 0.1 para a probabilidade de falso alarme, o ED requer por volta de 10^4 amostras para atingir altos valores de probabilidade de detecção, quando operando em valores de SNR acima de -15[dB].

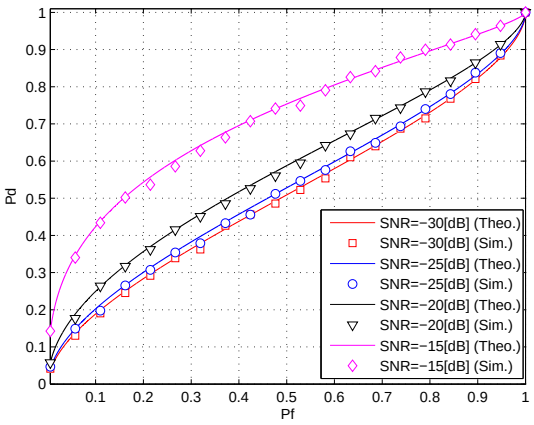

(a) ROC @ $N = 1000$

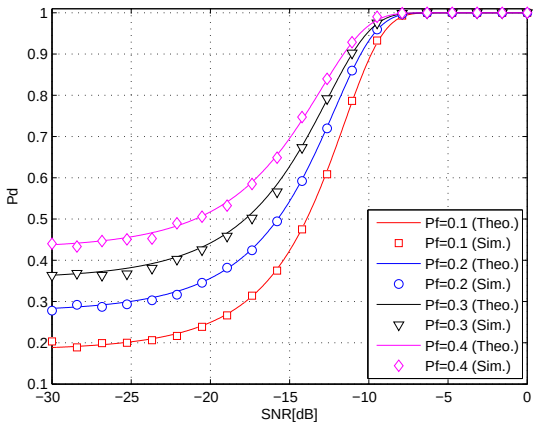

(b) $\mathrm{P_d} \times \mathrm{SNR}$, @ $N = 1000$

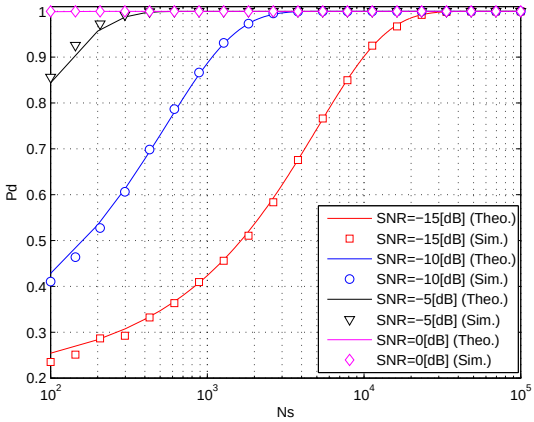

(c) $\mathrm{P_d} \times \mathrm{N}$, @ $\mathrm{P_f} = 0.1$

Figura 2.2: Performance do ED.

Figura 2.3 mostra o desempenho do MF. Na Fig. 2.3.(a) pode-se observar que a ROC converge rapidamente para a região de operação de interesse, por

exemplo, quando a SNR $= -20$[dB] a probabilidade de detecção é superior a 90%, enquanto que a probabilidade de falso alarme é somente 5%. Em (b), pode-se observar que a probabilidade de detecção converge para 1 para uma SNR de aproximadamente -20[dB], considerando apenas 1000 amostras. Finalmente, na Fig. 2.3.(c) é evidenciado que, por exemplo, 1000 amostras são suficientes para uma bom desempenho em termos de SS.

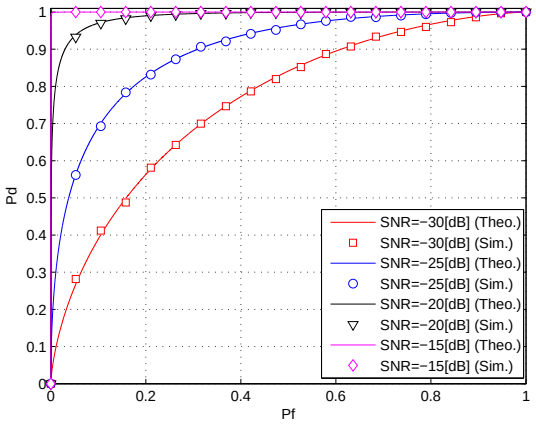

(a) ROC @ $N_s = 1000$

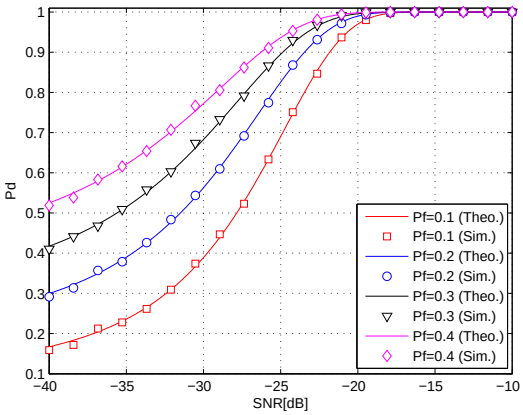

(b) $\mathrm{P_d} \times \mathrm{SNR}$, @ $N_s = 1000$

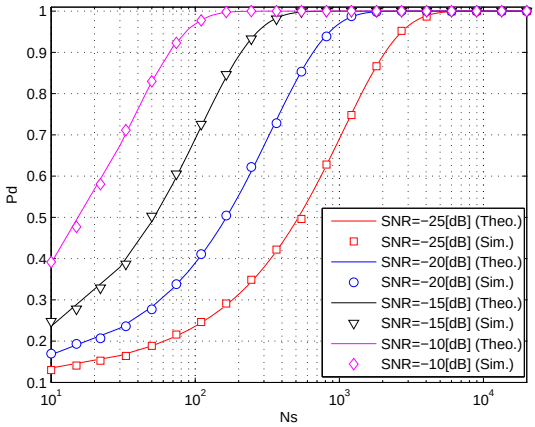

(c) $\mathrm{P_d} \times \mathrm{N_s}$, @ $\mathrm{P_f} = 0.1$

Figura 2.3: Performance do MF.

A Figura 2.4 mostra o desempenho do detector cicloestacionário, obtido apenas via simulação, para $N_s = 1000$ amostras. Em (a), a ROC considerando SNR de -15[dB] e probabilidade de falso alarme de 0.1 pode-se verificar pela curva que a probabilidade de detecção resulta $\simeq 0.53$. Em (b), com a probabilidade de falso alarme de 0.1 e SNR de -15[dB], a probabilidade de detecção fica em torno de $\simeq 0.5$; note-se que para SNR ≤ -15[dB], o desempenho do detector cicloestacionário decresce rapidamente, tornando-se inadequado por volta de $\simeq -20$ a $\simeq -25$ [dB]. Finalmente, examinando-se a Fig. 2.4.(c) pode-se concluir que o detector cicloestacionário deve operar com um número de amostras igual ou

superior a 10^5 amostras para uma SNR de -15[dB] tendo em vista garantir um desempenho próximo à região ideal de operação.

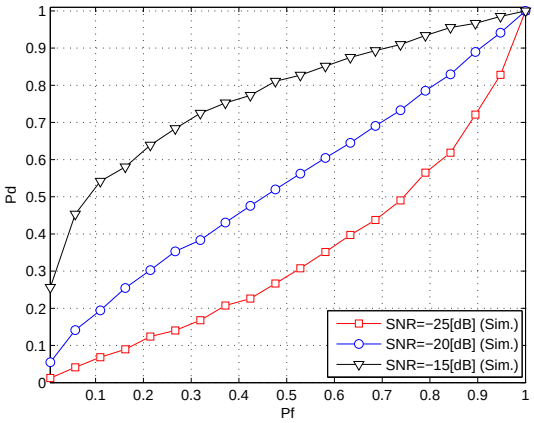

(a) ROC @ $N_s = 1000$

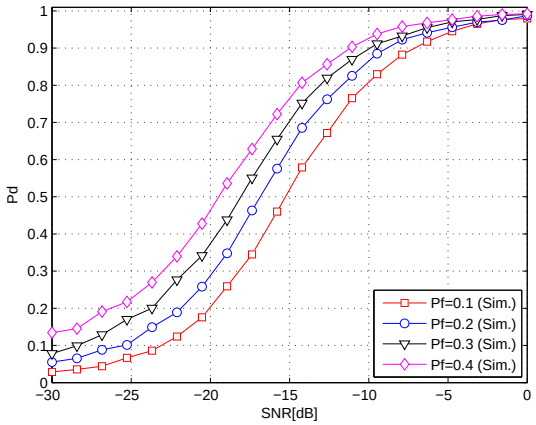

(b) $\mathrm{P_d} \times \mathrm{SNR}$, @ $N_s = 1000$

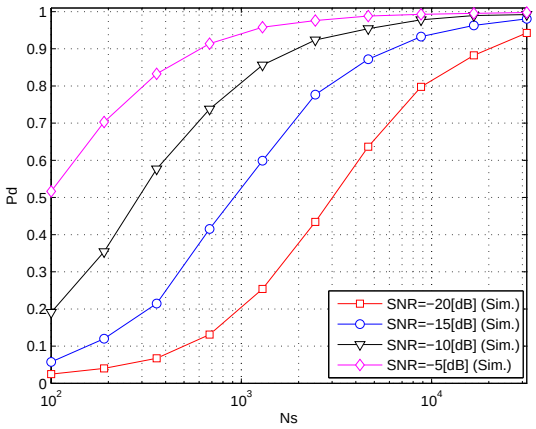

(c) $\mathrm{P_d} \times \mathrm{N_s}$, @ $\mathrm{P_f} = 0.1$

Figura 2.4: Desempenho do detector cicloestacionário.

Para o desempenho do detector de covariância, observa-se que os resultados apresentados na Figura 2.5.(a) e (b) indicam que as probabilidades de detecção P_d são inadequados para valores de SNR abaixo de -15[dB]. Entretanto, deve-se levar em consideração que o detector de covariância para operar não necessita de uma estimação da SNR. Ressalte-se, porém, que caso a estimativa para o segundo momento estatístico for imprecisa, o desempenho do detector será muito degradado. Em (c) pode-se observar que 2000 amostras são suficientes para o detector de covariância atingir alta probabilidade de detecção (≥ 0.9), dado 10% de probabilidade de falso alarme e SNR de -15[dB].

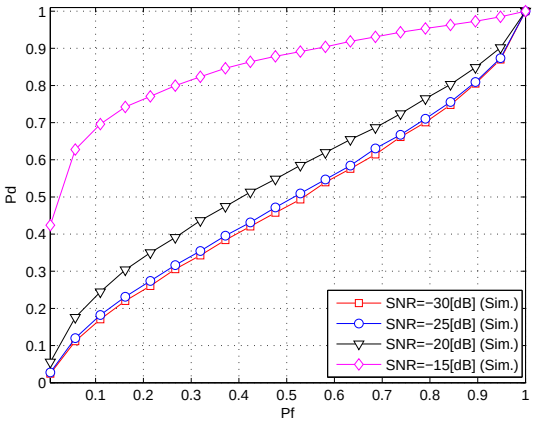

(a) ROC @ $N_s = 1000$

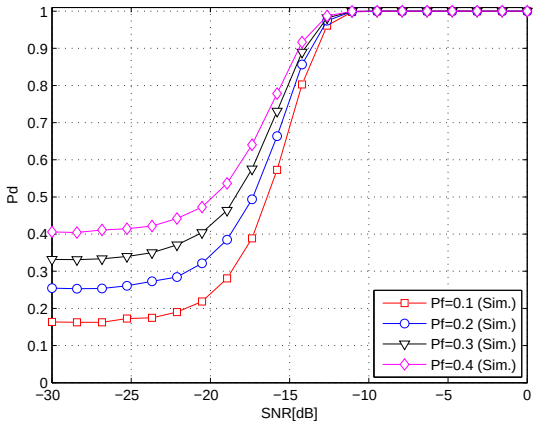

(b) $\mathrm{P_d} \times \mathrm{SNR}$, @ $N_s = 1000$

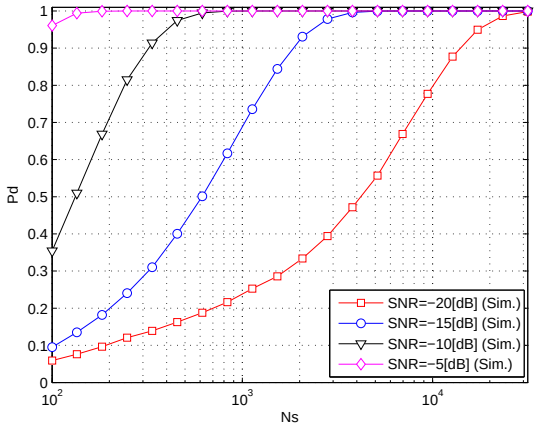

(c) $\mathrm{P_d} \times \mathrm{N_s}$, @ $\mathrm{P_f} = 0.1$

Figura 2.5: Performance do detector de covariância.

O desempenho do detector baseado em Autovalores é mostrado na Fig. 2.6. Pode-se observar em (a) e em (b) que a probabilidade de detecção converge rapidamente para região de interesse (i.e., $P_d \geq 0.9$) quando a SNR ≥ -15[dB]. Em (c), valores de $N_s \approx 1000$ amostras indicam desempenho adequado para o detector de covariância operando sob SNR> -15dB, dada a probabilidade de falso alarme abaixo de 10%.

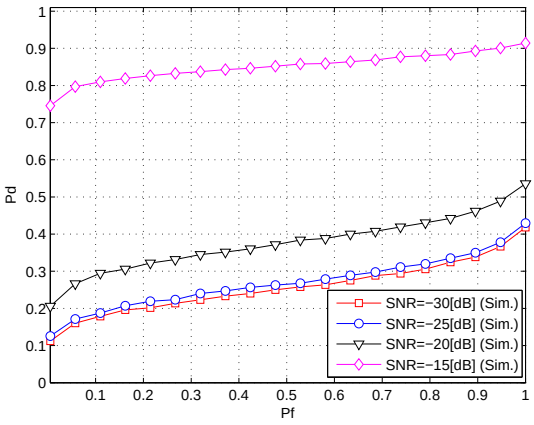

(a) ROC @ $N_s = 1000$

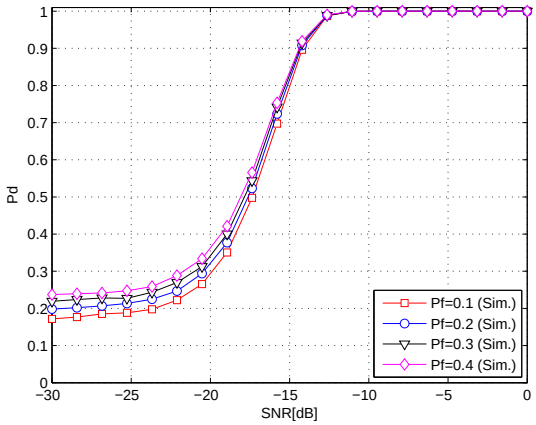

(b) $\mathrm{P_d} \times \mathrm{SNR}$, @ $N_s = 1000$

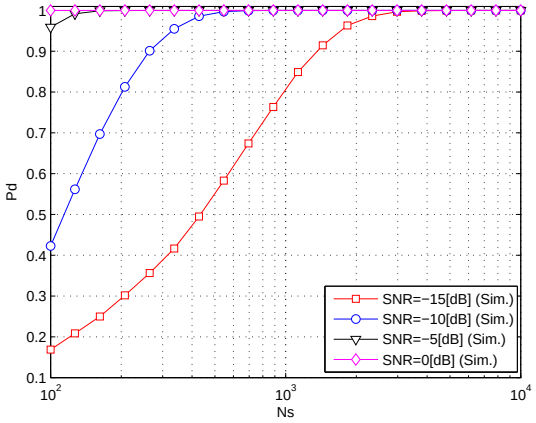

(c) $\mathrm{P_d} \times \mathrm{N_s}$, @ $\mathrm{P_f} = 0.1$

Figura 2.6: Performance do detector de autovalores.

Figura 2.7 mostra a comparação de todos detectores SS mono-banda tratados nesta Dissertação. Em (a), sintetizam-se as curvas de desempenho obtidas com número de amostras de 1000 e SNR fixa em -15[dB]. Pode-se observar que ED possui o pior desempenho dentre todos os detectores até valores de probabilidade de falso alarme de 0.6. Por outro lado, o detector de autovalores possui melhor performance do que o detector de covariância até uma probabilidade de falso alarme de 0.15, quando o detector de covariância supera o detector de autovalores. O detector de covariância possui melhor perfomance do que o ED para todos os valores de probabilidade de falso alarme. Como esperado, confirma-se o melhor desempenho do detector MF em cenários puramente AWGN.

Na Fig. 2.7.(b) tomam-se 1000 amostras e probabilidade de falso alarme fixa em 0.1. Para valores de SNR até -20[dB] todos os detectores SS, exceto o MF apresentam desempenhos em termos de P_d desprezíveis. No entanto, observe-se que o ED resulta marginalmente menos degradado, com $P_d \approx 0.23$, em relação aos detectores de covariância, de autovalores e cicloestacionario. Para faixa de

valores de probabilidade de detecção mais adequados ($P_d > 0.5$), pode-se observar de (c) que o ED apresenta o desempenho mais degradado, enquanto que o detector de autovalores e covariância apresentam desempenhos em termos de P_d similares e mais adequados para faixa de SNR> -15dB. Mais uma vez, o MF possui o melhor desempenho.

Na Fig. 2.7.(c) com probabilidade de falso alarme fixa de 0.1 e SNR de -15[dB], os detectores de energia, cicloestacionário, de autovalores e covariância apresentaram desempenhos bastante degradados para $N_s \leq 500$ amostras, sendo que na faixa $N_s \leq 300$ amostras, o ED resulta no desempenho menos degradado deste grupo de detectores. Adicionalmente, para valores na faixa de $N_s \in [700; 2000]$ amostras, o ED possui o pior desempenho entre todos. Os detectores de autovalores e covariância apresentam desempenhos semelhantes. Para valores acima de 3000 amostras, o detector de autovalores, covariância e o cicloestacionário resultam em desempenhos bastante adequados. Desempenho adequado é obtido com o detector MF a partir de $N_s \geq 200$ amostras.

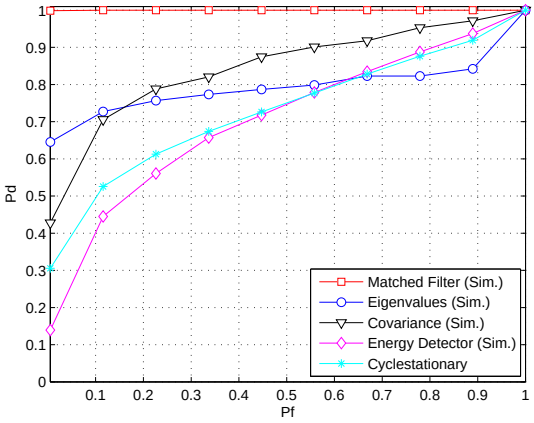

(a) ROC @ $N_s = 1000$, $SNR = -15$ dB

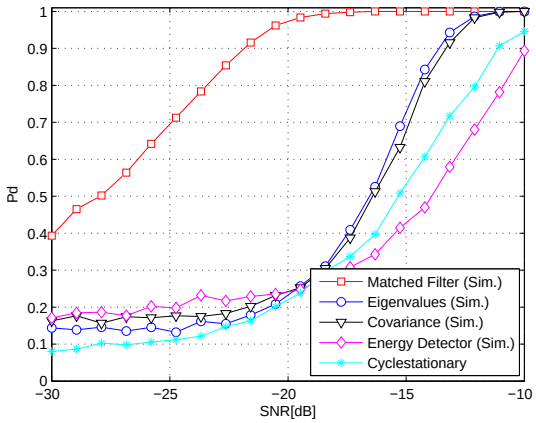

(b) $\mathrm{P_d} \times \mathrm{SNR}$, @ $N_s = 1000$, $\mathrm{P_f} = 0.1$

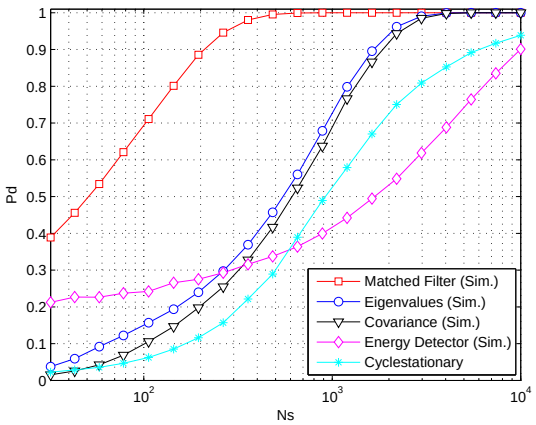

(c) $\mathrm{P_d} \times \mathrm{N_s}$, @ $\mathrm{P_f} = 0.1$, $SNR = -15$ dB

Figura 2.7: Comparação entre as técnicas de SS operando sob ruído AWGN.

Portanto, pode-se concluir que o detector de energia (ED) possui menor complexidade computacional se comparado aos outros detectores analisados neste trabalho. Entretanto, o ED apresenta baixo desempenho quando operando em baixa SNR, *i.e* quando o sinal recebido possui baixa potência em relação à potência do ruído sendo por isso um detector que apresenta baixa robustez. Esta característica pode ser observada nos resultados apresentados neste capítulo. Por outro lado, o MF possui desempenho ótimo entre todos os detectores analisados quando operando em canais AWGN, entretanto, o MF requer informações *a priori* do sinal do PU, que geralmente não estão disponíveis ao SU em aplicações práticas. O detector cicloestacionário resultou em desempenhos superiores em termos ROC ou ainda em termos de SNR e número de amostras, mostrando-se mais robusto que o ED para a maioria dos casos analisados neste trabalho; ademais, o detector cicloestacionário requer que o sinal do PU contenha a propriedade cicloestacionária, isto é, mantenha suas propriedades estatísticas em períodos cíclicos o que permite diferenciar o sinal do PU do ruído AWGN. No entanto, o detector cicloestacionário apresenta maior complexidade computacional em comparação ao ED. Finalmente, os detectores de covariância e o de autovalores são baseados nas medidas de correlação do sinal do PU, oferencendo um SS robusto e pouco dependente de informações *a priori* do PU; no entanto para a obtenção de desempenhos adequados, estes detectores devem operar em SNR mais elevadas, como pode ser observado nos resultados numéricos apresentados neste capítulo.

3 Compromisso Tempo de Sensoriamento *versus* Vazão em Redes de Rádio Cognitivo

Recentemente, muita importância vem sendo dada ao problema do compromisso entre tempo de sensoriamento *versus* vazão (*sensing-throughput tradeoff*) no contexto de CRNs (LIANG et al., 2007), (LIANG et al., 2008) e (PEH; LIANG; GUAN, 2009). O esquema que permite lidar com este tipo de problema consiste em formular e resolver satisfatoriamente o problema de otimização associado à maximização da vazão sujeito a diferentes restrições, tais como probabilidade de detecção, probabilidade de falso alarme, tempo máximo de *frame*, *threshold* ótimo, etc. Neste sentido, faz-se necessário definir o tempo de *frame*, que está associado com a camada MAC (*Medium Acess Control*) do modelo OSI (*Open System Interconnection*). Basicamente, o tempo de *frame* pode ser representado pela Figura 3.1.

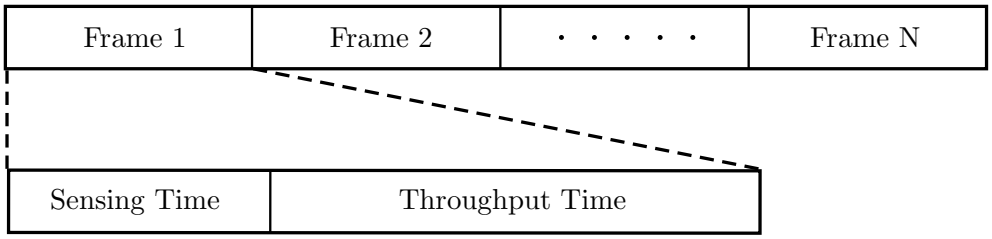

Figura 3.1: Estrutura básica de um tempo de *frame* associado à camada MAC. Neste modelo representa-se o tempo de sensoriamento (*sensing time*) e o tempo de vazão (*throughput time*).
Fonte: Próprio Autor.

A primeira porção do tempo de *frame* é usado para sensoriar o espectro, isto é, realizar o SS e a segunda porção é utilizada como tempo de transmissão (*spectrum sharing*), que impacta diretamente na vazão. Considerando que o tempo de *frame* é fixo, então o tempo de sensoriamento e a vazão são parâmetros que estão em permanente conflito.

Em (LIANG et al., 2008), um problema de otimização não-linear (NLP, *nonlinear problem*) foi formulado para lidar com a otimização do tempo de sensoriamento (STO, *sensing time optimization*) em uma CRN monobanda (SB). Basicamente, o problema de otimização que retrata o compromisso entre o tempo de sensoriamento e a vazão, pode ser descrito pela equação (3.1).

$$\begin{aligned} \max_{\tau} \quad & R(\tau) \\ \text{s.t.} \quad & \text{(C.1.)} \qquad 0 \leq \tau \leq T \\ & \text{(C.2.)} \qquad P_d(\tau) \geq \overline{P_d} \end{aligned} \tag{3.1}$$

sendo $\overline{P_d} = 0.9$ a probabilidade de detecção mínima de acordo com o padrão IEEE 802.22 WRAN; R é a expressão para a função objetivo, a qual descreve a vazão em uma CRN em função de τ, o tempo de sensoriamento; finalmente, T define o tempo de quadro (*frame*) de uma CRN (LIANG et al., 2008). As restrições de desigualdade (C.1.) e (C.2.) são também condições de igualdade para manter o conjunto de busca convexo.

O problema de otimização em (3.1) pode ser interpretado como tendo o objetivo de identificar o tempo de sensoriamento ótimo τ^* para cada tempo de *frame* T distinto. Tal otimização é realizada na camada MAC da rede, tal que a vazão do SU é maximizada, enquanto é assegurada a proteção ao PU, que está relacionado ao valor mínimo assumido por P_d.

Neste sentido, a contribuição deste trabalho de Dissertação consiste na extensão da análise numérica do trabalho feito em (LIANG et al., 2008). O problema STO pode ser resolvido de forma expedita usando o *Matlab Optimization Toolbox*. Foi usada a função *fmincon* que permite resolver problemas de otimização não-linear utilizando-se para isso um algoritmo interno do tipo pontos-interiores.

3.1 Resultados Numéricos

Neste seção são apresentadas as principais contribuições e resultados desenvolvidos no trabalho do Apêndice A.2 em relação à segunda parte do trabalho de dissertação relacionado com o tema de Compromisso entre o Tempo de Sensoriamento e Vazão.

3.1.1 Contribuições

As principais contribuições do segundo trabalho são:

1. Formulação de uma expressão analítica obtida a partir de outra já existente na literatura (LIANG et al., 2008), a qual descreve a probabilidade de detecção considerando-se a probabilidade de ocupação do canal pelo PU;

2. Análise numérica comparada relacionando a solução do problema de otimização com diversas probabilidades de ocupação do canal;

3. Avaliação da qualidade das soluções com ou sem a simplificação da função objetivo do problema de otimização proposto.

Usando a função *fmincon* do pacote *MATLAB Optimization Toolbox* do software MATLAB, o STO pode ser resolvido de modo expedito, resultando em um tempo de sensoriamento ótimo de $\tau^* = 2.6$ [ms] para os diferentes cenários de ocupação de canal analisado, isto é, para baixa (probabilidade de ocupação de 0.2), média (probabilidade de ocupação de 0.5) e alta ocupação do canal (probabilidade de ocupação de 0.8). Os valores estimados a partir da expressão simplificada para: a) vazão ótima $\widehat{R^*}$; b) a expressão original da vazão ótima; c) a diferença percentual entre as duas são mostrados na tabela 3.1.

Tabela 3.1: Vazão ótima estimada, original e diferença percentual considerando os casos de baixa, média e alta ocupação do canal por PU.

$\Pr(\mathcal{H}^1)$	0.2	0.5	0.8
$\widehat{R^*}\ \left[\frac{\text{bits}}{\text{s}\cdot\text{Hz}}\right]$	5.1659	3.228	1.2815
$R^*\ \left[\frac{\text{bits}}{\text{s}\cdot\text{Hz}}\right]$	5.2945	3.55	1.807
$\Delta R^*\ \%$	12.81	32.2	52.55

Obviamente, quando a probabilidade de ocupação do canal pelo usuário primário cresce há uma tendência de crescimento da discrepância entre a vazão ótima estimada e a vazão ótima original devido à simplificação da função objetivo do problema de otimização.

Obtido o tempo de sensoriamento espectral ótimo, pode-se então, determinar a quantidade de amostras necessárias para satisfazer o problema de otimização do tempo de sensoriamento espectral.

$$N_s^* = \tau^* f_s = 15600 \quad [\text{amostras}]. \tag{3.2}$$

O comportamento da vazão em função do tempo de sensoriamento, que é a função objetivo em (3.1), pode ser visto na Fig. 3.2. Para os resultados de simulação, $3 \cdot 10^4$ realizações Monte Carlo foram empregadas e comparadas com a curva teórica. A função vazão tem apenas um ponto de máximo, que é um ponto de ótimo global. Portanto, a função objetivo é côncava no domínio de interesse.

Além disso, examinando a Fig. 3.2, observa-se por inspeção que o valor máximo da vazão é obtido quando o tempo de sensoriamento é de ≈ 2.55 [ms] para os três casos de probabilidade de ocupação do canal, o qual também pode ser confirmado pelas soluções dos problemas de otimização associados na eq. (3.1).

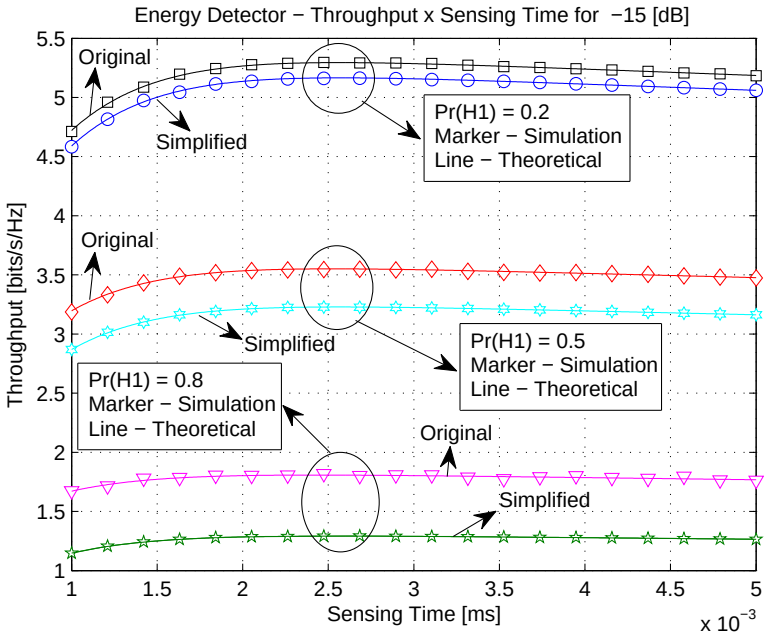

Figura 3.2: Vazão *versus* tempo de sensoriamento para $\text{SNR}_p = -15$[dB].

Para se obter a probabilidade de detecção *versus threshold* de um ED operando no tempo de sensoriamento ótimo, um número de $3 \cdot 10^4$ realizações Monte Carlo foi escolhido. A Fig. 3.3 mostra curvas de probabilidade de detecção *versus threshold* adotando-se $N_s^* = \tau^* f_s = 15600$ amostras. Pode-se concluir que o valor ótimo de limiar de decisão do ED é deslocado (incrementado) à medida que a probabilidade de ocupação do canal cresce, de baixa para média, alta e também quando o canal está completamente ocupado (probabilidade de ocupação igual a 1). Examinando a Fig. 3.3 pode-se concluir que a probabilidade de detecção miníma de $\overline{P_d} = 0.9$ é obtida para diferentes valores de *threshold* que podem ser diretamente obtidos da equação (3.3).

$$P_d(\tau) = Q\left((\lambda - \beta - 1)\sqrt{\frac{\tau f_s}{2\beta + 1}}\right), \tag{3.3}$$

onde $\beta = \text{P}_\text{r}(\mathcal{H}^1)\text{SNR}_p$. Os valores de SNR_p são ponderados por $\text{P}_\text{r}(\mathcal{H}^1)$, que é a probabilidade do canal estar ocupado.

Utilizando-se a equação (3.3) pode-se calcular os valores analíticos para o valor de limiar (*threshold*). O resultado é sintetizado na tabela 3.2, indicando ótima concordância entre valores teóricos e obtidos via simulação Monte-Carlo.

Tabela 3.2: Valores Numéricos e Analíticos para o *threshold* considerando-se $\overline{P_d} = 0.9$ e variando os valores de ocupação do canal pelo PU.

$\mathrm{P_r}(\mathcal{H}^1)$	0.2	0.5	0.8	1
Numérico	0.9955	1.0047	1.0147	1.020
Analítico	0.9960	1.0054	1.0148	1.0210

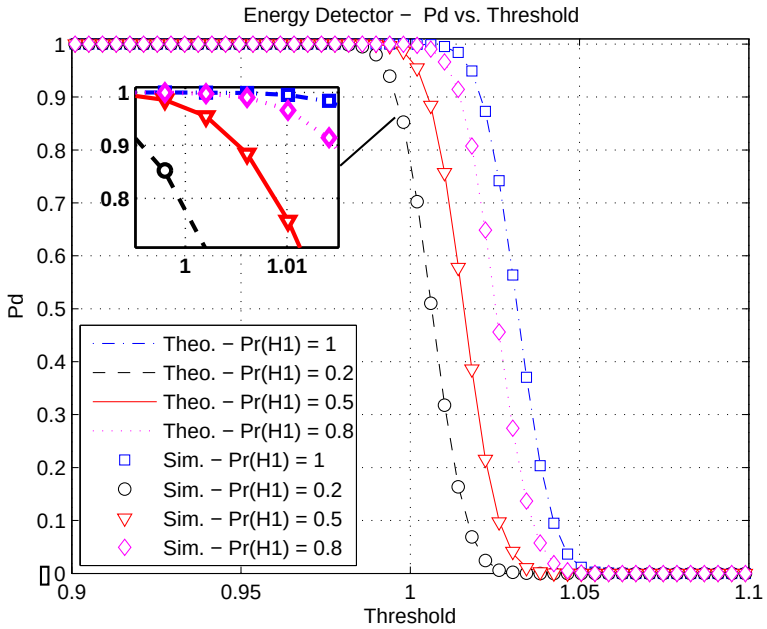

Figura 3.3: Probabilidade de detecção *versus* threshold para $N_s = 15600$ amostras. Ótima aderência dos valores teóricos com aqueles obtidos via simulação Monte Carlo.

Para se obter a probabilidade de detecção *versus* N_s, onde N_s é o número de amostras, o mesmo número de realizações Monte Carlo ($3 \cdot 10^4$) foi escolhido. Como consequência, Fig. 3.4 mostra a probabilidade de detecção *versus* N_s adotando valor de $\overline{P_d} = 0.9$ e valor para a SNR do PU como $\mathrm{SNR}_p = -15$ [dB]. Na Fig 3.4, comparou-se valores em que a probabilidade do canal ocupado seja baixa, média, alta e também quando o canal está completamente ocupado e para os quatro cenários a probabilidade de detecção está acima de 0.9 para $N_s = 15600$ amostras, como garantido pela solução do problema de otimização em (3.1).

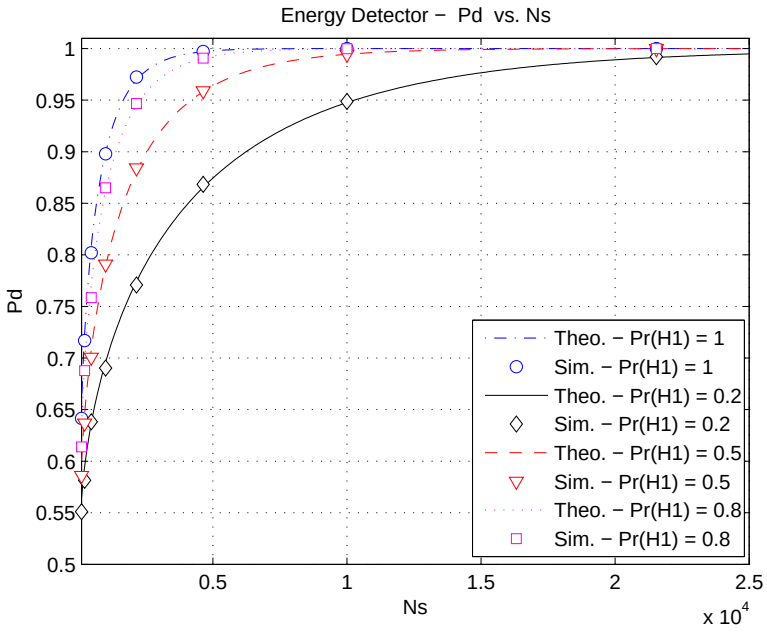

Figura 3.4: Probabilidade de detecção *versus* N_s.

Desta forma, pode-se concluir que o problema de otimização (STO) apresentado neste capítulo resultou convexo, possibilitando assim ser resolvido pelo MATLAB, garantindo a obtenção do ótimo global. Portanto, utilizando-se da função *fmincon* do *MATLAB Optimization Toolbox*, os resultados numéricos discutidos mostram que o ponto de máximo é um ótimo global e a função objetivo é uma função côncava garantindo a solução ótima do problema. Analisando-se os resultados obtidos conclui-se que a simplificação da função objetivo, *i.e* da vazão só é válida para valores de baixa ocupação do canal. Também é observado que os valores de probabilidade de detecção crescem com a probabilidade de ocupação do canal, como esperado, pois a definição de probalidade de detecção depende do sinal recebido do PU.

4 Sensoriamento Espectral Cooperativo Distribuído em Redes de Rádio Cognitivo

Um tema interessante e com bastante apelo atualmente consiste na análise e caracterização de técnicas de sensoriamento espectral cooperativas distribuídas e como isso impacta no CSS em comparação com as técnicas centralizadas, as quais requerem uma central de fusão das informações relativas ao SS.

De fato, as técnicas de sensoriamento espectral centralizadas necessitam de uma FC para realizar a decisão final, o que leva a um maior consumo de energia pelo uso da FC, reduzindo a eficiência energética da CRN, além da qualidade da transmissão do sinal do SU para a FC e depois da FC para o SU que pode ser deteriorada pela condição do canal, podendo impactar negativamente, portanto, tanto na eficiência espectral quanto na confiabilidade do sensoriamento espectral da CRN. Tendo em vista tais desvantagens, recentemente, têm sido propostas na literatura técnicas de sensoriamento espectral distribuído, as quais visam o menor consumo de energia e a melhoria na qualidade do sinal recebido.

Uma das técnicas que permite que o sensoriamento espectral cooperativo seja feito de forma distribuída é a técnica de consenso baseada no cálculo da média (AC, *average consensus*) (TEGUIG et al., 2015),(ZHANG et al., 2015), (LI; YU; HUANG, 2010), (YAN et al., 2012), (HONGNING; XIANJUN; LEILEI, 2014), (VOSOUGHI; CAVALLARO; MARSHALL, 2016), (WEI; HAIXI; ZHEN, 2015), (ASHRAFI; MALMIRCHEGINI; MOSTOFI, 2011), (LI; YU; HUANG, 2009), (SULEIMAN; PESAVENTO; ZOUBIR, 2016), (YU; HUANG; TANG, 2010) e (ZHENG; YANG; LOU, 2011). A técnica AC nada mais é do que a troca de informação de um SU (no caso do ED, o teste estatístico) entre os SUs vizinhos da rede até que atinjam o mesmo valor final de decisão, tudo isso sem a necessidade de uma FC. Por questão de facilidade, será considerado que cada SU utilize ED para realizar o SS.

Basicamente, o modelo de sistema (rede) pode ser descrito como uma CRN

com N SUs cooperativos. Pode-se representar a CRN a partir da teoria de grafos (ZHANG et al., 2015). Matematicamente, o AC pode ser definido como sendo a estimação do i-th SU atualizado no tempo de iteração $k = 1, 2, ...$ de acordo com a seguinte regra (YU; HUANG; TANG, 2010):

$$x_i(k+1) = x_i(k) + \alpha \sum_{j \in \mathcal{N}_i} \mathrm{g}_{ij}(x_j(k) - x_i(k)), \tag{4.1}$$

onde α representa o passo da iteração que satisfaz $0 < \alpha < (\max(\aleph_i))^{-1}$. O símbolo $\aleph$ representa a cardinalidade, i.e., o número de elementos no modelo por grafo (rede). A matriz de adjacência do grafo é definida por $\mathbf{G}$, cujos elementos g_{ij} determinam as conexões entre os SUs na rede. O conjunto de SUs vizinhos ao i-th SU é definido por $\mathcal{N}_i$. A estatística inicial antes da fusão na iteração $k = 0$ é considerada como sendo $x_i(0) = T_i$, onde T_i é o teste estatístico do i-th SU.

As regras de consenso podem ser calculadas sem peso (AC) e com pesos WAC (*weighted average consensus*), e também se dividem em máximo consenso, mínimo consenso e consenso médio (AC). Neste trabalho será dado enfoque à regra de consenso médio com pesos, pois é a que apresenta melhor desempenho, de acordo com (ZHANG et al., 2015).

A regra de consenso com peso (WAC) pode ser escrita como sendo (ZHANG et al., 2015):

$$x_i(k+1) = x_i(k) + \frac{\alpha}{\omega_i} \sum_{j \in \mathcal{N}_i} \mathrm{g}_{ij}(x_j(k) - x_i(k)), \tag{4.2}$$

sendo ω_i os pesos de cada SU (condição do canal) definidos conforme (ZHANG et al., 2015).

As técnicas atuais de consenso permitem que se obtenham desempenhos semelhantes às técnicas de cooperação centralizadas. Assim, a técnica AC possibilita que se obtenha desempenhos para o sensoriamento espectral semelhantes à técnica *soft combining* - EGC, enquanto que a técnica WAC permite que se obtenha performance semelhante à técnica *soft combining* - MRC. As técnicas *hard combining* possuem desempenho inferior comparado às técnicas de consenso médio e *soft combining* (ZHANG et al., 2015) e condizem com as regras de máximo e minimo consenso.

Nesta parte do trabalho de Dissertação analisou-se duas técnicas de consenso melhoradas, sendo proposta aqui a regra denominada IWAC (*improved weighted average consensus*), além de uma regra pré-existente na literatura, porém não explorada no contexto de SS chamada WAC-AE (*weighted average consensus - accuracy exchange*). Em resumo, as duas regras de consenso se tornam respecti-

vamente:

$$\text{(IWAC)} \qquad x_i(k+1) = x_i(k) + \frac{\alpha}{\omega_i} \sum_{j \in \mathcal{N}_i} \omega_j g_{ij}(x_j(k) - x_i(k)), \tag{4.3}$$

$$\text{(WAC-AE)} \qquad x_i(k+1) = x_i(k) + \alpha \sum_{j \in \mathcal{N}_i} \omega_j g_{ij}(x_j(k) - x_i(k)), \tag{4.4}$$

onde ω_j são os pesos dos SUs vizinhos que cooperam.

Na regra IWAC proposta, a regra de consenso é atualizada levando-se em consideração a condição do canal através dos pesos do i-th SU além dos pesos de seus nós vizinhos. Em contrapartida, na regra WAC-AE somente os pesos dos nós vizinhos são levados em consideração para o cálculo do consenso.

4.1 Resultados Numéricos

Neste seção são apresentadas as principais contribuições e resultados desenvolvidos no trabalho do Apêndice A.3 em relação à terceira parte do trabalho de Dissertação relacionado ao tema de Sensoriamento Espectral Cooperativo Distribuído baseado em diferentes regras de consenso.

4.1.1 Contribuições

As principais contribuições do terceiro trabalho são:

1. Análise sistemática das técnicas de consenso AC, WAC e WAC-AE;
2. Proposta de um método de consenso melhorado, denominado IWAC;
3. Análise numérica (via simulação Monte-Carlo) extensiva dos métodos de consenso considerados, com o objetivo de corroborar e comparar o desempenho dos diferentes detetores de consenso distribuídos.

A convergência numérica foi tomada como uma das figuras de mérito para análise das técnicas de consenso. Como foi usado o ED, então o critério de convergência adotado foi considerar a diferença de energia entre os SUs como sendo $\Delta E \leq 1$ dB. As quatro técnicas de consenso foram comparadas considerando diferentes cenários conforme o artigo anexado no Apêndice A.3 nesta Dissertação. Os resultados são mostrados na Tabela 4.1.

Foram adotados quatro cenários para simulação como descrito no trabalho do Apêndice A.3. O primeiro cenário (Cenário A) é uma rede fixa com 6 e

10 SUs, sujeitas a canais AWGN e valores de SNR entre $[-10, 0]$ dB. O segundo cenário (Cenário B) é uma rede móvel, com probabilidade de falha na comunicação de $\mathrm{P_{rfail}} = 0.4$. Uma probabilidade de falha de 0.4 é um valor razoável para caracterizar a mobilidade dos SUs e que vem sendo adotado na literatura (ZHANG et al., 2015). Foram adotados redes com 10 e 20 SUs, sujeitas a canais AWGN e valores de SNR entre $[-10, 0]$ dB. O terceiro cenário (Cenário C) é uma rede fixa com 6 e 10 SUs, sujeitas a canais Rayleigh e valores de SNR entre $[-2, 5]$ dB. O último cenário (Cenário D) é uma rede móvel ($\mathrm{P_{rfail}} = 0.4$) com 10 e 20 SUs, sujeitas a canais Rayleigh e valores de SNR entre $[-2, 5]$ dB.

Tabela 4.1: Número de iterações para que os métodos de consenso médio atinjam convergência sob o critério $\Delta E \leq 1$ [dB].

Cenário	**#SUs**	**AC**	**WAC**	**WAC-AE**	**IWAC**
A-AWGN	6	4	15	5	15
(Fixo)	10	4	6	9	10
B-AWGN	10	4	6	9	10
(Móvel)	20	22	25	30	31
C-Rayleigh	6	15	19	35	34
(Fixo)	10	19	11	18	27
D-Rayleigh	10	19	11	18	27
(Móvel)	20	42	48	> 50	> 50

Observa-se que quanto maior o número de SUs na rede mais iterações são necessárias para a convergência final. Para o cenário A, a rede com 10 SUs necessita de mais iterações do que a rede com 6 SUs; como esperado, o mesmo comportamento se observa para os outros cenários. Na média, o método proposto IWAC possui performance semelhante comparado aos métodos WAC-AE e WAC, para um mesmo número de iterações para convergência.

Nos cenários de canais Rayleigh, todos os métodos requerem um número maior de iteração para alcançar convergência devido às características do canal. Note que nas simulações, consideramos apenas uma realização de canal e os coeficientes de canal de Rayleigh e a localização de SU foram implantados para caracterizar a convergência dos detectores SS.

A Figura 4.1 representa o comportamento de convergência para os quatro detectores no caso de 10 SUs operando sob canais AWGN em rede fixa.

O mesmo comportamento para a convergência é válido para todos os detectores CSS em canais Rayleigh para redes fixa e dinâmica. Por exemplo, a Figura 4.2 ilustra o comportamento de convergência para o caso de 10 SUs operando

sob canais Rayleigh de rede fixa, que podem ser comparados diretamente com a convergência sob o comportamento de rede dinâmica do canal Rayleigh (Cenário D).

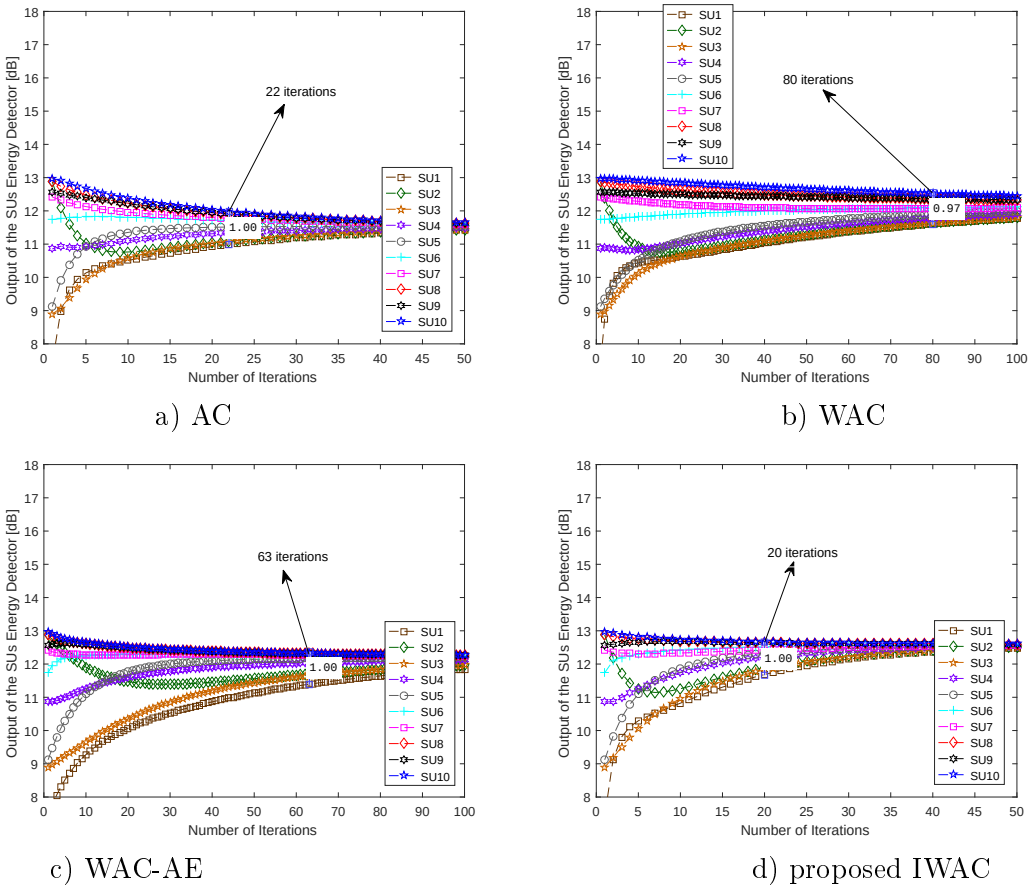

a) AC b) WAC

c) WAC-AE d) proposed IWAC

Figura 4.1: Convergência para 10 SUs e Rede Fixa em canal AWGN.

A ROC Global para os vários métodos de SS é comparada numericamente considerando diferentes cenários (A, B, C e D) como definidos no trabalho do Apêndice A.3 com o objetivo de demonstrar a eficácia dos métodos de SS sob os canais AWGN e Rayleigh. Portanto, Figura 4.3 ilustra a ROC para vários sensores clássicos, bem como o proposto WAC considerando 6, 10 e 20 SUs, sob canais AWGN e Rayleigh, Redes Fixas e Dinâmicas.

Para uma rede de 6 SUs, os métodos WAC e WAC-AE têm desempenho semelhante e podem ser comparados com a regra MRC (cujo desempenho é ótimo). O método IWAC proposto apresenta uma ligeira degradação em comparação com os métodos WAC e WAC-AE, mas mantém um melhor desempenho em comparação com o método AC, que possui desempenho semelhante à regra EGC. Por outro lado, as regras clássicas de combinação *hard* resultam em baixo desempenho em comparação com a regra de combinação *soft*. Entre todas as regras clássicas, a regra OR tem o melhor desempenho enquanto a regra AND apresenta a pior performance. Conclusão semelhante pode ser obtida observando-se a Figura 4.3

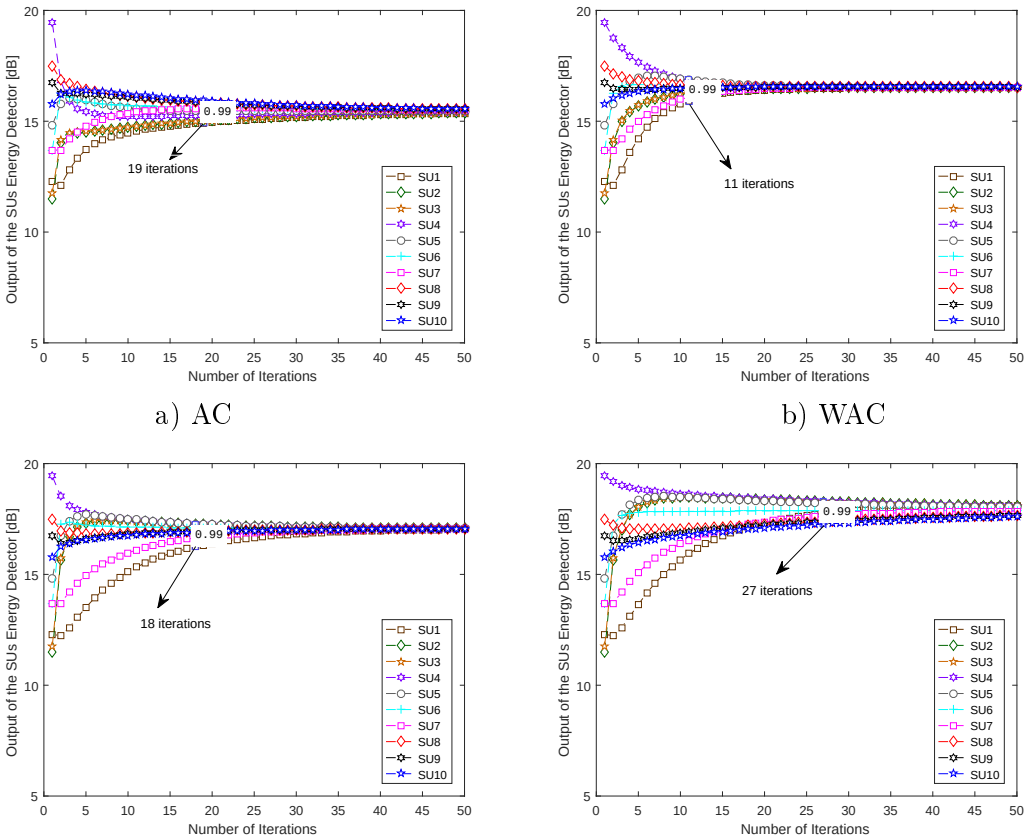

a) AC b) WAC

c) WAC-AE d) proposed IWAC

Figura 4.2: Convergência para 10 SUs e Rede Fixa em canal Rayleigh.

para 10 e 20 SUs. Além disso, a mobilidade da rede não afeta substancialmente o desempenho da ROC de todas as técnicas de detecção de espectro operando em canais AWGN.

A Figura 4.4 descreve a ROC para todos os métodos CSS aqui considerados operando em canais Rayleigh com redes de 6, 10 e 20 SUs, fixas e dinâmicas. Novamente, para 6 SUs os métodos IWAC, WAC e WAC-AE demonstram desempenho semelhante quando comparado ao desempenho ótimo (regra MRC). O método AC tem desempenho semelhante à regra EGC e, neste caso, tem desempenho semelhante aos métodos MRC e WAC. Examinando-se o conjunto de resultados para ROC, pode-se concluir que, em cenários de canais de desvanecimento, a regra OR resulta em desempenho adequado, enquanto os desempenhos da regra AND pioram. Conclusão semelhante pode ser obtida para diferentes números de SU em redes cooperativas. Finalmente, a mobilidade da rede afeta apenas marginalmente o desempenho em termos de ROC.

Desta forma, conclui-se que as regras de consenso com pesos (IWAC proposta, WAC-AE e WAC) tiveram desempenho muito próximo do esquema cooperativo ótimo que é baseado na regra MRC centralizada, conforme pode ser observado

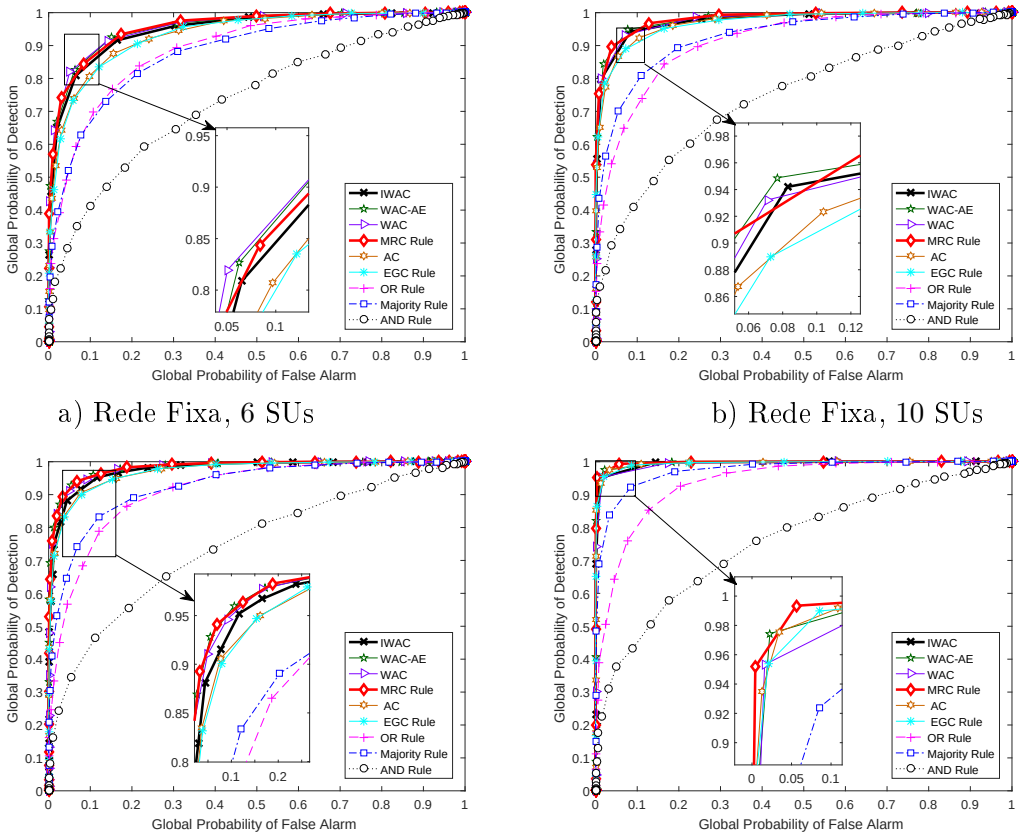

a) Rede Fixa, 6 SUs

b) Rede Fixa, 10 SUs

c) Rede Móvel, 10 SUs

d) Rede Móvel, 20 SUs

Figura 4.3: ROC Global para 6, 10 e 20 SUs em Rede Fixa e Móvel operando em canal AWGN.

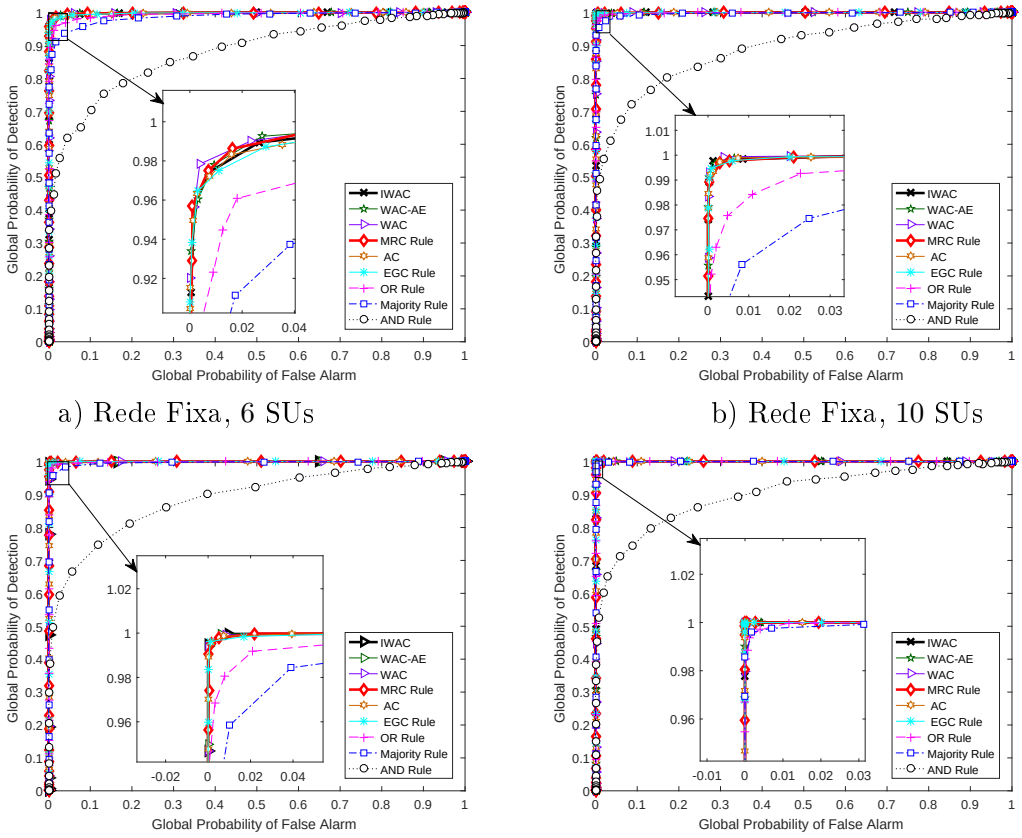

a) Rede Fixa, 6 SUs

b) Rede Fixa, 10 SUs

c) Rede Móvel, 10 SUs

d) Rede Móvel, 20 SUs

Figura 4.4: ROC Global para 6, 10 e 20 SUs em Rede Fixa e Móvel sujeito a canal Rayleigh.

nos resultados numéricos. A regra AC se assemelha ao esquema cooperativo subótimo baseado na regra EGC centralizada. As demais regras centralizadas baseadas em *hard combining* possuem desempenho inferior as demais anteriores. Para os cenários com canal Rayleigh, houve pouca diferença entre os detectores analisados, tantos os decentralizados como os centralizados com pesos, devido aos valores de SNR do canal e também pelo fato de que considerou-se para as simulações a condição de que o canal era completamente conhecido pelos SUs, portanto, nenhuma estimação de canal foi realizada. Por fim, pode-se concluir também que para a regra IWAC proposta mostrou-se ser necessário um número aproximadamente igual de iterações para a convergência final comparado com as outras técnicas analisadas.

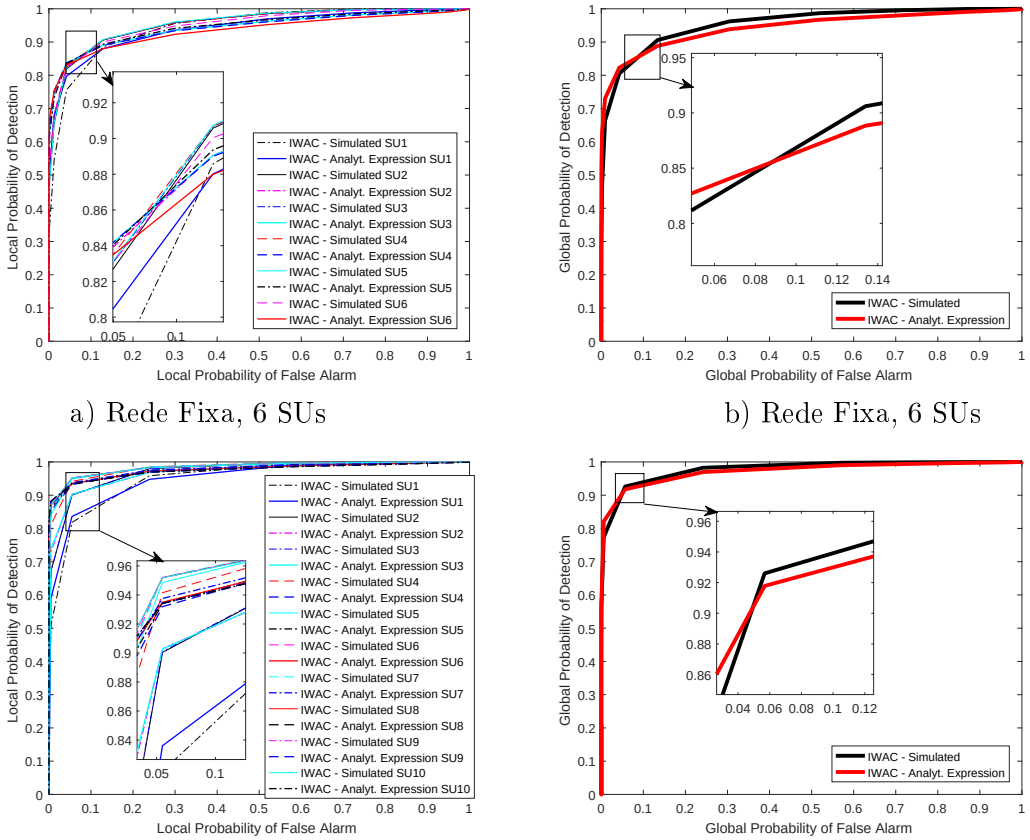

a) Rede Fixa, 6 SUs

b) Rede Fixa, 6 SUs

c) Rede Fixa, 10 SUs

d) Rede Fixa, 10 SUs

Figura 4.5: ROC Local e Global para 6 e 10 SUs sujeitos a canal AWGN - Cenário A.

Finalmente, a Figura 4.5 demonstra o ROC local (distribuída) para o método IWAC proposto, considerando apenas o Cenário A (6 e 10 SUs em um canal fixo AWGN). A expressão analítica é dada no trabalho do Apêndice A.3. e foi comparada com os resultados numéricos por simulação Monte Carlo.

Conclui-se que para o cenário A, Figura 4.5 demonstra um ajuste adequado entre os resultados simulados de Monte Carlo e a expressão analítica, evidenciando que

o conjunto das equações descritas no Apêndice A.3. é uma descrição analítica válida para caracterizar a ROC para o método IWAC.

5 Conclusões

5.1 Conclusões Gerais

Foram desenvolvidas três diferentes abordagens nesta Dissertação. Todas estão relacionadas ao tema de Sensoriamento Espectral em Redes Cognitivas. O primeiro trabalho de investigação relaciona os principais sensores em Redes Cognitivas para sistemas Monobanda, Multibanda e Cooperativos. O segundo trabalho analisa o compromisso entre o Tempo de Sensoriamento e a Vazão e sua solução a partir de um problema de otimização convexa. Por fim, o terceiro e último trabalho propõe uma nova técnica de Sensoriamento Espectral Cooperativo Distribuído caracterizando e comparando-a com técnicas existentes na literatura, incluindo técnicas clássicas em redes cooperativas.

5.2 Conclusões - Sensoriamento Espectral em Redes de Rádio Cognitivo

A primeira parte deste trabalho de Dissertação analisa técnicas de sensoriamento do espectro (SS) em sistemas de rádio cognitivo (CR) monobanda (SB); foram exploradas cinco técnicas básicas: ED, MF, detector cicloestacionário, detector de covariância e o detector baseado em autovalores. Em termos de complexidade, o detector de energia (ED) oferece um menor custo computacional. Entretanto, o ED apresenta baixo desempenho quando operando em baixa SNR, sendo por isso um detector pouco robusto às incertezas do ruído. Por outro lado, o MF possui desempenho ótimo quando operando em canais AWGN, porém, o MF requer informações do sinal do PU, que geralmente não estão disponíveis ao SU. Como alternativa, o detector cicloestacionário resultou em desempenhos superiores em termos de probabilidade de deteção (P_d) *versus* probabilidade de falso alarme (P_f) ou ainda SNR *versus* número de amostras (N_s), mostrando-se mais robusto que o ED; ademais, o detector cicloestacionário requer que o sinal do PU contenha a propriedade cicloestacionária, isto é, mantenha suas propriedades estatísticas

em períodos cíclicos o que permite diferenciar o sinal do PU do ruído térmico. No entanto, o detector cicloestacionário apresenta maior custo computacional em comparação ao ED. Finalmente, os detectores de covariância e o de autovalores são baseados nas medidas de correlação do sinal do PU, oferecendo um SS robusto e pouco dependente de informações do PU; no entanto para a obtenção de desempenhos adequados, estes detectores devem operar em SNR mais elevadas.

5.3 Conclusões - Compromisso Tempo de Sensoriamento *versus* Vazão em Redes de Rádio Cognitivo

O segundo trabalho abordou um problema de otimização para lidar com o tempo de sensoriamento *versus* vazão em uma CRN com um PU e um SU sob um esquema de SS-SB utilizando o detector de energia (ED). O problema de otimização equivalente e simplificado (STO) resultou convexo e não-linear na variável τ, possibilitando assim ser resolvido facilmente a partir de qualquer ferramenta computacional de otimização, garantindo a obtenção do ótimo global. Neste contexto, utilizou-se a função *fmincon* do *MATLAB Optimization Toolbox*. Os resultados numéricos discutidos mostram que o ponto de máximo é um ótimo global e a função objetivo é uma função côncava garantindo a solução do problema.

5.4 Conclusões - Sensoriamento Espectral Cooperativo Distribuído em Redes de Rádio Cognitivo

O terceiro trabalho analisa o desempenho de metodologias de CSS distribuído baseadas em regras de consenso, incluindo uma nova técnica melhorada (IWAC) em comparação com técnicas existentes na literatura, tais como, as técnicas distribuídas baseadas em consenso (AC, WAC e WAC-AE), técnicas centralizadas baseadas em combinação *soft* (MRC e EGC) e técnicas de combinação *hard* (AND, OR e Majority). Observou-se que as regras de consenso com pesos (IWAC, WAC-AE e WAC) tiveram desempenho muito próximo do esquema cooperativo ótimo que é baseado na regra MRC centralizada, para um mesmo número de iterações para a convergência final e mesma complexidade computacional.

Apêndice A – Trabalhos Desenvolvidos

Neste Apêndice são apresentados os trabalhos desenvolvidos desde o início do Mestrado Acadêmico. O primeiro trabalho foi publicado na forma de capítulo de livro, cujo tema explora as diversas técnicas utilizadas no SS em CRNs. O segundo trabalho foi publicado na categoria artigo de conferência, cujo foco consiste da otimização do tempo de sensoriamento em redes CRNs, permitindo aumentar a vazão de informações de um SU. Já o terceiro trabalho foi submetido como um artigo completo para revista. Este *full paper* trata do CSS distribuído baseado na técnica de *average consensus* e possui diversas vantagens em comparação ao CSS centralizado.

A seguir são apresentados os três trabalhos formatados, na ordem temporal em que foram desenvolvidos.

A.1 Sensoriamento Espectral em Redes de Rádio Cognitivo

Título:	*Spectrum Sensing Techniques in Cognitive Radio Networks: Achievements and Challenges;*
Autores:	Aislan Gabriel Hernandes, Ricardo Tadashi Kobayashi and Taufik Abrão;
Categoria:	*Book Chapter*
Publicação:	2016 (online); 2017 (impresso)
Livro:	*Introduction to Cognitive Radio Networks and applications*
Editora:	CRC, Taylor and Francis Publication Group, USA

Resumo das Contribuições: as principais contribuições deste trabalho foram desenvolvidas nas seções 4.3.6, 4.4.5 e 4.5.3 do texto a seguir, na qual é feita a comparação entre os diversos detectores monobanda em termos de ROC, a comparação entre os principais detectores MB sumarizada na forma de tabela, bem como a comparação entre os principais esquemas cooperativos também é discutida, sendo sintetizada na forma de tabela.

4

Spectrum-Sensing Techniques in Cognitive Radio Networks: Achievements and Challenges

Aislan Gabriel Hernandes, Ricardo Tadashi Kobayashi, and Taufik Abrão

CONTENTS

4.1 Introduction

The usage of wireless communication resources, mainly energy and spectrum, has increased tremendously in the recent past. Considering its scarcity and misuse, spectrum becomes an even more important and challenging resource to deal with. Spectrum is a natural resource that has suffered even more limitation thanks to the growth of numerous services such as social networks, video streaming, and cloud storage. Another contributing factor is the geographical location of services. Indeed, there are many geographical areas where communication systems do not make usage of specific bandwidths (BWs) and/or these BWs are only partially used, featuring a misuse or inefficient use of the spectrum.

One of the most important parameter related with the use of spectrum is the spectrum efficiency (SE). In the last few years, many techniques and methods have been proposed to improve the SE, including the capacity and performance of the wireless systems. A promising solution for this challenge is the cognitive radio (CR) concept [1] that allows licensed or primary users (PUs) and nonlicensed or secondary users (SUs) to share the same spectrum. In this scheme, SU accesses the spectrum of PU without causing harm to the PU operation; it is called the *underlay* scheme. Alternatively, the SU can occupy the licensed spectrum when the PU is absent, which is known as the *overlay* scheme; in this context, the SU is seen as an opportunistic user. CR has been one of the promising access methods for future 5G communications; it is an intelligent radio that can be reconfigured dynamically and basically operates in sensing and sharing the spectrum.

Spectrum sensing (SS) is the ability of the radio systems to detect an idle portion of the spectrum or any busy licensed band that allows its usage for SU, depending on the constraints of the PU. Spectrum sharing is the momentary utilization of a portion of spectrum by SU without causing interference to the PU [2].

During sensing, the CR must reliably detect the presence of PUs without causing any interference to them. There are many ways to detect the presence or absence of a PU in a portion of spectrum, starting with a hypothesis, constructing a statistic test, and, based on this, comparing the signals at a threshold level. The simplest and low computational complexity SS is by *energy detection*. The main disadvantage of the energy detection method is its high noise sensitivity. There are many other kinds of detectors, such as coherent detector [matched filter (MF)], feature detector [cyclostationary (CS)-based sensing], covariance matrix detector, and eigenvalue-based detector [3,4].

Another important task carried out by CRs is the *spectrum handoff* (SH) [5]. Whenever a PU returns to its operation, the SU using the PU band must switch its channel to a free one, to avoid interfering the PU. This procedure should be implemented carefully to avoid disturbance to SU communication. There are two types of SHs: *reactive* and *proactive* [3]. In the reactive handoff, SU would sense other available channels when the PU returns and waste some time sensing the spectrum again. On the other hand, in the proactive handoff the SU has a list of candidate channels to access once the PU returns, i.e., the SU

constructs a list of available channels and accumulates data records about the behavior of the PUs in order to predict which channels are going to be available for future access. The SH in CRNs depends on the behavior of the PUs. This is a major challenge since the PUs, behavior is random.

We can expand the concept of singleband CRNs (SB-CRNs) to multiband CRNs (MB-CRNs) [3]. MB-CRNs have recently received much attention from several research organizations, as they can significantly enhance the SUs throughput. With MB-CRNs, the SU not only has a set of candidate channels, but can also reduce handoff frequency and data interference due to the return of PUs.

MB-CRNs sensing can be proceeded by *serial-SS* or *parallel-SS techniques* [3]. In serial spectrum sensing (SS), any singleband (SB) detector using a reconfigurable bandpass filter (BPF) or a tunable oscillator sweeps the entire spectrum sequentially. In parallel SS, a filter and detector band structure working in parallel allows it to sense the entire spectrum more rapidly. In this chapter, we focus on the following MB-SS techniques: *angle-based sensing* (AS), *compressed sensing*, and *wavelet sensing*, which have gained more research interest and attention in the last few years [3].

Two hybrid schemes that can be used jointly with CRNs are *cooperative relays* [6] and *cooperative SUs* [3], which provide spatial diversity, i.e., analogous to multiple inputs multiple outputs (MIMOs). Through the use of cooperative networks, destructive effects of wireless channels, such as fading, path loss, and shadowing can be minimized. Spatial diversity of cooperative networks is called macrodiversity, since the distance between relays and/or SUs is in order of meters. On the other hand, spatial diversity of MIMO is called microdiversity because the distance between antennas is comparable with wavelengths, considering the carrier frequency.

There are many schemes and protocols in cooperative communication such as *relays*, *cooperative secondary users* (*coop-SUs*), and *cooperative spectrum sensing* (*CSS*) [3]. The frequently used ones are *amplify-and-forward (AF)* and *decode-and-forward (DF)* [3] in the relay network, and *hard* and *soft* combined with *or-and-majority* rules in coop-SUs scheme. The AF relay is the simplest scheme which receives a signal version of the source node in a first time-slot, while an amplified version of it is sent by the relay node to the destination node in a second time-slot. This scheme is known as *transparent relaying protocol* because the relay does not modify the information represented by a known waveform. In contrast, the DF relay scheme decodes the received signal at relay node coming from the source node, and then re-encodes and retransmits it to the receiver node. This scheme is known as *regenerative relaying protocol* because the information (bits) or waveform (samples) is modified before being retransmitted by the relay node. This procedure requires digital baseband operations and thus more powerful hardware. The advantage of the AF relay scheme is its simplicity, but the disadvantage is the amplification of the input noise along with the source signal. The DF relay scheme has the advantage of decoding; therefore the noise is not amplified. The disadvantage of the DF relay scheme is that if the signal received by the source node is not decoded correctly, the cooperative communication has to be instantly interrupted.

In CSS scheme, *hard combiner* is simply the sum of decision of all SUs in the network, i.e., the SUs send the final one-bit decision to the other SUs. In *soft combining*, the SU shares its original sensing information or original statistical test weighted by a factor that matches the importance of the decision of each SU.

One of the most used transmission systems in conjunction with CR method is the *orthogonal frequency division multiplexing (OFDM)* because it allows more flexibility for spectrum allocation. OFDM technique splits a user data stream into several substreams, which are sent in parallel to several subcarriers, obtained by splitting the total BW in narrower

channels. The OFDM for multiple access called *orthogonal frequency division multiple access (OFDMA)*, also known as multiuser OFDM (MU-OFDM), allows choosing which users will be allocated to which subcarriers in each time-slot. Currently, OFDMA technique is the basis of many operating technologies, e.g., IEEE 802.16 (WiMax) and 3GPP LTE-Advanced used in 4G systems [7,8].

Another important issue in current and future efficiency-based communication systems and methods is the *energy efficiency* (EE). In CRNs, improving EE poses a challenging problem, because it focuses on optimizing SE and EE jointly. What parameter needs to be sacrificed for the overall system to achieve satisfactory EE: QoS, fairness, PU interference increasing, network architecture, security?

In the CRN context, it is noteworthy that on the one hand, PUs put strict requirements on the interference and channel usage by the SUs; on the other hand, the SUs expect high QoS from the operator at a lower cost; finally, the operator desires to operate at low-operating and low-management costs [9], which represent a challenging and complex optimization problem.

The rest of this chapter is organized as follows. In Sections 4.2 through 4.2.3, the main concepts and principles associated with CRNs are explored. The main SB-SS detectors are discussed and compared in Section 4.3. Recent MB-CRNs concepts and methods are examined in Section 4.4, while cooperative CRNs are put into perspective in Section 4.5. Final remarks and perspectives are offered in Section 4.6. Lists of symbols and acronyms used across this chapter are shown in Tables 4.1 and 4.2, respectively.

TABLE 4.1

List of Symbols

Symbol	Note
α	Cyclic frequency
B	Bandwidth
C	Capacity
F	Frequency
Γ	Signal-to-noise ratio (SNR)
G	Effective throughput
$h_{r,d}$	Channel coefficient between relay and destination
$h_{s,d}$	Channel coefficient between source and destination
$h_{s,r}$	Channel coefficient between source and relay
H_0, H_1	Free and occupied channel hypotheses, respectively
Λ	Threshold
$n_{s,d}$	Addictive Gaussian noise between source and destination
$n_{s,r}$	Addictive Gaussian noise between source and relay
N	Number of samples
σ_n^2	Noise power
P	Power
P_d	Detection probability
P_f	False-alarm probability
ρ_{max}	Maximum eigenvalue
ρ_{min}	Minimum eigenvalue
S	Signal
$T(\cdot)$	Statistic test

TABLE 4.2

List of Acronyms

Acronym	Expansion
AF	Amplify-and-forward
AWGN	Additive white Gaussian noise
CS	Compressive sensing
CRN	Cognitive radio network
CWT	Continuous wavelet transform
CSS	Cyclic spectral density
DF	Decode-and-forward
ED	Energy detector
EE	Energy efficiency
MF	Matched filter
MIMOs	multiple inputs multiple outputs
MME	Maximum–minimum eigenvalue ratio
MB	Multiband
OFDM	Orthogonal frequency division multiplexing
OFDMA	Orthogonal frequency division multiple access
QoS	Quality of service
PSD	Power spectral density
PU	Primary user
ROC	Receiver operating characteristic
SB	Single band
SE	Spectral efficiency
SNR	Signal-to-noise ratio
SH	Spectrum handoff
SS	Spectrum sensing
SU	Secondary user
WMM	Wavelet modulus maxima
WMP	Wavelet multiple product
WMS	Wavelet multiple sum
WSS	Wavelet spectrum sensing

4.2 Spectrum Sensing: Concepts and Principles

Spectrum idles must be sensed by the SU for opportunistic spectrum access. Successful SS allows the overlay access scheme. Let us first consider the most simple case of SS, in which the channel can be used by its PU. From a given observation, the SU must determine whether or not the spectrum is occupied [3,4,10], which implies two hypotheses, i.e., when the channel is free and when it is occupied:

$$\begin{cases} H_0 : \boldsymbol{y} = \eta \\ H_1 : \boldsymbol{y} = \boldsymbol{x} + \eta \end{cases} \tag{4.1}$$

When the channel is free, only additive noise will be observed on the SU side, i.e., $\boldsymbol{y} = \eta$, characterizing the hypothesis H_0. However, if the channel is being used, the SU will sense the PU signal $\boldsymbol{x}$ plus the noise η, hence hypothesis H_1 will be taken. It is noteworthy that $\boldsymbol{x}$

contains the message of the PU and effect of the wireless channel on it. To decide between the two hypotheses, the SU receiver evaluates a test statistics $T(\boldsymbol{y})$ based on its observed signal and compares it with a specific *threshold* λ:

$$\begin{cases} H_0 : T(\boldsymbol{y}) < \lambda \\ H_1 : T(\boldsymbol{y}) \geq \lambda. \end{cases} \tag{4.2}$$

Thus, spectrum idles are identified when $T(\boldsymbol{y})$ is above its threshold and is considered free otherwise.

Although SS may seem a simple task, it still remains a challenging area for CRNs. Important and remaining open issues on SS include the following:

- A more reliable detector than the traditional detectors is required, because any missed-detection creates unacceptable interference among SUs and PUs.
- To identify a spectrum hole a wider BW needs to be sensed, e.g., 4G mobile communications use up to 20 MHz BW and one channel less than this cannot be used. Thus, different bands experience different signal propagation characteristics, while the design of a detector with suitable performance becomes a challenging task.
- The classical sensing/detection techniques may fail in CRNs, because the knowledge of PUs, parameters at SUs is restricted, while computational complexity and implementation cost are the other restricted factors.

4.2.1 SB-Sensing versus MB-Sensing Techniques

SB-sensing technique allows the SU to detect a PU in an SB-spectral sensing environment, with the possibility to use this band to transmit. This provides a better use of available spectrum, since it is a scarce resource nowadays. MB-sensing technique is the extension of SB sensing to many bands (Figure 4.1). The main benefit in operating under MB-SS is the increased system throughput while reducing the SH, which is challenging in CRNs. Indeed, when an SU needs higher throughput or has to maintain a certain quality of service (QoS), it may naturally transmit over a larger BW available by accessing multiple bands.

In MB sensing, the wideband spectrum is divided into M nonoverlapping subbands as shown in Figure 4.1. For simplicity, one can assign the same BW value for all subbands,

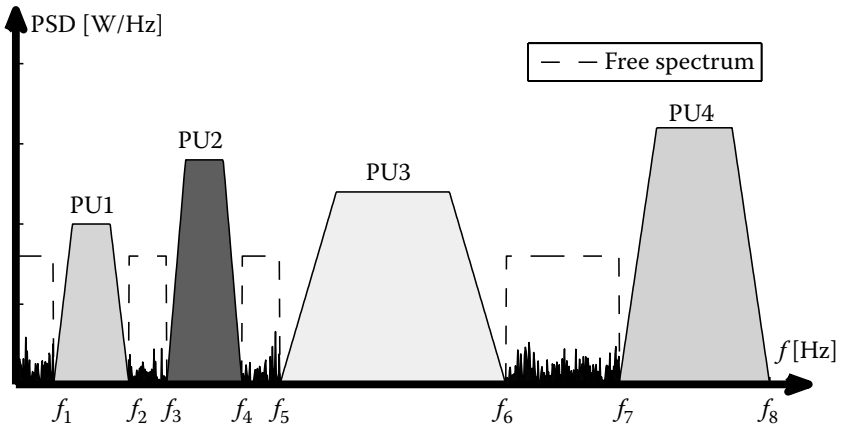

FIGURE 4.1
Multiband spectrum, considering $M = 8$ and unequal subband sizes, i.e., $B_m \neq B_n$.

$B_1 = B_2 = \cdots = B_M$. The main task for the SU sensing is to determine which subchannels are available for the spectrum access. This is, in general, a challenging task, since the available bands are not necessarily contiguous, and the activity of the PUs might be correlated across these bands.* In addition, each particular band is considered occupied even if only a small portion of it is being used.

In Figure 4.1, the wideband spectrum is divided into unequal subband (or subchannel) sizes. Thus, the problem becomes an MB detection problem. Hence, when an SU needs to minimize the data interruptions due to return of PUs to their respective priority bands, a seamless handoff from one band to another becomes a vital feature to guarantee QoS. As a consequence, in MB-CRN the SUs are provided with backup channels, since such channels have already been accessed. Hence, under MB-CRNs, SUs do not only have a set of candidate channels, but MB mode also allows handoff rate reduction.

4.2.2 Noncooperative versus Cooperative Sensing Techniques

- CSS is conceived and implemented to enhance the performance of SB noncooperative detectors. In CSS, the SUs help the network, sensing the spectrum and sharing the sensing results with other SUs. Cooperative sensing scheduling is the case where sensing scheduling is performed in a way that leverages the sensing performance by selecting the best set of cooperating SUs for each channel. On the other hand, in noncooperative wireless networks the SS procedure may be impaired because of the fading channel effects or due to unknown noise. There are many methods to combine the signals arriving at the receiver. In this chapter we discuss two classes of cooperative schemes: cooperative relay and cooperative SS.
- The cooperative relay scheme allows increasing the diversity using relay node, which retransmits the signal to the destination. Such methods boost the probability of detection and lower the probability of false alarm by utilizing the diversity of the measurements from multiple SUs. In addition, *or-and-majority* rules with hard or soft combining are usually deployed to construct hypothesis testing in CSS.
- Even considering the large number of channels to be sensed and the minimum number of sensing SUs for each channel, plenty of SUs should perform sensing all over the service area at any time. However, if almost all SUs perform sensing continuously, enormous energy expenditure is expected, reducing the SU battery lifetime. Therefore, the channels to be sensed as well as the set of SUs that should sense each channel must be selected carefully [11]. Cooperative sensing procedures are responsible to do this selection effectively in order to improve the performance of the CRNs. Cooperative and relay cooperation techniques for SS are treated in more details in Section 1.5.

4.2.3 Spectrum Handoff

In the context of CRNs, the SH consists band changing by the SUs due to return of PUs at the licensed band that was being momentarily used by the SUs. When this happens, there are two possible scenarios. First, the SU remains in the band on silent mode until the PU evacuates the band. Second, the SU moves to another channel. The first scenario is inefficient

* For instance, the primary users in wireless local area networks (WLAN) and broadcast television.

because the SU does not know how long the PU would be active. In the second scenario, two different methods can be implemented for sensing the band: reactive and proactive.

In the reactive method, the SU would again sense to detect other available channels when the PU returns. This way the SU wastes some time sensing the spectrum even if the sensing occurs instantaneously. The target channels are sensed in a demand manner. In the proactive method, the SU makes the target channel ready for SH before transmitting any information. In this method, the SU periodically observes all channels to obtain channel statistics and detects the possible candidate set of idle channels.

In the context of CRNs, the SU throughput and handoff delays are two major parameters of interest for comparing different handoff techniques. The main feature of the spectrum searchers is to initiate a fast and smooth handoff, to avoid performance degradation while reducing the time during SH, namely handoff delay.

Another way to define SH is the cell-based SH, i.e., in the macroview context. There are two major types of SHs in the cell-based type: *intracell* SH and *intercell* SH. The intracell SH occurs commonly in the wireless regional area networks' (WRANs) internal cell, when the PU appears or when the SU QoS decreases in a specific band. On the other hand, the intercell SH generally occurs when the mobile cognitive user (SU) is moving from one WRAN cell to another WRAN cell.

Efficient schemes for fast and smooth handoff are discussed in [5,12]. Generally, the SH degrades SUs performance because of the interruptions that cause delay in the transmissions. Maheshwari and Singh [5] discuss new techniques that allows a fast and smooth SH, such as those based on *queueing theory*, *fuzzy-based*, *neural networks*, *support vector machines* (SVMs), and *hidden Markov model* (HMM).

4.3 SB-SS Detectors

This section explores the fundamentals of SB-SS, covering the most widespread sensing techniques found in literature, including energy detector (ED), MF, covariance detector, CS detector, and eigenvalue detector. The features, operation, and performance are covered under these classical SS techniques. Sensing performance will be discussed through Monte Carlo simulations and theoretical performance will be presented, whenever it is available considering, for simplicity, additive white Gaussian noise (AWGN) channels.

For this section, let us consider the following model for SS

$$\begin{cases} H_0: & \mathbf{y}(n) = \boldsymbol{\eta}(n) \\ H_1: & \mathbf{y}(n) = \mathbf{x}(n) + \boldsymbol{\eta}(n) \end{cases}, \tag{4.3}$$

where $\mathbf{y}(n)$ is a vector containing N observations made at distinct times by the SU receiver, $\mathbf{x}(n)$ is the PU signal, which is probably affected by the channel between the PU and SU, and $\boldsymbol{\eta}(n)$ is the zero mean, variance σ^2, n-power AWGN on the SU receiver. In this case, the terms on Equation 4.3 are

$$\begin{aligned} \mathbf{y}(n) &= [\mathrm{y}(n)\mathrm{y}(n-1)\mathrm{y}(n-2)\ldots\mathrm{y}(n-N+1)]^T, \\ \mathbf{x}(n) &= [\mathrm{x}(n)\mathrm{x}(n-1)\mathrm{x}(n-2)\ldots\mathrm{x}(n-N+1)]^T, \\ \boldsymbol{\eta}(n) &= [\eta(n)\eta(n-1)\eta(n-2)\ldots\eta(n-N+1)]^T. \end{aligned} \tag{4.4}$$

Hence, SS is carried out by the SU through its observations $\mathbf{y}(n)$, which will be compared with a specific threshold λ

$$\begin{cases} H_0 : T\left(\mathbf{y}(n)\right) < \lambda \\ H_1 : T\left(\mathbf{y}(n)\right) \geq \lambda \end{cases}, \tag{4.5}$$

where H_0 implies on free spectrum and H_1 on occupied channel. When the threshold is reached, i.e., $(y(n) > \lambda$, there are two possible outcomes in an SS:

- $P_f = \Pr\left(\mathbf{y}(n) > \lambda \,|\, H_0\right)$, the false-alarm probability, i.e., the probability of an SU not detecting an idle channel. Misleading spectrum detection comes, mainly, from noisy measurements
- $P_d = \Pr\left(\mathbf{y}(n) > \lambda \,|\, H_1\right)$, detection probability, i.e, correct detection probability

The detector performance can be characterized by curves. Hence, it is straightforward that a spectrum sensor should operate with a high detection and low false-alarm probabilities. The most common way of characterizing an SS technique is through receiver operating characteristic (ROC), which is a $P_d \times P_f$ curve. Given the definitions of P_f and P_d, one can conclude that it is very desirable that an ROC curve converges to a step function.

In the following section, the main SS detectors are characterized and compared in terms of ROC curves. Hereafter, for the sake of simplicity, let us drop the discrete time index (n), resulting in $y(n) = y$, $\mathbf{x}(n) = \mathbf{x}$, and $\boldsymbol{\eta}(n) = \boldsymbol{\eta}$.

4.3.1 Energy Detector

When the SU does not have prior knowledge of the PU's transmitted signal, the ED is a suitable choice. It simply computes the energy of the received signal over a time period associated with N samples and within the predefined BW. This detector does not require the channel gains and other parameter knowledge or estimates, while holds a low design cost, as shown in Figure 4.2. However, its performance degrades substantially with noise power and/or increasing interference, i.e., when the ED operates in a low SNR region.

4.3.1.1 Statistic Test and Threshold Level

The test statistics for a typical ED is expressed as [3]

$$T^{\mathrm{ED}}\left(\mathbf{y}\right) = \frac{\left\|\mathbf{y}\right\|_{\mathrm{F}}^2}{\sigma_n^2}, \tag{4.6}$$

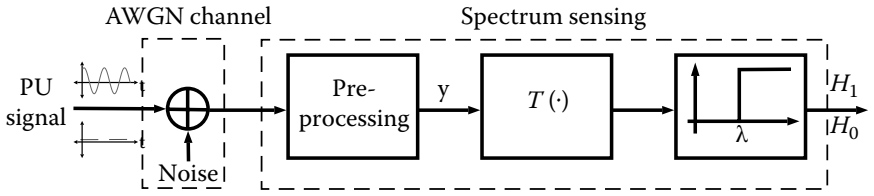

FIGURE 4.2
General singleband detection topology for spectral sensing purpose.

where $\|\boldsymbol{y}\|_{\mathrm{F}}^2$ is the Frobenius norm, N is the number of samples, and σ^2 is the noise power. The numerator of Equation 4.6 represents the received energy power, ε_y. In practice, one cannot dispose off the actual received energy power. Instead, the ED uses the following approximation [13]

$$\hat{\varepsilon}_y = \frac{1}{N}\sum_{k=1}^{N}\left|y(k)\right|^2,$$

where as the number of samples N becomes large, by the law of the large numbers, $\hat{\varepsilon}_y$ converges to ε_y. After evaluating the $T^{ED}(\mathbf{y})$, it is compared with a threshold to satisfy a given target false-alarm probability P_{f} and a given SNR γ

$$\lambda^{\mathrm{ED}}(\mathbf{y}) = \left[Q^{-1}(P_{\mathrm{f}}) + 1\right]\gamma, \tag{4.7}$$

where $Q^{-1}(\cdot)$ is the inverse Q function.

4.3.1.2 Performance Analysis

Considering AWGN channels and a given threshold λ, specified by SNR, the number of samples N and target false-alarm probability P_{f}, the theoretical detection probability can be described as [4]

$$P_{\mathrm{d}}^{\mathrm{ED}} = \frac{\Gamma\left(NB, \frac{\lambda}{2}\right)}{\Gamma(NB)}, \tag{4.8}$$

where B is the total BW, the function $\Gamma(\cdot,\cdot)$ is the incomplete Gamma function. However, through the central limit theorem, the detection probability can be simplified to

$$P_{\mathrm{d}}^{\mathrm{ED}} = Q\left(\frac{1}{\sqrt{2\gamma+1}}\left[Q^{-1}(P_{\mathrm{f}}) - \sqrt{N}\gamma\right]\right). \tag{4.9}$$

The performance of ED in SS applications under SNR $\in$ [–30; –15] [dB] is depicted in Figure 4.3. One can observe that with $N = 1000$ samples, the ROC curve (a) is far from the ideal, even for SNR = –15 [dB]. It should be remarked that spectrum sensors should operate reliably under low SNR, in order to avoid interference in case of misleading SS. In Figure 4.3(b), it can be seen that high detection probabilities are reached for SNR values superior to –10 [dB]; hence, more samples are required if the detector is to operate under lower SNR values. Finally, in Figure 4.3(c) it can be pointed out that, setting a low false-alarm probability, the ED requires around $N = 10^4$ samples to reach high detection probability, when operating under SNR values higher than –15 [dB].

4.3.2 Matched Filter

When the SU has a perfect knowledge of PU signal structure, e.g., modulation type, code, and wave shape, it can correlate the receive signal with a known copy of the PU signal. In this scenario, the MF or coherent receiver is the optimal detector which maximizes the SNR in the presence of AWGN. However, its computational complexity is excessively high while its performance decreases as the channel response changes quickly, i.e., under short coherence time in fading channels scenarios.

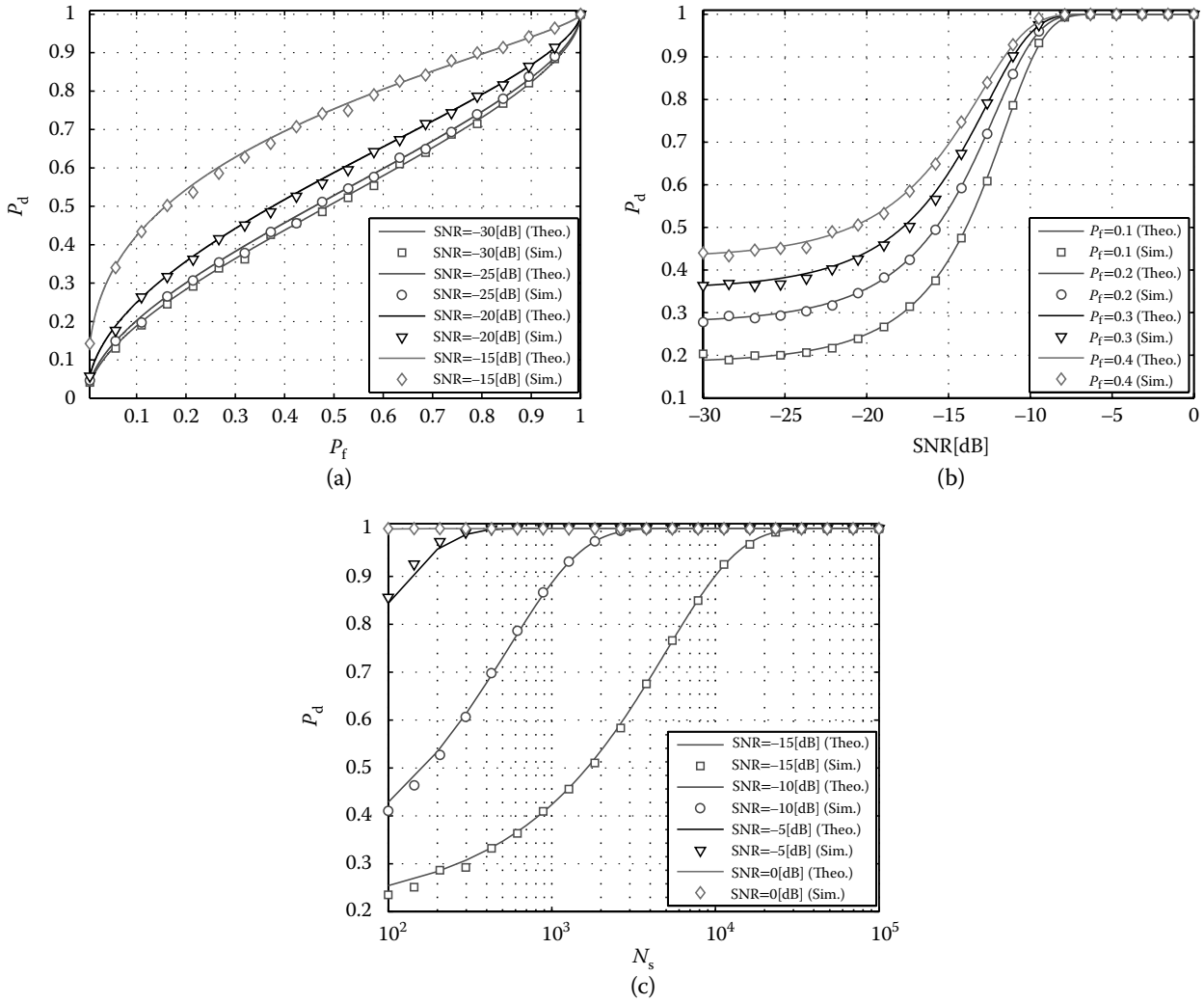

FIGURE 4.3
Energy-detector performance in terms of detection and false-alarm probabilities, as well as number of samples N, operating under AWGN channels. (a) ROC @ $N = 1000$; (b) $P_d \times$ SNR, @ $N = 1000$; (c) $P_d \times N$, @ $P_f = 0.1$.

4.3.2.1 Statistic Test and Threshold Level

To determine whether or not the spectrum is occupied, the MF evaluates the following test [3]

$$T^{\mathrm{MF}}(\mathbf{y}) = \Re\left[\mathbf{x}^H \mathbf{y}\right], \tag{4.10}$$

which correlates the transmitted signal with the received one, where $\Re[\cdot]$ is the operator real part and $(\cdot)^H$ is the Hermitian operator. After calculating $T^{\mathrm{MF}}(\mathbf{y})$, the detection sensing compares it to a specific threshold for the MF, which is defined, for AWGN, as

$$\lambda^{\mathrm{MF}} = Q^{-1}(P_f)\sqrt{N\gamma}\,. \tag{4.11}$$

Thus, the MF threshold is a function of the number of samples N, SNR γ and the target false-alarm probability P_f. Figure 4.2 depicts a general topology for the MF detection, with statistical test and threshold given by (10) and (11), respectively.

4.3.2.2 Performance Analysis

If the the MF-SS detector operates under AWGN scenarios, the theoretical detection can be expressed by [4]

$$P_{\mathrm{d}}^{\mathrm{MF}} = Q\left(\frac{\lambda^{\mathrm{MF}}}{\sqrt{N\gamma}}\right). \tag{4.12}$$

Figure 4.4 shows the MF performance considering different perspectives, i.e., graphs of the ROC, $P_{\mathrm{d}} \times \mathrm{SNR}$ and $P_{\mathrm{d}} \times N$. In these figures, continuous lines represent the theoretical performance, while markers represent simulated performance. In (a), one can observe that the ROC converges rapidly to its optimal point, e.g., with a SNR $\gamma = -20$ [dB] the probability of detection is higher than 90%, while the probability of false alarm is just 5%. In (b), it can be observed that the probability of detection converges to 1 around $\gamma = -20$ [dB], considering only $N = 1000$ samples. Also, (c) shows that $N = 1000$ samples are enough to perform reliable SS in such a way that false-alarm probability is quite low.

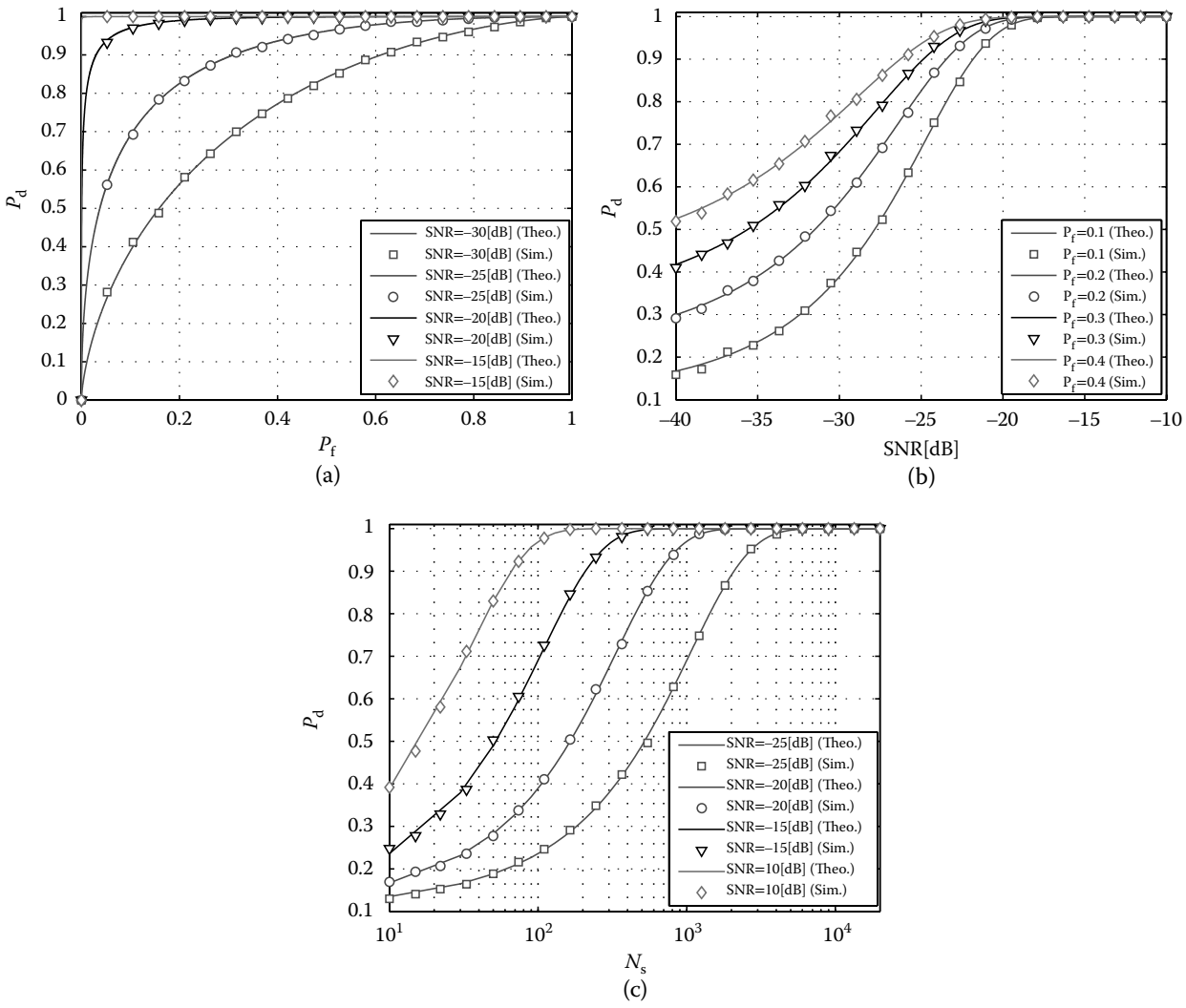

FIGURE 4.4
Matched-filter performance operating under AWGN channels. (a) ROC @ $N_{\mathrm{s}} = 1000$; (b) $P_{\mathrm{d}} \times \mathrm{SNR}$, @ $N_{\mathrm{s}} = 1000$; (c) $P_{\mathrm{d}} \times N_{\mathrm{s}}$, @ $P_{\mathrm{f}} = 0.1$.

4.3.3 CS Feature Detector

To perform a reliable SS, the CS detector takes advantage of the knowledge of the second moment statistics of the PU signal. If the PU signal presents periodic statistical properties, i.e., periodic mean and autocorrelation, the received signal on the SU side also features periodic properties in the CS sense. Since white noise is, generally, uncorrelated in time, this detector can easily verify if a CS signal is present on a given spectrum band. However, if the noise is correlated in time, CS detection may require a higher sample rate, which is a concerning drawback, as it increases the sensing complexity. Hence, if the PU signal is known to present statistical periodicity, CS detection can be used to perform SS in a CRN.

In order to determine whether or not a signal is CS, the spectral correlation density or cyclic spectral density (CSD) function must be evaluated. The evaluation of CSD is based on the cyclic autocorrelation of the signal $\boldsymbol{y}$

$$R_y^{\alpha}(\tau) = \mathbb{E}\left[\mathbf{y}(t)\mathbf{y}(t)e^{j2\pi\alpha n}\right], \tag{4.13}$$

which forms the following Fourier transform pair

$$S_y^{\alpha}(f) = \int_{-\infty}^{\infty} R_y^{\alpha}(\tau)e^{-j2\pi f\tau}\,\mathrm{d}\tau, \tag{4.14}$$

where S_y^{α} is the power spectral density (PSD) of $\mathbf{y}(t)$. Alternatively, the SCD function can be obtained, for example, using the FFT accumulation method (FAM) [14], which uses two FFT blocks to estimate the SCD of a given signal in order to get a better SCD approximation.

4.3.3.1 Statistic Test and Threshold Level

The CS statistics test and threshold for the SS problem under AWG noise are given, respectively, by [15]

$$T^{\mathrm{CS}}(\mathbf{y}) = \max\left(S_y^{\alpha}(f)\right), \tag{4.15}$$

and

$$\lambda^{\mathrm{CS}} = \sqrt{\frac{\sigma_n^4}{2\sigma_x^2}\ln\left(\frac{1}{P_{\mathrm{f}}}\right)}, \tag{4.16}$$

where σ_x^2 is PU signal variance and σ_n^2 is the noise variance.

4.3.3.2 Performance Analysis

The detection probability is defined as [15]

$$P_{\mathrm{d}}^{\mathrm{CS}} = Q_m\left(\frac{\max\left(S_y^{\alpha}(f)\right)}{\sigma_1}, \frac{\lambda^{\mathrm{CS}}}{\sigma_1}\right), \tag{4.17}$$

where $Q_m(\cdot,\cdot)$ is the generalized Marcum Q-function [16] and variance

$$\sigma_1^2 = \frac{\sigma_n^4}{2\sigma_x^2}\left(1 + \frac{S_x\left(f+\frac{\alpha}{2}\right)}{\sigma_n^2} + \frac{S_x\left(f-\frac{\alpha}{2}\right)}{\sigma_n^2}\right).$$

Figure 4.5 shows the CS-simulated performance considering different parameters, i.e., graphs of ROC, $P_d \times$SNR and $P_d \times N$. In (a), the ROC considering $\gamma = -15$ dB and $P_f = 0.1$ shows a probability of detection $P_d \simeq 0.53$. Besides, in (b) if the $P_f = 0.1$ and $\gamma = -15$ dB, the probability of detection is around $P_d \simeq 0.5$, and for a SNR $\gamma \leq -15$ dB the performance decreases rapidly, becoming very poor around $\gamma \approx -30$ dB. Finally, in (c) the CS detector shows that it must operate under $N = 10^5$ samples for a SNR of $\gamma = -15$ dB in order to achieve a near-optimal performance, i.e., operate with greater number of samples and excessive computational processing.

4.3.4 Covariance Matrix Detector

Covariance sensing determines whether or not the channel is being occupied, based on the covariance matrix of the observed signal, considering L temporal lags. In this case

$$\begin{cases} H_0 : \hat{\mathbf{y}}(n) = \hat{\boldsymbol{\eta}}(n) \\ H_1 : \hat{\mathbf{y}}(n) = \hat{\mathbf{x}}(n) + \hat{\boldsymbol{\eta}}(n) \end{cases}' \tag{4.18}$$

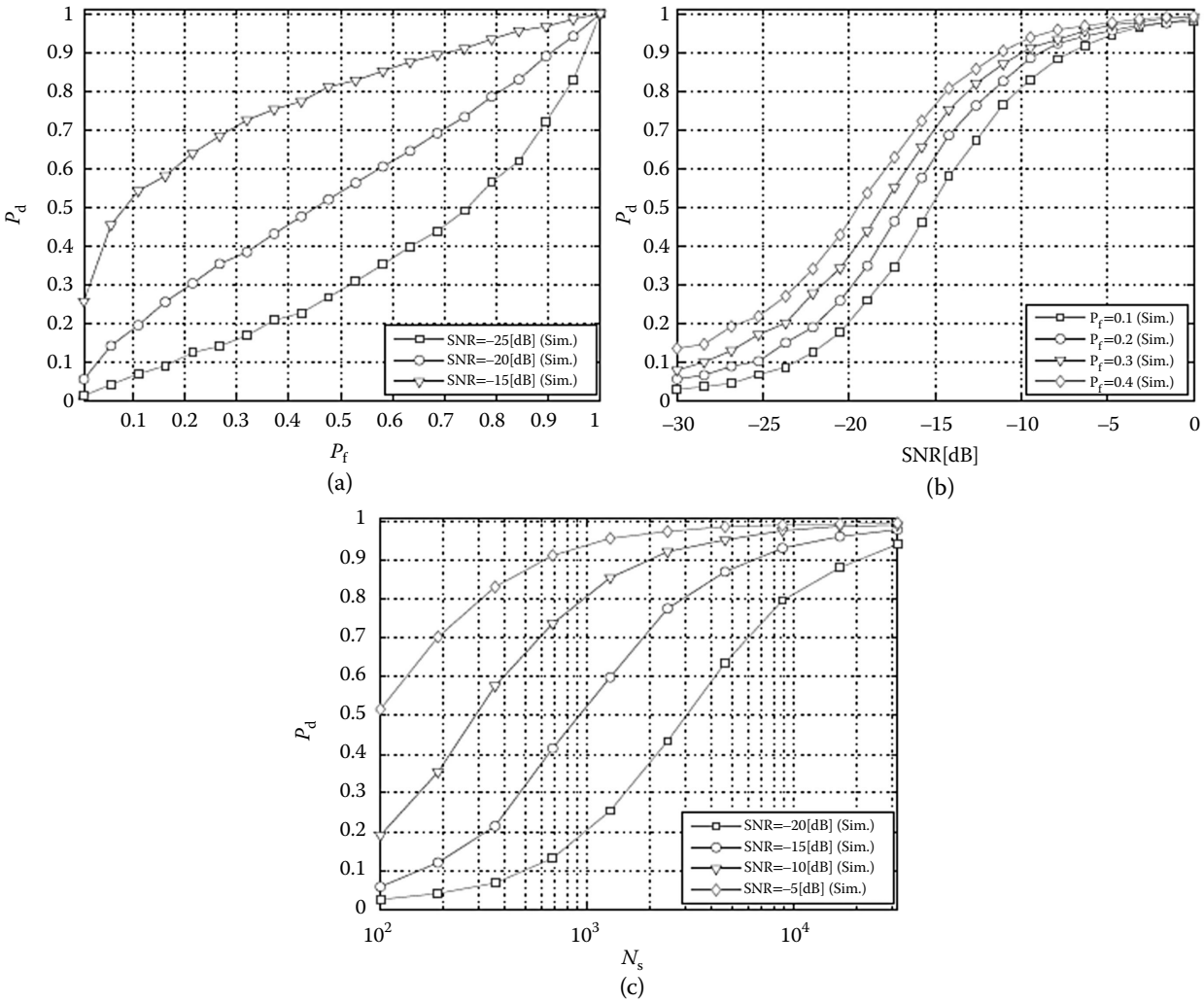

FIGURE 4.5
Cyclostationary-detector performance under AWGN channels. (a) ROC @ N_s = 1000; (b) $P_d \times$ SNR, @ N_s = 1000; (c) $P_d \times N_s$, @ P_f = 0.1.

where $\hat{\mathbf{y}}(n)$, $\hat{\mathbf{x}}(n)$ and $\hat{\boldsymbol{\eta}}(n)$ are windowed versions, of length* $N \leq L$, of the received SU signal, PU signal x and the SU side noise η. More specifically

$$\begin{aligned}\hat{\boldsymbol{y}}(n) &= \left[y(n)\ y(n-1)\ y(n-2),\ldots,y(n-L+1)\right]^T,\\ \hat{\boldsymbol{x}}(n) &= \left[x(n)\ x(n-1)\ x(n-2),\ldots,x(n-L+1)\right]^T,\\ \hat{\boldsymbol{n}}(n) &= \left[\eta(n)\ \eta(n-1)\ \eta(n-2),\ldots,\eta(n-L+1)\right]^T.\end{aligned} \tag{4.19}$$

Since SS is proceeded with a finite number of samples, the covariance matrix of $\mathbf{y}$ can only be estimated. The reason for windowing $\mathbf{y}$ into $\hat{\mathbf{y}}$ is to obtain a better covariance matrix estimate just for L lags, instead of a poor covariance matrix over N lags. Hence, L is associated with the covariance matrix estimation quality and is usually referred as the smoothing factor. Considering these observations, we define the following estimated covariance matrices

$$\mathbf{R}_{\mathbf{y}}(N) = \frac{1}{N}\sum_{n=L-1}^{L-2+N} \hat{\mathbf{y}}(n)\hat{\mathbf{y}}(n)^H, \tag{4.20}$$

and

$$\mathbf{R}_{\mathbf{x}}(N) = \frac{1}{N}\sum_{n=L-1}^{L-2+N} \hat{\mathbf{x}}(n)\hat{\mathbf{x}}(n)^H. \tag{4.21}$$

Finally, taking the noise as uncorrelated in time

$$\mathbf{R}_{\mathbf{y}} = \mathbf{R}_{\mathbf{x}} + \sigma_n^2\mathbf{I}_L. \tag{4.22}$$

It is known that x is probably correlated in time,† thus $\mathbf{R}_{\mathbf{x}}$ is not diagonal. Hence, covariance-based detection verifies if the covariance matrix of the received signal is diagonal or not.

4.3.4.1 Statistic Test and Threshold Level

Based on the previous observations, a straightforward test is

$$T^{\mathrm{COV}}(\mathbf{y}) = \frac{T_1}{T_2}, \tag{4.23}$$

where the expressions for T_1 and T_2 are given by

$$T_1 = \frac{1}{L}\sum_{\substack{n=1\\m=1}}^{L} |r_{nm}|, \tag{4.24}$$

and

$$T_2 = \frac{1}{L}\sum_{n=1}^{L} |r_{nn}|. \tag{4.25}$$

Thus, if $T_1/T_2 \geq \lambda^{\mathrm{COV}}$ the spectrum is occupied and if $T_1/T_2 < \lambda^{\mathrm{COV}}$ it is idle. Finally, given a target false-alarm probability, the threshold can be obtained as

---

* Since $\hat{\mathbf{y}}$(n) is a windowed version of y, $L \leq N$.

† Mainly due to the carriers of transmitted signals and due to time dispersion introduced by the channel (multi-tap channel).

$$\lambda^{\mathrm{COV}} = \frac{1+(L-1)\sqrt{(2/N\pi)}}{1-Q^{-1}(P_{\mathrm{f}})\sqrt{(2/\pi)}}. \tag{4.26}$$

4.3.4.2 Performance Analysis

Though many analytical formulas for covariance SS performance are available in the literature, unfortunately, such formulas are just approximated expressions. Zeng [17] proposed the following approximation for the probability of detection of covariance detector

$$P_{\mathrm{d}}^{\mathrm{COV}} \cong 1-Q\left(\frac{\frac{1}{\lambda^{\mathrm{COV}}}+\frac{\gamma \mathrm{Y}_L}{\gamma+1}-1}{\sqrt{2/N}}\right), \tag{4.27}$$

where

$$\mathrm{Y}_L = \frac{2}{L}\sum_{l=1}^{L-1}\frac{(L-l)\,\mathbb{E}\left[x(n)x(n-l)\right]}{\sigma_x^2}, \tag{4.28}$$

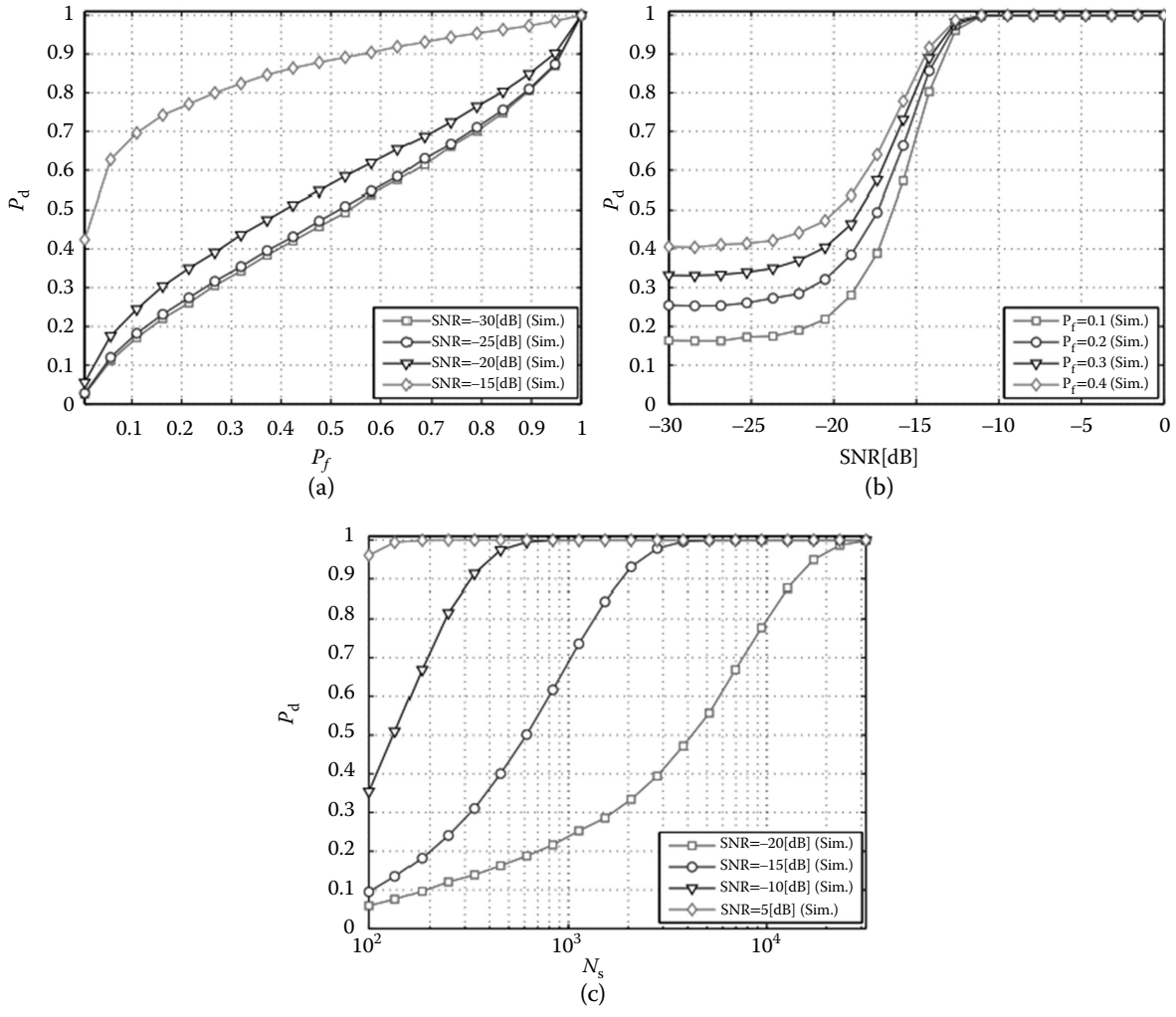

FIGURE 4.6
Covariance detector performance. (a) ROC @ N_s = 1000; (b) P_d × SNR, @ N_s = 1000; (c) P_d × N_s, @ P_f = 0.1.

is a measure of temporal correlation of the PU signal. Since the analytical performance available in the literature is inaccurate, next section will present only simulation results. Figure 4.6 depicts the performance of the covariance detector. First, it can be observed in (a) and (b) that the detection probability may not be as high as expected for SNR lower than $\gamma = -15$ [dB]. It should be pointed out that the covariance detector does not require SNR estimates; however, if the second statistical moment is poorly estimated, the performance of the covariance detector will be impacted negatively. Through Fig. 4.6(c) one can see that $N = 2000$ samples are enough to reach a high detection probability ($\geq$0.9), given 10% of false alarm and $\gamma = -15$ [dB].

4.3.5 Eigenvalue Detector

The eigenvalue detector can exploit the eigenvalue structure of the covariance matrix of PUs signals. The ratio between the maximum and minimum eigenvalue of the covariance matrix of receiver signal vector (PUs signal vector) is compared with a specific threshold. Nevertheless, if the correlation of the PUs signal is zero (white noise feature), the detection may fail.

The eigenvalues of a covariance matrix of a signal can reveal some of its characteristics. If the eigenvalues are similar, it is very likely that the matrix is well-behaved, tending to a diagonal matrix. The eigenvalue detector exploits this feature, i.e., for the idle channel, a diagonal $\mathbf{R}_y$ matrix will be generated due to white noise temporal decorrelation feature for lags other than zero.

4.3.5.1 Statistic Test and Threshold Level

First, the SU must estimate the correlation matrix of $\mathbf{y}$ using Equation 4.20. Then the eigenvalues of $\mathbf{R}_y$ are evaluated in order to proceed with the test, which is given by the maximum–minimum eigenvalue (MME) ratio

$$T^{\mathrm{MME}}(\mathbf{y}) = \frac{\rho_{\max}}{\rho_{\min}}, \tag{4.29}$$

where $\rho_{\max}$ is the maximum and $\rho_{\min}$ is the minimum eigenvalue of covariance matrix of the received signal. Fixing a target false-alarm probability, the threshold for this sensing technique is written as [18]

$$\lambda^{\mathrm{MME}} = \left(\frac{\sqrt{N}+\sqrt{L}}{\sqrt{N}-\sqrt{L}}\right)^2 \left(1+\frac{\left(\sqrt{N}+\sqrt{L}\right)^{-\frac{2}{3}}}{(NL)^{\frac{1}{6}}} F_1^{-1}(1-P_f)\right), \tag{4.30}$$

where $F_1(\cdot)$ is the cumulative distribution function (CDF) of Tracy–Widom distribution.*

4.3.5.2 Performance Analysis

For the MME test, the detection probability is given by

$$P_f^{\mathrm{MME}} = 1 - F_1\left(\frac{\lambda^{\mathrm{MME}}\left(\sqrt{N}-\sqrt{L}\right)^2 - \mu}{\nu}\right), \tag{4.31}$$

* Tracy–Widom distribution is the limiting law of the largest eigenvalues of random matrices and has no closed form for the CDF function [19,20].

where $\mu = \left(\sqrt{N-1}+\sqrt{L}\right)^2$ and $\nu = \left(\sqrt{N-1}+\sqrt{L}\right)\left(\frac{1}{\sqrt{N-1}}+\frac{1}{\sqrt{L}}\right)^{1/3}$. Numerical results performance for eigenvalue detector are presented in Figure 4.7. It can be observed through Figure 4.7(a) and (b) that the detection probabilities converge rapidly for $\gamma \geq -15$ [dB], while (c) corroborates that $N = 1000$ samples are enough to perform a reliable SS, given a target false-alarm probability as low as 10%.

4.3.6 Performance Comparison of SB-SS Methods

- There is no detector to confirm that the performance is better than others in all channel and system scenarios. The choice of the detector depends on many factors, such as how much information SU has about the PU signal, SNR level, and signal processing resource availability.
- ED is highly indicated when no prior knowledge about the PU is available and when the performance is not much affected by uncertain noise, i.e., the system

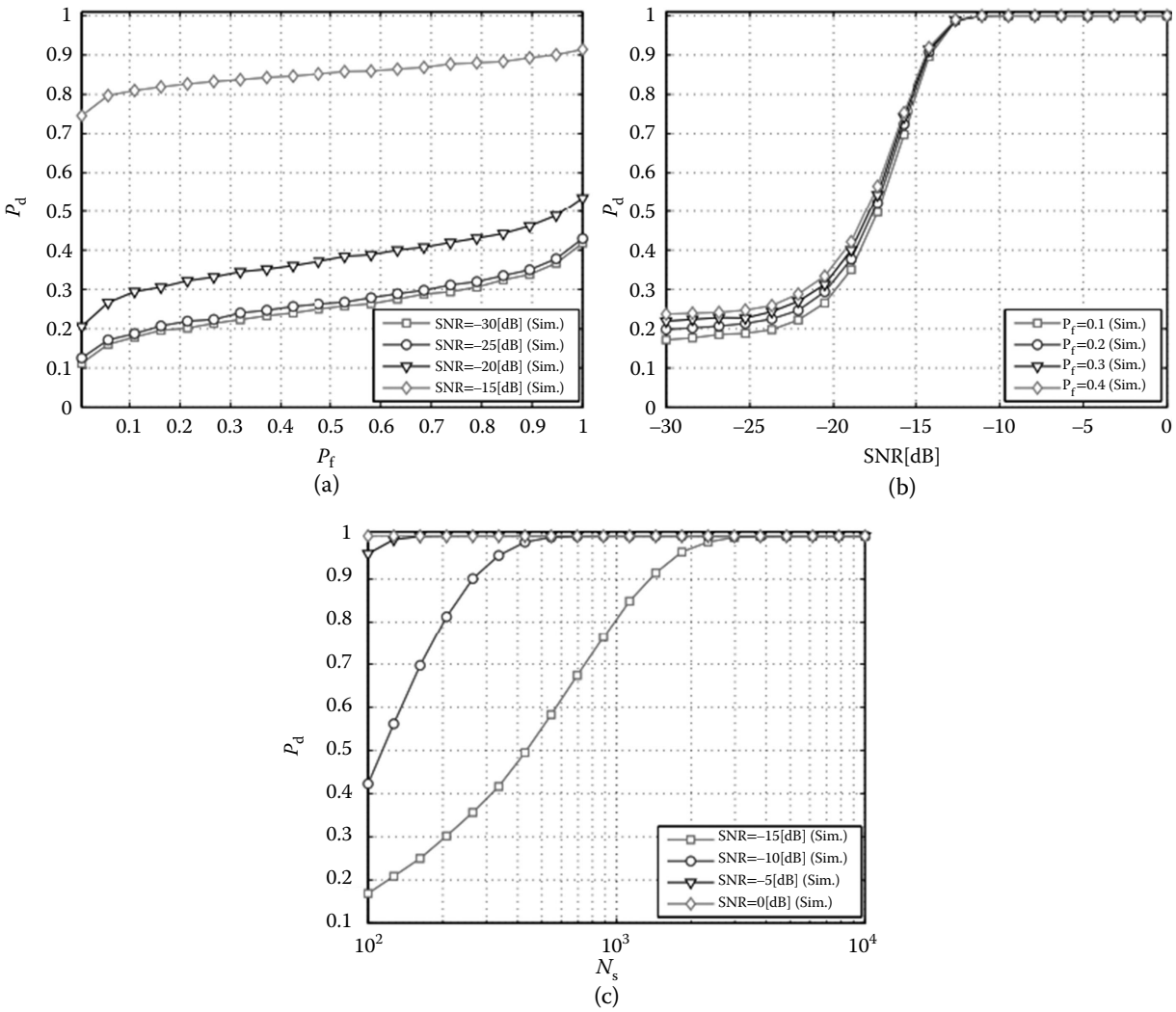

FIGURE 4.7
Eigenvalue detector numerical simulation performance under AWGN channels. (a) ROC @ N_s = 1000; (b) P_d × SNR, @ N_s = 1000; (c) P_d × N_s, @ P_f = 0.1.

operates in not-so-low SNR. This detector results in low computational complexity compared with other SS detectors analyzed in this chapter.

- The MF (coherent detector) is used when the SU has full knowledge of the PU signal, i.e., when the SU knows about modulation, wave format, codification, and other PU features.
- A CS detector is used when the SNR is quite low and knowledge regarding the PU signal is partial. In this situation, the CS detector has better performance and robustness, substituting ED with advantage in performance. However, this detector has a high computational complexity and some parameters must be known by the detector, such as cycle prefix or cycle frequency. In addition, the PU signal must present the CS statistical properties.
- Covariance matrix (cov) detector is based on the estimated covariance matrix of the PU signal. Similar to CS, eigenvalue, and MF detectors, the cov spectral sensing detector has the ability to distinguish the PU signal from other signals, such as other SUs. No other information a priori of signal, channel, and noise is necessary.
- Eigenvalue detector is also based on the estimated covariance matrix of PU signal. The difference between (cov) detector is given by the statistic test. The statistic test of eigenvalue detector is determined only by the ratio of maximum and minimum eigenvalues. Table 4.3 summaries the main characteristics of the principal SB-SS methods in CRNs.

Figure 4.8 shows the numerical performance analysis comparing all the SB detectors treated in this chapter. In (a), the sample number is $N = 1000$ and SNR is fixed as $\gamma = -15$[dB] which are realistic values that can be deployed in practical scenarios of CRNs. One can observe that the ED has the worst performance among all the detectors until $P_f = 0.6$. On the other hand, the eigenvalue detector has better performance than the covariance detector until $P_f = 0.15$, when the covariance detector is replaced by better performance than the eigenvalue detector. The covariance detector has better performance than ED for all values of P_f. As expected, the MF detector has the optimal performance, because the system is operating under AWGN scenarios.

TABLE 4.3

Singleband Spectrum-Sensing Detector Comparison

	Required Knowledge		Identify PU From		
SS detectors	σ_n^2	**PU Signal, x**	**Noise**	**Other Signals**	**Remark**
Energy	✓		Limited by SNR		Simple method
MF		✓	✓	✓	Max. SNR under AWGN
Cyclostationary		✓	✓	✓	High sensing time
Covariance			✓	✓	Require reliable estimates of covariance matrix
Eigenvalue			✓	✓	Performance similar to COV detector

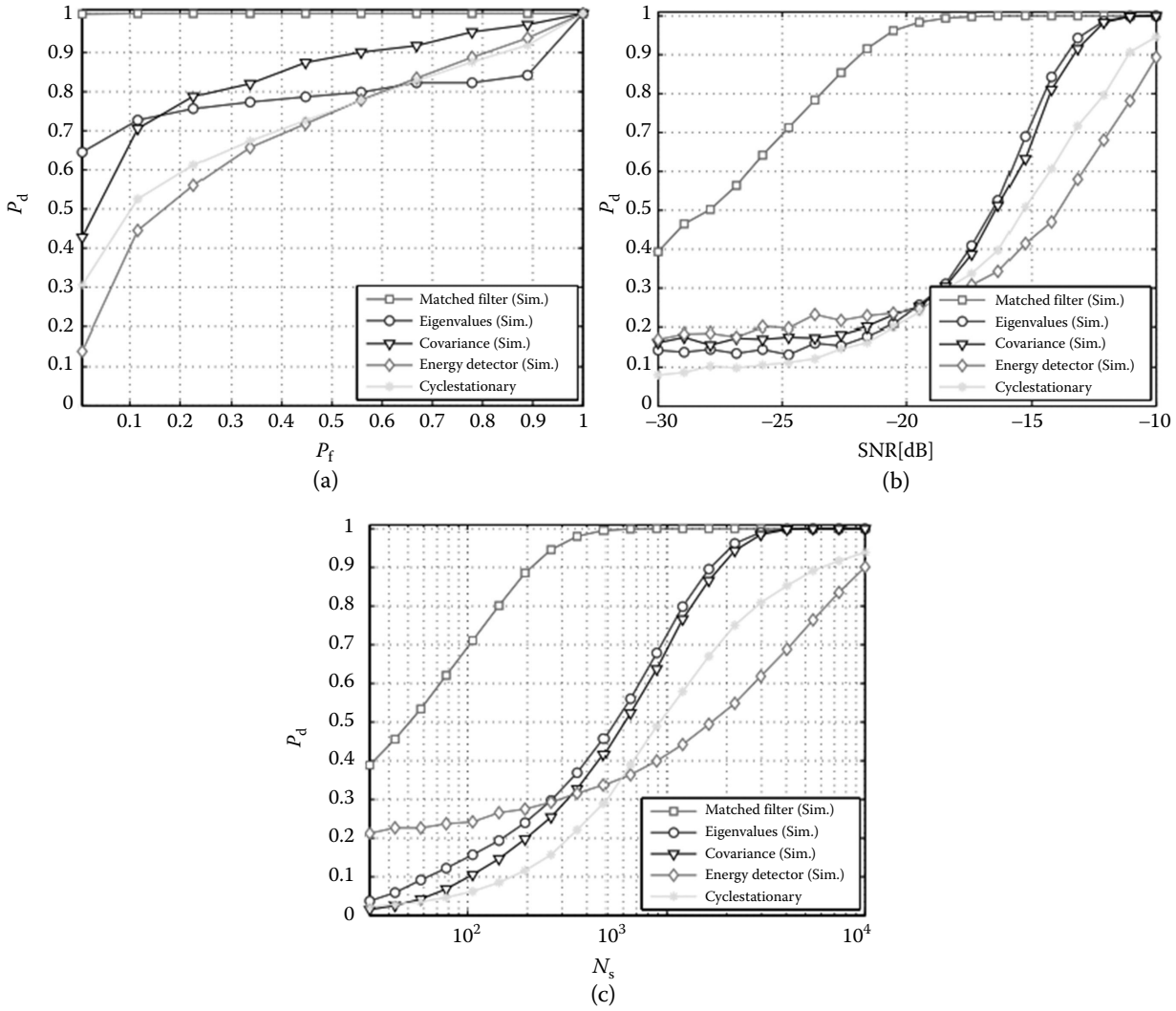

FIGURE 4.8
Comparison of spectrum-sensing techniques operating under AWGN channels. (a) ROC @ N_s = 1000, SNR = –15 dB; (b) P_d × SNR, @ N_s = 1000, P_f = 0.1; (c) P_d × N_s, @ P_f = 0.1, SNR = –15 dB.

In Figure 4.8(b), sample number is $N = 1000$ and false-alarm probability is fixed as $P_f = 0.1$, which are the real parameter values found in a practical system configurations. Until $\gamma = -20$ dB the ED is slightly better than the covariance detector, which in turn is better than eigenvalue detector. After SNR = –20 dB, ED becomes the worst detector and the eigenvalue and covariance present equivalent performance, with eigenvalue slightly better than covariance detector. Once again, the MF has the best performance, even for very low SNR values, demonstrating satisfactory operation for a wide range of low SNR values, i.e., $\gamma \geq -22$ [dB].

In Figure 4.8(c), the false-alarm probability is fixed as $P_f = 0.1$ and the SNR in $\gamma = -15$ dB; indeed, we are interested in determining the minimum number of samples with which SS detectors can operate satisfactorily. For these parameters, the CS, eigenvalue, and covariance detectors give poor performance under a lower number of samples $N \in [300; 500]$ samples, but the ED results in a better performance in terms of detection probability. For medium–high values of samples, $N \in [700; 2000]$, the ED gives the worst performance among all. The eigenvalue and covariance have approximate performances, with the eigenvalue being slightly better than the covariance detector. For high values of samples,

N = 3000, the eigenvalue, covariance, and even CS detector result in good performance. The best performance is obtained with MF with lower number of samples N_s = 500. For each chosen parameter ($P_{f,\,SNR}$), the number of samples (N) impacts on the performance and complexity of the detector.

4.4 MB Cognitive Radio Networks

MB-CRNs have recently caught the attention of several researcher organizations, since MB techniques can significantly enhance the SU's throughput. For example, the *ultrawideband* (UWB) channel can be divided in multiple subchannels and the sensing problem becomes an MB detection problem. Alternatively, MB sensing can be seen in an OFDMA perspective, where each subchannel is treated as subband sensing.

Another advantage of MB-CRNs is that they provide simultaneous sensing to the SUs and access to multiple channels, reducing the handoff frequency, i.e., diminishing the SUs, transmission interruptions. In addition, with MB-CRNs, the SU not only has a set of candidates channels, but reduces handoff frequency which generates data interference upon return of the PU.

CRNs deploy MB mode when the SUs aim is to achieve higher throughput or keep the QoS without interfering the PUs.

4.4.1 MB Sensing Problem

Spectrum idles must be sensed by the SU for opportunistic spectrum access by expanding spectrum-sensing techniques to MB mode. Let us consider a classical binary hypothesis testing problem

$$\begin{cases} H_{0,m} : \mathrm{y}_m = \mathrm{n}_m \\ H_{1,m} : \mathrm{y}_m = x_m + \mathrm{n}_m \end{cases}, \tag{4.32}$$

where m is the individual subchannel of a wideband consisting M subchannels in total and $\mathbf{y}_m = [y_m(1), y_m(2), \ldots, y_m(N)]^T$ is the N number of samples of the received signal at the SU receiver in subband m; transmitted PU signal in the same subband m is $\mathbf{x}_m = [x_m(1), x_m(2), \ldots, x_m(N)]^T$; and $\mathbf{n}_m$ is the AWGN noise vector sample with $n_m \sim N\left(0, \sigma^2; {}_nI\right)$.

In order to decide between absence or presence of PU signal hypotheses, H_0 and H_1 on subchannel m, one can compare a test statistics $T(\mathbf{y}_m)$ with a default threshold λ

$$\begin{cases} H_{0,m} : T\left(\mathrm{y}_m\right) < \lambda \\ H_{1,m} : T\left(\mathrm{y}_m\right) \geq \lambda \end{cases}. \tag{4.33}$$

Spectrum idles are identified when $H_{0,m}$ is true. When the PU signal is detected, the hypothesis $H_{1,m}$ is true.

There are many techniques to use MB-CRNs in sensing, such as serial spectrum-sensing techniques, parallel spectrum-sensing techniques, wavelet sensing, compressed sensing, and AS. However, few important issues still remain open in MB-CRNs, such as trade-off between sensing time and throughput [3]. In the next section, we will discuss the last three techniques.

4.4.2 Wavelet Spectrum Sensing

Continuous wavelet transform (CWT) in the spectrum-sensing context was firstly deployed by Tian and Giannakis (2006) [21], who showed how to identify the edges (or boundaries) of subchannels and how to estimate the PUs allocated to each subchannel of a wideband spectrum [22–26].

This mode of spectrum sensing is employed when the SU has no knowledge of the number of subbands M, associated with subbands $B_1, B_2, \ldots, B_M$ B_2 B_M, and the correspondent localization of frequencies $f_1, f_2, \ldots, f_M$, where the mth subband is defined as $B_m = f_m - f_{m-1}$ (Figure 4.1). In this kind of sensing, the CWT [27] is deployed due to its suitable properties, which is enabled to search the boundaries of spectral occupancy of PU signals across the entire subband set.

CWT has the ability to construct a time–frequency representation of a signal that offers a very good simultaneous localization of time and frequency. If $\mathbf{y}_m(t)$ is a received signal, $s > 0$ and r are the scaling and shifting factors respectively, with $s \in R^+$ and $r \in R$, the CWT is defined as [27]

$$w_{y_m} = \frac{1}{\sqrt{|s|}} \int_{-\infty}^{\infty} \mathrm{y}_m(t) \psi\left(\frac{t-r}{s}\right) \mathrm{d}t, \tag{4.34}$$

where $\psi(t)$ is a continuous function called the mother function with $s = 1$ and $r = 0$. Daughter functions are originated from the mother function with $s \neq 1$ and $r \neq 0$, i.e., functions built from scaled and shifted version of the mother function. There are many types of mother functions available in the literature, which include beta, hat mexican wavelet, and Gaussian continuous wavelet functions. However, the most used wavelet function in spectrum sensing is the Gaussian wavelet function that shows recurrent regularity which can be written as

$$\psi(t) = \frac{\mathrm{d}^n \exp\left(\dfrac{-t^2}{2}\right)}{\mathrm{d}t^n}. \tag{4.35}$$

Figure 4.9 depicts the continuous Gaussian wavelet functions of order $n = 1$–6. It is to be noted that there is a preference for nonorthogonal smoothing function, e.g., Gaussian wavelet function in SS, because orthogonal wavelet families can degrade the performance in detecting the limit of subband occupancy, i.e., orthogonal wavelet function can smooth the edges. Being capaable of determining the boundaries of occupied subbands, CWT allows singularities detection in the wideband spectrum in wavelet sensing. Wavelet sensing is also called edge detection and while analyzing the power spectrum density (PSD), the SUs are able to determine which subchannel is vacant for access. In this technique, the sensing PSD should be smooth in order to obtain reliable ROC.

PSD is smooth and almost flat within each subband B_m, but exhibits discontinuities from its neighboring bands B_{m-1} and B_{m+1}. Hence, irregularities in PSD appear only at the edges of the those subbands. PSD of the mth received signal can be written as

$$S_{y_m}(f) = \sum_{m=1}^{M} \alpha_m^2 S_{x_m}(f) + S_{n_m}(f), \tag{4.36}$$

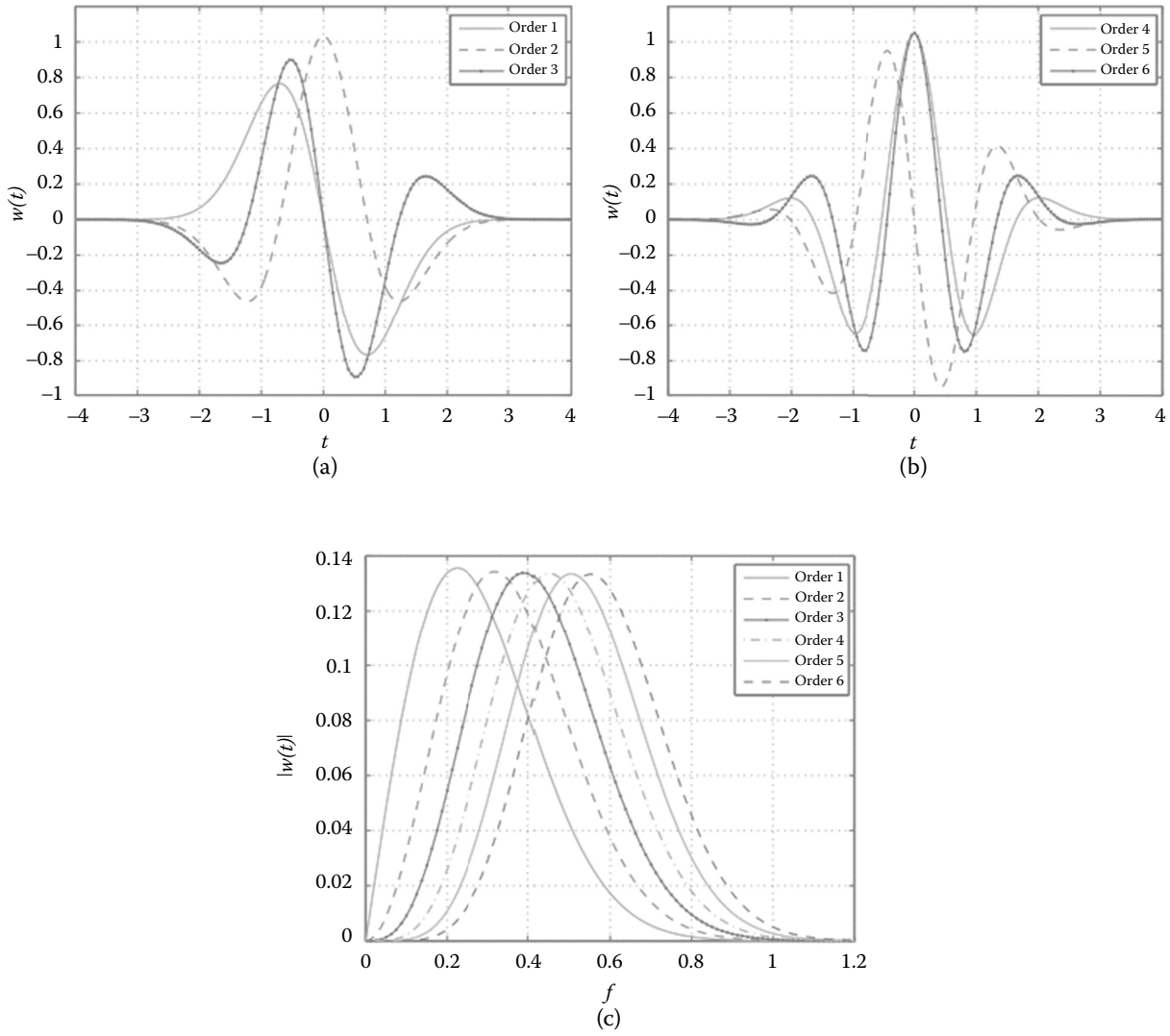

FIGURE 4.9
Continuous Gaussian wavelet functions of order $n = 1,2$, and 3 (a) and 4, 5, and 6 (b) in the frequency domain. (c) Frequency representation.

where α_m^2 indicates the signal power density within the mth band; furthermore, in the absence of noise, $S_{\mathbf{x}_m}(f)$ represents the normalized (unknown) power spectral shape within each band B_m, satisfying three conditions:

$$S_{x_m}(f) = 0, \quad \forall f \neq B_m \qquad \text{(a)}$$

$$w_{y_m} = \int_{f_m - 1}^{f_m} S_{x_m}(f)\,df = f_m - f_{m_1} \qquad \text{(b)} \qquad (4.37)$$

$$S_{x_m}(f) = \begin{cases} 1, & \forall f \in B_m \\ 0, & \text{otherwise} \end{cases} \qquad \text{(c)}$$

Condition (c) holds true since PSD within each subband B_m is smooth and almost flat; PSD of the mth PU signal defined by $\alpha_m^2 S_{x_m}(f)$ and $S_{\boldsymbol{n}_m}(f)$ is the noise PSD that can be described as AWGN noise, i.e., $S_{\boldsymbol{x}_m}(f) = N_0/2$.

CWT of the PSD of received signal is given as

$$W_s(f) = S_{y_m}(f) * \Psi_s(f), \tag{4.38}$$

where $\Psi_s(f) = \frac{1}{s}\Psi\left(\frac{f}{s}\right)$ is the wavelet smoothening function with $\Psi(f)$ being the Fourier transform of $\psi(t)$, the * is the convolution operator and $s = 2^j$ for $j = 1, 2, \ldots, J$ is the scale factor. Equation 4.38 is able to take a frequency interval and enlarge the details in the analysis of a specific subband. As a consequence, to obtain the subband edges, derivatives of $W_s(f)$ can be deployed in order to allow a better identification of edges in the PSD signal.

4.4.2.1 Wavelet Modulus Maxima Method

In the wavelet modulus maxima (WMM) method, the edges of the subchannels f_n can be determined by first and second derivatives of wavelet signal $W_s(f)$. Setting as local variation point of $S_{y_m}(f)$ smoothed by $\Psi_s(f)$, the local maxima (LM) is obtained via the first derivative of wavelet $W_s(f)$ as follows

$$f_n = \max_f \left| W_s'(f) \right|, \tag{4.39}$$

where f_n is the nth edge frequency. Another criterion based on derivative is the zero crossing (ZC) rule. It is obtained from the second derivative of wavelet $W_s(f)$

$$f_n = \left\{ f \mid \left| W_s''(f) \right| = 0 \right\}, \tag{4.40}$$

where $W_s'(f)$ and $W_s''(f)$ are the first and second derivatives of the wavelet smoothing function with scale factor s, given respectively by

$$W'_{s=2^j}(f) = s\frac{\mathrm{d}}{\mathrm{d}f}\left(S_{y_m} * \Psi_s\right)(f) = S_{y_m} * \left(s\frac{\mathrm{d}\Psi_s}{\mathrm{d}f}\right)(f), \tag{4.41}$$

$$W''_{s=2^j}(f) = s^2\frac{\mathrm{d}^2}{\mathrm{d}^2 f}\left(S_{y_m} * \Psi_s\right)(f) = S_{y_m} * \left(s^2\frac{\mathrm{d}^2\Psi_s}{\mathrm{d}^2 f}\right)(f). \tag{4.42}$$

The LM- and ZC-based WMM methods have the same objective, to determine the edges, i.e., allow to identify the occupancy of mth subchannel B_m associated to the edge frequencies f_m and f_{m-1}.

4.4.2.2 Wavelet Multiscale Product Method

Wavelet multiscale product (WMP) method uses the first PSD wavelet derivative. It is simply the product of J first order derivatives of the frequency-scaled wavelet

$$\mathcal{U}_j^p = \prod_{j=1}^{J} W'_{s=2^j}(f), \tag{4.43}$$

where the derivative of the smoothed PSD of the received signal is given in Equation 4.41.

The desired local maxima of wavelet modulus are tracked by their propagation to multiple coarse scale $s = 2^j$ for $j = 1, 2, \ldots, J$ with the goal of decreasing the noise effect in the spectrum sensing, where false edges caused by noise are very common in the WMM method.

The WMP approach is intended to enhance multiscale peaks due to edges or singularities, while suppressing noise. Boundaries of consecutive frequencies bands $\{f_m\}$ can be acquired from $\mathbf{y}_m$ picking the LM of the multiscale product, which can be written as

$$f_m = \max_f \left| \mathcal{U}_j^p \right|, \; f \in \left[f_0 ; f_M \right]. \tag{4.44}$$

4.4.2.3 Wavelet Multiscale Sum Method

In the wavelet multiscale sum (WMS) method again the first derivative of the PSD wavelet is deployed. The difference is that the product is replaced by the sum of the PSD wavelet derivative

$$\mathcal{U}_j^s = \sum_{j=1}^{J} W'_{s=2^j}(f). \tag{4.45}$$

The problem in applying the WMP method to narrowband spectral sensing is a subband signal appears with slow variation on the PSD signal. This slow variation could result in edge detection fault, because they are attenuated when the multiplication method of Equation 4.43 is used. This problem can be solved using the WMS method that replaces the product by the sum.

4.4.3 Compressive Sensing

The compressive sensing (CS) method uses the concept of compressive sampling (CS) [3,28]. The CS method allows reducing the sampling rate below the Nyquist rate when the signal is sparse in a certain domain. A signal is sparse when it has low PSD, i.e., when the signal produces a white space. Therefore, a wideband spectrum is underutilized when the wideband is sparse in the frequency domain. This fact can be exploited in the MB-CRNs SS context.

Suppose a hypothetical model [29] $Q \leq M$, where Q is a subset of the M subbands of a wideband system. The received signal of a SU can be given by

$$y(t) = \sum_{q=1}^{Q} a_q x_q(t) \exp\left(j2\pi f_q t\right) + n(t), \tag{4.46}$$

where t is the time index, a_q is the amplitude of the qth primary signal, x_q is the baseband representation, f_q is the carrier frequency of the qth primary signal and also is the center frequency of one of the occupied subbands, and $n(t)$ is the AWG noise. If the sampling rate is defined as f_y, suppose this frequency is much higher than the date rate of each source, i.e., the Nyquist rate is obeyed. Then, the data sample in the SU can be defined as

$$y\left(\frac{n}{f_y}\right) = \sum_{q=1}^{Q} a_q x_q\left(\frac{n}{f_y}\right) \exp\left(j2\pi f_q \frac{n}{f_y}\right) + n\left(\frac{n}{f_y}\right), \tag{4.47}$$

where $n = 1, 2, \ldots, N$ and N is the number of samples.

Following the previous description the discrete-time signal received vector $\mathbf{y}_m$ with dimension $N \times 1$ can be written in a matrix form as

$$\mathbf{y}_m = \mathbf{B}_{am} + \mathbf{n}_m, \tag{4.48}$$

where $\mathbf{B}$ is a matrix defined as

$$\mathbf{B} = \left[\mathbf{b}_1, \mathbf{b}_2, \ldots, \mathbf{b}_Q\right],$$

with each vector given by

$$b_q = \left[x_q\left(\frac{1}{f_y}\right)\exp\left(\frac{j2\pi f_q}{f_y}\right), \ldots, x_q\left(\frac{N}{f_y}\right)\exp\left(\frac{j2\pi f_q N}{f_y}\right)\right]^T, \tag{4.49}$$

where $q = 1, \ldots, Q$, $\mathbf{a}_m = \left[a_{1_m}, \ldots, a_{Q_m}\right]$ and $\mathbf{n}_m = \left[n_{1_m}\left(\frac{1}{f_y}\right), \ldots, n_{Q_m}\left(\frac{1}{f_y}\right)\right]^T$.

For a sparse representation of the previous signal, a basis must be considered that represents the signal. Therefore, considering Π is the sparsity basis matrix that must be written in terms of all possible channel occupancy states [29]. Let $\left[\hat{f}_1, \ldots, \hat{f}_M\right]$ be a sampling set of the frequencies of M subbands that matches the frequency components of the received signal [29]. The received signal can be represented in a sparse form as follows

$$\mathbf{y}_m = \prod \mathbf{s}_m + \mathbf{n}_m. \tag{4.50}$$

The sparsity basis matrix can be constructed as $\prod = \left[\mathbf{b}\left(\hat{f}_1\right), \mathbf{b}\left(\hat{f}_2\right), \ldots, \mathbf{b}\left(\hat{f}_M\right)\right]$ where

$$\mathbf{b}\left(\hat{f}_i\right) = \left[x_q\left(\frac{1}{f_y}\right)\exp\left(\frac{j2\pi\hat{f}_i}{f_y}\right), \ldots, x_q\left(\frac{N}{f_y}\right)\exp\left(\frac{j2\pi\hat{f}_i N}{f_y}\right)\right]^T. \tag{4.51}$$

Making the following change of variables $\mathbf{z}_m = \mathbf{Y}\mathbf{y}_m = \mathbf{Y}\prod \mathbf{s}_m + \mathbf{Y}\mathbf{n}_m$ where $\mathbf{z}_m$ is the measurement vector with dimension $L \times 1$ and Υ is a measurement matrix with dimension $L \times N$ that can be choosen by considering that the correlation between Υ and Π must be low, a good choice for Υ is a totally random matrix [29]. Then $\mathbf{z}_m$ is called L-sparse if $L << N$ and $\mathbf{y}_m$ is compressible.

CS problem can be defined as a stable matrix Υ, where the signal $\mathbf{y}_m$ is transformed into $\mathbf{z}_m$ without losing signal information that characterizes the transformation of sparse domain $R^{N\times 1}$ into compressed domain $R^{L\times 1}$.

The reconstruction of the sparse signal can be described as an optimization problem. The analysis of the sparsity measure can be done by the p-norm, where $p \in [0,2]$ [29]. The optimal sparsity measure is done by a pseudonorm, called 0-norm, defined as [30]

$$\begin{aligned} &\underset{\mathbf{z}_m}{\text{minimize}} && \left\|\mathbf{z}_m\right\|_0 \\ &\text{s.t.} && \mathbf{z}_m = \mathbf{Y}\mathbf{y}_m = \mathbf{Y}\prod \mathbf{s}_m + \mathbf{Y}\mathbf{n}_m \end{aligned} \tag{4.52}$$

where the 0-norm is defined for a vector $\boldsymbol{x}$ as [30]

$$\|x\|_0 = n(i \mid x_i \neq 0)\,, \tag{4.53}$$

where n is the number or quantity and 0-norm is number of nonzero elements in a vector.

The 0-norm sparsity performance is a challenge, because the optimization problem is not convex and makes it a nondeterministic polynomial time hard problem (NP-hard problem). An alternative approach is to formulate the optimization problem as 1-norm, called *basis pursuit* (BP) [31]. Hence, the linear convex problem is written as [30]

$$\begin{aligned} &\underset{\mathbf{z}_m}{\text{minimize}} \ \|\mathbf{z}_m\|_1 \\ &\text{s.t.} \qquad \mathbf{z}_m = \mathbf{Y}\mathbf{y}_m = \mathbf{Y}\prod \mathbf{s}_m + \mathbf{Y}\mathbf{n}_m \end{aligned} \tag{4.54}$$

where $\|\mathbf{x}\|_1$ is the 1-norm of $\mathbf{z}_m$.

The signal reconstruction and sparsity measurement can also be defined and calculated by other criterion and algorithms in the literature, such as matching pursuit (MP), LASSO, and AIC [10].

4.4.4 Angle-Based Sensing

AS can exploit the available spectrum in a space dimension, similar to a MIMO system, by increasing the spatial diversity. The major feature in AS is that not all subchannels occupy the same physical space for PUs. For example, if an SU is aware of the azimuth angle* of the PUs, then when the PUs transmit in a certain direction, the SU can simultaneously transmits in another direction using the same band in the same geographical area without interference.

The AS problem is capable of determining the *direction of arrival* (DoA) or *angle of arrival* (AoA), wherein each PU is transmitting. The main techniques described in literature to realize the AS include the *MUltiple SIgnal Classification* (MUSIC), Bartlett, Root MUSIC, Capon, and *estimation of signal parameters via rotational invariance technique* (ESPRIT) [32,33]. In this chapter, we only describe the MUSIC technique [34], which is one of the most important techniques to determine array angle and direction. MUSIC is a technique based on eigen space methods used for the signal and noise separation in different subspaces during signal processing which simplifies the signal analysis.

The system considered herein represents the array distribution with their directions, according to the Figure 4.10, modeled as [34,35]

$$\mathbf{y}_m = \mathbf{A}(\theta)\mathbf{x}_m + \mathbf{n}_m\,, \tag{4.55}$$

where $\mathbf{y}_m$ is the received signal at the mth subband B_m; the transmitted signal $\mathbf{x}_m$ by the array configuration with dimension $N \times 1$, and $\mathbf{n}_m$ is AWGN vector with dimension $N \times 1$, with statistical distribution $\mathbf{n}_m \sim N(0, \sigma^2\mathbf{I})$. In this model, the sources (PUs) are considered

* Azimuth angle is the angular measurement formed between a reference and a line from the observer until a point of interest is reached in the same horizontal plane.

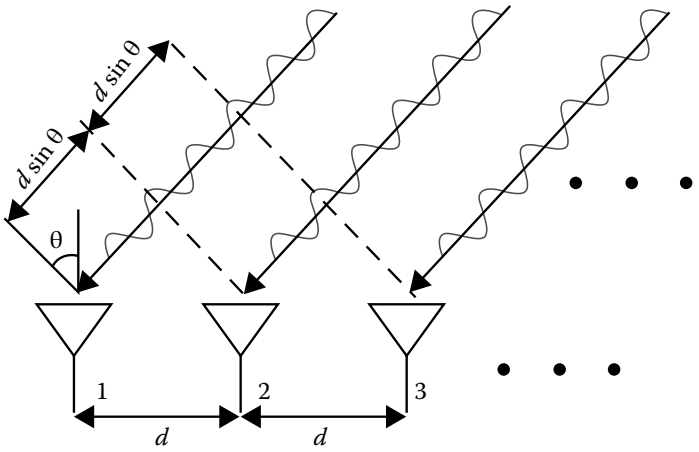

FIGURE 4.10
Schematic representation for the DoA analysis.

independent and the noise is uncorrelated. The $N \times D$ matrix $\mathbf{A}(\Theta)$ is called the steering matrix corresponding to the angles of distribution of arrays, and defined as [34]

$$\mathrm{A}(\theta) = \left[\mathbf{a}(\theta_1), \mathbf{a}(\theta_2), \ldots, \mathbf{a}(\theta_D)\right], \tag{4.56}$$

where $\mathbf{a}(\theta_i)$ is the steering vector with dimension $N \times 1$ defined as the angle, and the direction of PUs transmission are as follows

$$\mathbf{a}(\theta_i) = \left[1, \exp\left(\frac{-j\omega d \sin\theta_i}{c}\right), \ldots, \exp\left(\frac{-j\omega(N-1) d \sin\theta_i}{c}\right)\right], \tag{4.57}$$

where d is the distance between antennas and c is the speed of light.

Under this model, the correlation matrix of the received signal with dimension $D \times D$ is readily obtained as follows

$$\begin{aligned} \mathbf{R}_{\mathbf{y}_m} &= \mathbb{E}\left[\mathbf{y}_m \mathbf{y}_m^H\right] \\ &= \mathbb{E}\left[\mathbf{A}(\theta)\mathbf{x}_m \mathbf{x}_m^H \mathbf{A}(\theta)^H\right] \; + \; \mathbb{E}\left[\mathbf{n}_m \mathbf{n}_m^H\right] \\ &= \mathbf{A}(\theta) \cdot \mathbf{A}(\theta)^H + \sigma^2 \mathbf{I}_D \\ &= \mathbf{R}_{\mathbf{x}_m} + \sigma^2 \mathbf{I}_D, \end{aligned} \tag{4.58}$$

where $\mathbf{R}_{\mathbf{x}_m}$ is the correlation of the transmitted signal and $\mathbf{X} = \mathbb{E}\left[\mathbf{x}_m \mathbf{x}_m^H\right] = \mathrm{diag}\left(\sigma_1^2, \ldots, \sigma_N^2\right)$.

4.4.4.1 MUSIC Algorithm

MUSIC algorithm [34] estimates the angle or direction content of a signal autocorrelation matrix using an eigenspace method. In this method, the detector needs to know the array spatial distribution.

The correlation matrix $\mathbf{R}_{\mathbf{x}_m}$ can be related to its ith eigenvector $\mathbf{q}_m$ associated with its ith eigenvalue

$$\mathbf{R}_{\mathbf{x}_m} q_m = \mathrm{A}(\theta) \cdot \mathrm{A}(\theta)^H \mathrm{q}_m = 0\,. \tag{4.59}$$

Hence,

$$\mathbf{q}_m^H \mathbf{A}(\theta) \cdot \mathbf{A}(\theta)^H \mathbf{q}_m = 0\,. \tag{4.60}$$

Finally, from Equation 4.60 and assuming that $\mathbf{A}(\theta)$ is positive definite, it follows that the steering matrix is orthogonal to the eigenvector of $\mathbf{R}_{\mathbf{x}_m}$

$$\mathbf{A}(\theta)^H \mathbf{q}_m = 0\,. \tag{4.61}$$

Equation 4.61 implies that all N–M eigenvectors $\mathbf{q}_m$ of the matrix $\mathbf{R}_{\mathbf{x}_m}$ corresponding to the zero eigenvalues are orthogonal to all M signal steering vectors. This is the principle of the MUSIC technique which allows to separate the signal from the noise.

Now, let us consider $\mathbf{U}_N$, a $N \times (N–M)$ subspace of the noise eigenvectors. Then, the MUSIC *pseudospectrum* can be defined as [34]

$$P^{\text{MUSIC}} = \frac{1}{\mathbf{a}^H(\theta)\mathbf{U}_N\mathbf{U}_N^H\mathbf{a}(\theta)}\,. \tag{4.62}$$

In the CRN context, the important information of angle and direction is obtained by applying the following operation [36]

$$\theta^{\text{MUSIC}} = \arg\min_\theta \mathbf{a}^H(\theta)\mathbf{U}_N\mathbf{U}_N^H\mathbf{a}(\theta)\,. \tag{4.63}$$

As a consequence, the following statistic test can be applied

$$T^{\text{MUSIC}}(y) = \frac{1}{180^\circ}\sum_{\theta=-90^\circ}^{90^\circ} P^{\text{MUSIC}}, \tag{4.64}$$

where P^{MUSIC} is the spatial spectrum, also called pseudospectrum at time t.

4.4.5 Comparison of MB-SS Methods

The main characteristics of the MB-SS methods are summarized in Table 4.4. The MB-SS remains challenging in CR implementations; hence, further promissing MB techniques should be evolved in the future to improve this branch.

Wavelet sensing is deployed when the SUs do not know the frequency limits of the subbands. Wavelet is a technique which is common in image processing and is used to determine the image edges. Similarly, in the SS context, the wavelet sensing has the same properties, i.e., this technique is able to determine the edges of the occupied portion of spectrum. However, the wavelet-based detector is affected by the noise and can produce false-edges detection, which disrupts the SUs opportunities and can generate an interference in PUs.

TABLE 4.4

Performance Comparision—MB Sensing

MB–SS Detector	Advantages	Disadvantages
Wavelet	Unknown MB limits	False edges
Compressed	Low sampling rate	Known $\prod$ and Υ
Angle	New dimension to explore	MIMO system

Compressed sensing can be used when the signal is sparse, i.e., in the case of a major part of the spectrum in communication systems. This technique is able to reconstruct the signal using a subsample information. This fact makes the processing less complex and helps increase the EF. The main challenge in this technique is that the SUs must know the sparsity basis **matrix** Π and measurement matrix Υ.

In AS technique, a new dimension is explored, providing new forms of diversity to the system, such as angle and space diversities. However, in this case, multiple antennas must be used to detect the directions and angles of the PU's transmission, increasing the complexity of the applications.

4.5 Cooperative CRNs

Cooperative CRNs work in two ways: relays networks and CSS. CSS schemes provide spatial diversity, increased coverage, ubiquitous connectivity, and network throughput.

Cooperative CRNs can provide diversity in environment subject to fading, shadowing, and path-loss channel effects, which can degrade the SS performance substantially.

SU cooperative sensing has two methods for SS: *hard* and *soft* combining. There are some rules that allow to choose the best threshold for each application and channel scenario, called *or-and-majority* rules.

Furthermore, considering the context of the relay cooperative sensing, there are two main and widely deployed protocols: AF and DF.

The binary decision of cooperative SS can be formulated as same as SB SS. The next section desribes the principle of CSS with the main rules to construct the threshold λ.

4.5.1 Cooperative Spectrum Sensing

Detection of transmissions from licensed (or primary) users is challenging in CRN environment due to a few uncertainties, such as (a) channel uncertainty, i.e., dynamic variations in the channel fading and shadowing conditions; (b) aggregated-interference uncertainty, when there are too many unlicensed users in the same CRN, who interfere with each other; (c) and finally, the noise uncertainty which can affect the detection sensibility and ROC performance.

Aiming to mitigate the uncertainties in SS, a CSS approach can be deployed in CRN context. CSS offers diversity gain, which can remarkably improve the detection probability performance of an unlicensed (secondary) user. Multiple unlicensed users cooperatively sense the target spectrum and share the SS results with each other. Figure 4.11 depicts a general topology of CRN with CSS. Indeed, each SU is responsible to sense a small portion of the spectrum and sends the results to the fusion center (FC), which constructs and broadcasts an updated map of availability of spectrum rules to all CRN nodes [37].

One advantage of CSS is that unlicensed user SU_1 may not be able to detect transmission from licensed user PU_1 due to channel fading. If SU_1 (source node) starts transmission, it will interfere with data reception at the licensed user, say PU_1. However, if unlicensed user SU_1 senses the spectrum and reports the presence of licensed user PU_1 to the FC, SU_2 can be notified by the FC and will defer its transmission to avoid any interference to the licensed user PU_2.

Alternatively, the cooperative cognitive networks can deploy multiple relay users to forward the signal received from a PU to an SU aiming to improve the performance of SS

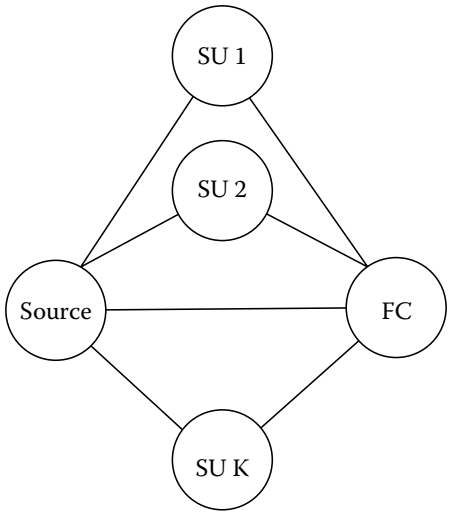

FIGURE 4.11
Cooperative CR scheme with K secondary users, one source node, and a fusion center.

while taking advantage of the spatial diversity [38]. In this mode, CSS is used to combat the noise and channel uncertainties, and therefore, the probability of misdetection and false alarm decreases substantially. Additionally, cooperative mode for SS reduces the sensing time while improving the accuracy. However, CSS implies higher complexity and energy consumption.

In CSS based on decision fusion, each cooperative partner makes a binary decision based on its local observation and then forwards one bit of the decision to the common receiver in FC. Let $d_k \in \{0,1\}$ denote the local SS result of the kth CR, including SUs and in some schemes relay nodes. Hence, $d_k = 0$ indicates that the CR infers the absence of the PU in the observed band. In contrast, $d_k = 1$ implies the PU operation in that band. At the common fusion receiver, all 1-bit decisions are fused together according to a specific logic rule [39].

FC uses different techniques for combining the SS results coming from different unlicensed SUs to make a decision in CSS. The simplest method is to use an OR operation among the received sensing results. Moreover, combining techniques based on maximal ratio combining (MRC) and equal gain combining (EGC) have been investigated in [40]. Following section briefly discusses the *hard combining*, *soft combining* and *or-and-majority* rules.

4.5.1.1 Hard Combining

In hard combining SS, K cooperative SUs are sensing the spectrum and the final decision is given for the following metric

$$T(y) = \sum_{k=1}^{K} d_k, \tag{4.65}$$

where the d_k is the decision of kth SU and $d_k \in \{0,1\}$, being $d_k = 0$ if PU is absent, or $d_k = 1$ if PU is present in the band.

4.5.1.2 Soft Combining

In soft combining SS, the metric is given as weight sum of the observations states for each SU's contribution. Hence, the most important contributions are associated to higher

weight, but the other less important contributions are also considered. The associated test statistic in the soft combining method is simply written as follows

$$T(y) = \sum_{k=1}^{K} c_k T_k(y), \tag{4.66}$$

where c_k is the weight coefficient and $T_k(\mathbf{y})$ is the test statistics of the kth SU. Taking $c_k = 1$ the soft combining becomes the classical EGC diversity combine. Besides, if c_k is proportional to SNR at the kth SU, the rule gets closer to the classical MRC.

4.5.1.3 Or-And-Majority Rules

The *or-and-majority* rules allow to describe different ways to construct the threshold λ in a CSS scheme; in summary

- *Or* rule: $\lambda = 1$. The rule *Or* ensures minimum interference to the PUs. The PU is considered present in a band, if only a single PU sends 1 to FC in its decision, i.e., if test statistic of an SU adds one. It can be seen that the Or rule is very conservative for CRs to access the licensed band. As such, the chance of causing interference to the PU is minimized.
- *And* rule: $\lambda = K + 1$, where K is the number of collaborative nodes sensing the same subband. It is much less conservative, ensuring a high rate of transmission to the SUs. The PU is considered present in the band, if all CRs sense the presence of a PU in the band.
- *Majority* rule: $\lambda = \left(\frac{K+1}{2}\right)$. The PU is considered present in the band, if the majority of SUs send 1 to the decision center.

4.5.2 Relay CSS

In this kind of CSS, one or more relay(s) help to realize the SS. There are many relay protocols in the communication systems, but the most important are AF and DF protocols. In the following sections, the AF and DF protocols are introduced.

4.5.2.1 AF Relaying Protocol

In the AF protocol, the relay scales the received version of the signal and retransmits it to a second time-slot, an amplified version of it, to the destination node. In the first time-slot, the signal transmitted from the source is received at both the relay and the destination, which respectively are [6,41]

$$y_{s,r} = \sqrt{P} h_{s,r} x + n_{s,r}, \tag{4.67}$$

$$y_{s,d} = \sqrt{P} h_{s,d} x + n_{s,d}, \tag{4.68}$$

where P is the RF transmit power deployed by the source node in the first time-slot; x is the transmitted signal; $h_{\mathrm{r}}^{\mathrm{s}}$ and $h_{\mathrm{d}}^{\mathrm{s}}$ are the channel fading coefficients between the source–relay and source–destination paths, respectively.

In the AF protocol, the relay node does the simple scaling on the received signal by a factor inversely proportional to the received power given as

$$\beta = \frac{\sqrt{P}}{\sqrt{P\left|h_{\mathrm{s,r}}\right|^2 + N_0}}. \tag{4.69}$$

As a consequence, the signal transmitted by the relay node to the destination node in the second time-slot is scaled by $\beta \cdot y_r^s$.

SNR at the destination node is the sum of SNRs from the source node and relay node, as a result of the macro-diversity gain offered by cooperative source–relay–destination scheme. SNR from the source node is given as follows

$$\gamma_{\mathrm{s,d}} = \frac{P}{N_0}\left|h_{\mathrm{s,r}}\right|^2. \tag{4.70}$$

4.5.2.2 DF Relaying Protocol

In DF relaying, the receiver signal is detected at relay node, re-encoded, and then retransmitted to the receiver node. The DF relaying scheme has an advantage over the AF relaying scheme in reducing the effects of additive noise at the relay node, but in a low SNR regime the decision errors of relay node propagates to the destination. On the other hand, if the relay is able to decode the transmitted symbol correctly, i.e., when relay node operates in medium and high SNR regimes, the relay retransmits the decoded symbol with power P to the destination node; otherwise the relay does not cooperate in the retransmission. This can be written as follows

$$y_{\mathrm{r,d}} = \sqrt{P} h_{\mathrm{r,d}} \hat{x} + n_{\mathrm{r,d}}, \tag{4.71}$$

where $\hat{x}$ is the decoded signal x at the relay node.

4.5.3 Comparison among Cooperative SS Methods

A comparison of the principal CSS methods are summarized in Table 4.5. The hard combining method is based on the fact that the SUs perform the SS and each SU has a decision, which is shared among the other SUs. This method has a simple decision, i.e., the sum of the decision of each individual SU. The disadvantage of this technique is if the SU misses the detection, the error is propagated to the decision fusion, affecting other decisions.

The soft combining method has advantages over other methods, but does not disregard others as less reliable. This makes the final decision less wrong, but this depends on the hits of some SUs.

In the AF relaying protocol, the signal receives a gain before retransmission to the destination node. The disadvantage of this protocol is that the noise is amplified jointly to the signal and is received by the destination node.

In the DF relaying protocol, the signal is re-encoded in the relay node, which makes the signal free of noise amplified. The biggest problem is if the relay decodes wrong or the

TABLE 4.5

Method Comparison—Cooperative Sensing

CSS method	Advantages	Disadvantages
Hard combining	Simple decision of each user	Subject to error propagation
Soft combining	Weights the best performance	More complexity
AF relaying	Simple propagation with a gain	Propagates noise with a gain
DF relaying	Reduce noise propagation	If decoding fails, it does not work (low SNR)

signal contains errors, then the relay does not retransmit the signal and the destination node only depends on the direct link or direct node.

4.6 Conclusions and Perspectives

Concerning SB-SS, this chapter explored five basic techniques capaable of analyzing spectrum usage in a specific BW, namely ED, MF, CS feature detector, covariance detector, and eigenvalue detector. In terms of complexity, ED offers SS at low computational cost. However, ED also presents low performance, especially under very low *SNR*, along with requiring precise *SNR* knowledge, which is not always available, to perform proper SS. On the other hand, MF performs optimal spectrum, but also requires a detailed description of the PU signal characteristics, which, in some cases, can be an unreasonable requirement. Despite presenting a reasonable spectral sensing performance, the CS method may require embedding more features of the signal in order to improve cyclostationarity on the PU signal, e.g., a header signal or a periodic pulse. In this sense, PU signal should experience a reduction in SE in order to ease SS for PUs, which may not bring benefits to PUs if they do not take advantage on SUs. Finally, covariance and eigenvalue detections are based on measuring temporal correlation of the PU signal, being capable of robust SS, which is bounded to the number of lags considered for correlation calculus.

MB-SS expands the SS from an SB model to an MB model. Basically, this chapter deals with three MB methods: wavelet sensing, compressed sensing, and AS. There are other methods to sense the spectrum in a MB model, but the three methods discussed here are the most promising. Wavelet SS is used when the limits of the subbands are unknown. So, wavelet technique is able to determine these limits. There are three kinds of wavelet methods to determine the limits of subbands: WMM, WMP, and WMS. The first is the most simple method and determines the limits using an LM through first derivative or zero crossing that uses the second derivative of the wavelet PSD. The second derivative is an improvement of the first and uses the idea of the product of the first derivative of the wavelet increasing the scale and is able to reduce the false edges in the SS, which is a very common problem in WMM. Third method is a variation of the second method and is simply the change of the product by the sum. This change reduces the edge fault, due to slow variation of PSD in narrowband systems.

Compressed sensing is another way to deal with SS in the MB systems. This method uses the concept of sparsity of signal combined to a norm optimization problem that is capable of measuring the sparsity of a channel. The optimal measure depends on a 0-norm, which

in essence results in a nonconvex optimization problem; so, it cannot be solved in a polynomial time. Based on that, other optimization metrics have been proposed, such as basis pursuit, match pursuit, and AIC.

The last SS method for MB-CRNs is angle sensing that provides another dimension to the MB-SS challenge. This method uses an algorithm to sense the DoA of a signal or a set of signals. A classical algorithm to deal with is MUSIC algorithm based on the signal separation from the noise subspace.

Another class of CRN is the cooperative CRNs. There are two ways in which the SUs can cooperate in a CRN. The first one is when one SU shares its sensing decision with another SUs through FC, or act as a relay helping the PU's transmission. In the first class, two options are avaliable to combine the information: hard and soft combining. First, the final decision is only the sum of all SU's decisions. The second one deploys weights that can act according to the importance of the decision. Another important rule is the *or-and-majority* rules that allow determining the threshold in a cooperative SS using different consensus rules. In the second class of CSS, two basic relay protocols arise: AF protocol and DF protocol. In the first class, the signal received by the destination node is only the signal of the source node with a gain. The problem with this method is that the noise is amplified along with the information. The second method decodes the signal coming from the source node and retransmits this signal to the destination without amplifying the noise. The problem with this method is if the signal contains decision error, basically due to SNR regime, the relay is unable to retransmit to the destination node.

CRNs is one of the techniques that will enable the future 5G communications. Due to scarcity of spectrum and high rates of 5G communications protocols, CRN is a candidate to operate under high spectral efficiency mode. The spectral sensing techniques addressed in this chapter can contribute to improving the performance, robustness, and efficiency of CRNs, till another promising technique appears to construct a solid knowledge area in the future.

References

1. Mitola, J., and Maguire, G. Q. (1999). Cognitive radio: Making software radios more personal. *Personal Communications, IEEE* 6 (4): 13–18.
2. Sharma, M., and Gupta, R. (2014). Comparative analysis of various communication systems for intelligent sensing of spectrum. In *2014 International Conference on Advances in Computing, Communications and Informatics (ICACCI)*, New Delhi, India, pp. 902–908.
3. Ibnkahla, M. (2014). *Cooperative Cognitive Radio Networks: The Complete Spectrum Cycle*. Boca Raton, FL: CRC Press.
4. Zhang, Y., Zheng, J., and Chen, H.-H. (2010). *Cognitive Radio Networks: Architectures, Protocols, and Standards*. Boca Raton, FL: CRC Press.
5. Maheshwari, P., and Singh, A. (2014). A survey on spectrum handoff techniques in cognitive radio networks. In *2014 International Conference on Contemporary Computing and Informatics (IC3I)*, Mysore, India, pp. 996–1001.
6. Dohler, M., and Li, Y. (2010). *Cooperative Communications: Hardware, Channel & PHY*. Chichester, West Sussex, U.K.; Hoboken, NJ: Wiley.
7. Parekh, P., and Shah, M. (2014). Spectrum sensing in wideband OFDM based cognitive radio. In *2014 International Conference on Communications and Signal Processing (ICCSP)*, Melmaruvathur, India, pp. 1476–1481.

8. Wang, N., Gao, Y., and Cuthbert, L. (2014). Spectrum sensing using adaptive threshold based energy detection for OFDM signals. In *2014 IEEE International Conference on Communication Systems (ICCS)*, Macau, pp. 359–363
9. Lunden, J., Koivunen, V., and Poor, H. (2015). Spectrum exploration and exploitation for cognitive radio: Recent advances. *IEEE Signal Processing Magazine* 32 (3): 123–140
10. Hattab, G., and Ibnkahla, M. (2014). Multiband spectrum access: Great promises for future cognitive radio networks. *Proceedings of the IEEE* 102 (3): 282–306.
11. Di Benedetto, M.-G., Cattoni, A. F., Fiorina, J., Bader, and Nardis, L. D. (2015). *Cognitive Radio and Networking for Heterogeneous Wireless Networks: Recent Advances and Visions for the Future* (1st edn). Volume 1 of Signals and Communication Technology. Switzerland: Springer International Publishing.
12. Feng, C. (2012). Cognitive learning-based spectrum handoff for cognitive radio network. *International Journal of Computer and Communication Engineering* 1 (4): 350–353
13. Kay, S. (1998). *Fundamentals of Statistical Signal Processing: Detection Theory*. Englewood Cliffs, NJ: Prentice-Hall PTR, p. 672.
14. Roberts, R., Brown, W., and Loomis, H. (1991). Computationally efficient algorithms forcyclic spectral analysis. *IEEE Signal Processing Magazine* 8 (2): 38–49.
15. Bhargavi, D., and Murthy, C. (2010). Performance comparison of energy, matched-filter and cyclostationarity-based spectrum sensing. In *2010 IEEE Eleventh International Workshop on Signal Processing Advances in Wireless Communications (SPAWC)*, Marrakech, pp. 1–5.
16. Gradshteyn, I. S., and Ryzhik, I. M. (2007). *Table of Integrals, Series, and Products*. Elsevier/ Academic Press, Amsterdam, seventh edition. Translated from the Russian. Translation edited and with a preface by Alan Jeffrey and Daniel Zwillinger, with one CD-ROM (Windows, Macintosh and UNIX).
17. Zeng, Y., and Liang, Y.-C. (2009b). Spectrum-sensing algorithms for cognitive radio based on statistical covariances. *IEEE Transactions on Vehicular Technology*, 58 (4): 1804–1815.
18. Zeng, Y., and Liang, Y.-C. (2009a). Eigenvalue-based spectrum sensing algorithms for cognitive radio. *IEEE Transactions on Communications*, 57 (6): 1784–1793.
19. Tracy, C. A., and Widom, H. (1996). On orthogonal and symplectic matrix ensembles. *Communications in Mathematical Physics* 177: 727–754.
20. Tracy, C. A., and Widom, H. (2000). The distribution of the largest eigenvalue in the Gaussian ensembles: β. In *Calogero-Moser-Sutherland Models* (Montreal, QC, 1997), CRM Ser. Math. Phys. New York: Springer, pp. 461–472.
21. Tian, Z., and Giannakis, G. (2006). A wavelet approach to wideband spectrum sensing for cognitive radios. In *2006 1st International Conference on Cognitive Radio Oriented Wireless Networks and Communications*. Mykonos Island, pp. 1–5.
22. Devi, T., and Sagar, S. (2014). Discrete wavelet packet transform based cooperative spectrum sensing for cognitive radios. In *2014 First International Conference on Computational Systems and Communications (ICCSC)*, Trivandrum, pp. 226–231.
23. El-Khamy, S., Abdel-Malek, M., and Kamel, S. (2014). An improved reconstruction technique for wavelet-based compressive spectrum sensing using genetic algorithm. In *2014 31st National Radio Science Conference (NRSC)*, Cairo, pp. 99–106.
24. Jadhav, A., and Bhattacharya, S. (2014). A novel approach to wavelet transform-based edge detection in wideband spectrum sensing. In *2014 International Conference on Electronics and Communication Systems (ICECS)*, Coimbatore, India, pp. 1–5.
25. Jindal, S., Dass, D., and Gangopadhyay, R. (2014). Wavelet based spectrum sensing in a multipath Rayleigh fading channel. In *2014 Twentieth National Conference on Communications (NCC)*, Kanpur, India, pp. 1–6.
26. Zhao, Y., Wu, Y., Wang, J., Zhong, X., and Mei, L. (2014). Wavelet transform for spectrum sensing in cognitive radio networks. In *2014 International Conference on Audio, Language and Image Processing (ICALIP)*, Shanghai, pp. 565–556.
27. Daubechies, I. (1992). *Ten Lectures on Wavelets*. Philadelphia, PA: Society for Industrial and Applied Mathematics.

28. Hosseini, H., Syed-Yusof, S., Fisal, N., and Farzamnia, A. (2015). Compressed waveletpacket-based spectrum sensing with adaptive thresholding for cognitive radio. *Canadian Journal of Electrical and Computer Engineering* 38 (1): 31–36.
29. Liu, F. L., Guo, S. M., Zhou, Q. P., and Du, R. Y. (2012). An effective wideband spectrum sensing method based on sparse signal reconstruction for cognitive radio networks. *Progress in Electromagnetics Research C* 28: 99–111.
30. Hayashi, K., Nagahara, M., and Tanaka, T. (2013). A user's guide to compressed sensing for communications systems. *IEICE Transactions* 96-B (3): 685–712.
31. Chen, S., and Donoho, D. (1994). Basis pursuit. Technical report, Department of Statistics, University of California, Berkeley.
32. Dhope, T., and Simunic, D. (2012). On the performance of AoA estimation algorithms in cognitive radio networks. In *2012 International Conference on Communication, Information Computing Technology (ICCICT)*, Mumbai, India, pp. 1–5.
33. Dhope, T., and Simunic, D. (2013). On the performance of DoA estimation algorithms in cognitive radio networks: A new approach in spectrum sensing. In *2013 36th International Convention on Information Communication Technology Electronics Microelectronics (MIPRO)*, Opatija, pp. 507–512.
34. Schmidt, R. (1986). Multiple emitter location and signal parameter estimation. *IEEE Transactions on Antennas and Propagation* 34 (3): 276–280.
35. Roy, R., Paulraj, A., and Kailath, T. (1986). Direction-of-arrival estimation by subspace rotation methods—ESPRIT. In *IEEE International Conference on ICASSP '86 Acoustics, Speech, and Signal Processing* (Volume 11), ICASSP 86, Tokyo, pp. 2495–2498.
36. Liping, D., Feifei, L., and Yueyun, C. (2012). Time-angle spectrum sensing based on sliding window music algorithm. In *2012 Fourth International Conference on Multimedia Information Networking and Security (MINES)*, Nanjing, pp. 644–647.
37. Zhang, Y., Yang, W.-D., and Cai, Y.-M. (2007). Cooperative spectrum sensing technique. In *Proceedings of IEEE International Conference on Wireless Communications, Networking and Mobile Computing (WiCom)*, Shanghai, pp. 1167–1170.
38. Ganesan, G., Li, Y., Bing, B., and Li, S. (2008). Spatiotemporal sensing in cognitive radio networks. *IEEE Journal on Selected Areas in Communications* 26 (1): 5–12.
39. Letaief, K., and Zhang, W. (2009). Cooperative communications for cognitive radio networks. *Proceedings of the IEEE* 97 (5): 878–893.
40. Ma, J., and Li, Y. G. (2007). Soft combination and detection for cooperative spectrum sensing in cognitive radio networks. In *Proceedings of IEEE Global Telecommunications Conference (GLOBECOM)*, Washington, DC, pp. 3139–3143.
41. Hossain, E., Kim, D. I., and Bhargava, V. K. (2011). *Cooperative Cellular Wireless Networks*. New York, NY: Cambridge University Press.

A.2 Compromisso Tempo de Sensoriamento *versus* Vazão em Redes de Rádio Cognitivo

Título:	*Sensing-Throughput Tradeoff in Cognitive Radio Networks;*
Autores:	Aislan Gabriel Hernandes and Taufik Abrão;
Categoria:	*Symposium Paper*;
Publicação:	2016;
Congresso:	XXXIV Simpósio Brasileiro de Telecomunicações e Processamento de Sinais - SBrT'2016.

Resumo das Contribuições: A principal contribuição deste trabalho encontra-se na seção III, onde é mostrada a formulação do problema de tempo de sensoriamento *versus* vazão na eq.(9), a qual descreve a probabilidade de detecção considerando-se a probabilidade de ocupação do canal pelo PU. Também há contribuições na seção de resultados, onde é comparada a solução do problema de otimização com diversas probabilidades de ocupação do canal.

Sensing-Throughput Tradeoff in Cognitive Radio Network

Aislan Gabriel Hernandes and Taufik Abrão

***Abstract*— This paper deals with the relationship between the sensing time and throughput in a cognitive radio network (CRN) using energy detector (ED). The sensing time is a period in the medium access control (MAC) protocol that the secondary user (SU) spent to sensing the spectrum. This parameter is critical to determine the performance of the SU and the interference to primary user (PU). In cognitive radio (CR), increasing the sensing time is equivalent to increase the SU performance; accordingly, the throughput of the SU decrease, reducing the SU quality of service (QoS). Such configuration set a tradeoff between sensing time and throughput. In this contribution, the sensing-throughput optimization (STO) problem is formulated to deal with such tradeoff, where the throughput of the SU is maximized. The STO resulting in a convex nonlinear optimization problem (NLP) that can be solved using efficient solvers. Numerical analysis examines the performance of the ED when the throughput is maximized, as well when distinct parameters values are assumed.**

***Keywords*— Cognitive Radio Network, Secondary User, Primary User, Spectrum Sensing, Energy Detection, Throughput Maximization.**

I. INTRODUCTION

Due to the growth of the wireless communication services, the available spectrum has become scarce. Measurements carried out by Federal Communications Commission (FCC) have demonstrated that the most part of the allocated spectrum is not utilized [1]. The period of time of the spectrum occupancy varies from milliseconds to hours. This motivates the use of the cognitive radio (CR) [2], [3] which is able to increase the spectrum efficiency (SE) considerably. In a wireless regional area networks (WRANs), the main objective is to maximize the spectrum utilization of the TV channels. The CR is the main technology in the WRAN 802.22, where each medium access control (MAC) frame consists of one sensing slot and one data transmission slot. The sensing duration strongly impacts the network throughput. If sensing duration increases the throughput decreases. However, a longer sensing time improves the detection performance, i.e, the SU become more aware about the received signal while more protection is given to the PU.

Aislan G. Hernandes and T. Abrão. Department of Electrical Engineering, Londrina State University, Londrina-PR, Brazil, E-mails: aislangabrielhernandes@gmail.com, taufik@uel.br. Homepage: http://www.uel.br/pessoal/taufik/UEL/Welcome.html.

Recently, more and more importance has been given to the sensing time *vs.* throughput tradeoff in the context of CRN [4], [5]. The scheme to deal with this challenging issue consists in formulate and efficiently solve the associated optimization problem that maximize the throughput subject to different constraints, such as probability of detection, probability of false alarm, maximum frame time, optimum threshold, and so forth. For instance, in [6], [7], the sensing-throughput optimization problem in ED spectrum sensing was formulated as convex nonlinear optimization problems. Moreover, in [8], [9] the non-cooperative double threshold spectrum sensing was analysed in the sensing-throughput tradeoff perspective. In [10], the multichannel cooperative sensing optimization problem was formulated as a nonconvex mixed-integer problem that is solved dividing the original problem into convex mixed-integer subproblems.

In [11], a convex nonlinear optimization problem is formulated to deal with the STO tradeoff in a singleband cognitive radio network. In this sense, this contribution consists in a numerical analysis extension of the work in [11]. The STO problem was solved expeditiously using the solver available into the *Matlab Optimization Toolbox*. Simulation results demonstrate the quality of solution and the impact in the ED performance and some interesting results are discussed when the parameters of simulation are different to the initial problem considerations, revealing the ED performance dependence with such parameters.

The rest of the paper is organized as follow. The CR system model is summarized in section II. The formulation of the sensing time *vs.* throughput optimization problem is developed in section III. Numerical results supporting our finding are discussed in section IV. Finally concluding remarks are offered in section V.

II. System Model

The transmitted PU signal samples is represented by $s(i)$ while a circular symmetric complex Gaussian (CSCG) noise samples are represented by $n(i)$. The received signal at the SU is written by

$$y(i) = s(i) + n(i), \qquad i = 1, 2, ..., \tau f_s. \tag{1}$$

where τf_s is the total number of samples, τ is the sensing time and f_s is the sampling frequency.

A binary decision hypothesis is taken if the channel is idle or busy, respectively, as

$$\begin{cases} \mathcal{H}^0 : y(i) = n(i), & i = 1, 2, ..., \tau f_s. \\ \mathcal{H}^1 : y(i) = s(i) + n(i), & i = 1, 2, ..., \tau f_s. \end{cases} \tag{2}$$

where $\mathcal{H}^0$ and $\mathcal{H}^1$ are the hypothesis of the absence and presence of the primary user.

The basic MAC frame time structure considered herein is depicted in the Fig. 1. The first portion of the frame time is used to sensing the spectrum and the second portion is related with the transmission time, that impacts in the throughput. Considered that the total frame time is fixed, then the sensing time and throughput are conflicting parameters.

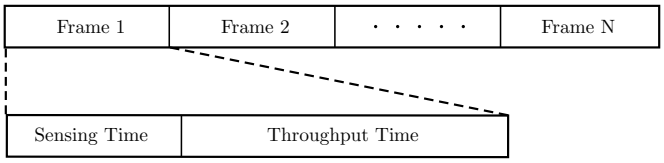

Fig. 1. Sensing-throughput frame time structure.

A. Energy Detector

The ED is the more simple form to spectrum sensing in CRN. It simply estimates the energy content in a determined spectrum bandwidth. The associated statistical test is formulated as

$$T(y) = \frac{1}{\tau f_s} \sum_{i=1}^{\tau f_s} |y(i)|^2. \tag{3}$$

Such statistical test is compared with a threshold level

$$T(y) \underset{\mathcal{H}^0}{\overset{\mathcal{H}^1}{\gtrless}} \lambda, \tag{4}$$

if the statistical test is smaller than threshold level λ, the SU chooses as a idle channel, otherwise the channel is busy and the SU will not transmit.

There are four scenarios that must be considered in the ED performance analysis:

1) If the channel is idle and the SU estimates that the channel is idle, then the SU will transmit and the throughput is maximum. A *correct detection* occurs;
2) If the channel is idle and the SU estimates that the channel is busy, then the SU will not transmit and a *false alarm* occurs;
3) If the channel is busy and the SU estimates that the channel is idle, then the SU will transmit and a *miss detection* occurs;
4) Finally, if the channel is busy and the SU estimates that the channel is busy, then the SU will not transmit and the PU is protected. A *correct detection* occurs.

In this work, the interest is concentrated on the first and third scenarios, *correct detection* and *miss detection* respectively.

III. Sensing-Time *vs.* Throughput Problem Formulation

The probability of false alarm $P_f(\cdot)$ and probability of detection $P_d(\cdot)$ associated to the ED can be formulated using the *central limit theorem* (CLT) approach, as function of sensing time parameter τ

$$P_f(\tau) = Q\left(\sqrt{2\text{SNR}_p + 1} Q^{-1}(\overline{P_d}) + \sqrt{\tau f_s}\text{SNR}_p\right), \tag{5}$$

$$P_d(\tau) = Q\left(\frac{1}{\sqrt{2\text{SNR}_p + 1}} Q^{-1}(\overline{P_f}) - \sqrt{\tau f_s}\text{SNR}_p\right), \tag{6}$$

where $\overline{P_d}$ and $\overline{P_f}$ are the probability of detection target and false alarm target, respectively, and the integral the of Gaussian probability density function is defined as

$$Q(x) \triangleq \frac{1}{\sqrt{2\pi}} \int_x^\infty \exp\left(\frac{-z^2}{2}\right) dz. \tag{7}$$

The value of the threshold λ can be related with the probability of detection $P_d(\tau)$ as [11]

$$P_d(\tau) = Q\left((\lambda - \text{SNR}_p - 1)\sqrt{\frac{\tau f_s}{2\text{SNR}_p + 1}}\right). \tag{8}$$

When different values of probability of channel occupancy occurs, then eq. (8) can be extended to:

$$P_d(\tau) = Q\left((\lambda - \beta - 1)\sqrt{\frac{\tau f_s}{2\beta + 1}}\right), \tag{9}$$

where $\beta = \text{P}_\text{r}(\mathcal{H}^1)\text{SNR}_p$. The value of SNR_p is weighted to $\text{P}_\text{r}(\mathcal{H}^1)$, which is the probability of the channel be busy.

The signal-to-noise ratio (SNR) of the primary user signal received in the primary user is given by $\text{SNR}_p = \frac{P_p}{N_0}$ and SNR of the secondary user signal is given by $\text{SNR}_s = \frac{P_s}{N_0}$, where P_p and P_s are the transmission power of the PU and the SU respectively, while the same level

of the noise power spectral density N_0 is assumed for both PU and SU user types.

As a consequence, the throughput of the SU in the absence and in the presence of the PU are given respectively by

$$C_0 = \log_2(1 + \text{SNR}_s), \tag{10}$$

$$C_1 = \log_2\left(1 + \frac{\text{SNR}_s}{1 + \text{SNR}_p}\right), \tag{11}$$

where C_0 is the throughput of the SU when it operates in the absence of the PU and C_1 is the throughput of the SU when it operates in the presence of the PU. Obviously, the value of C_0 is always larger than the value of the C_1, i.e the throughput when the channel is busy suffers interference from the PU signal. Therefore, the first and third scenarios lead to the sensing-throughput relations [11]

$$B_0(\tau) = \frac{T - \tau}{T} C_0, \tag{12}$$

$$B_1(\tau) = \frac{T - \tau}{T} C_1. \tag{13}$$

In the first case, the PU is not present then SU not generate false alarm. For the second case PU signal is active. Hence, $B_0(\tau)$ and $B_1(\tau)$ represent the SU throughput dependent on the sensing-time duration ($\tau < T$) when PU is absent and present, respectively.

The probabilities for occurrence of the first and third scenarios are given by [11]

$$\text{P}_\text{r}(\text{correct detection}) = [1 - P_f(\tau)] \cdot \text{P}_\text{r}(\mathcal{H}^0), \tag{14}$$

$$\text{P}_\text{r}(\text{miss detection}) = [1 - P_d(\tau)] \cdot \text{P}_\text{r}(\mathcal{H}^1), \tag{15}$$

where $\text{P}_\text{r}(\mathcal{H}^0)$ and $\text{P}_\text{r}(\mathcal{H}^1)$ is the probability of the channel is idle and busy (related to the first and third scenarios), respectively. The probability $(1 - P_d(\tau))$ is called miss detection probability.

So, the throughput $R_0(\tau)$ and $R_1(\tau)$ for the first and third scenarios are respectively

$$R_0(\tau) = \frac{T - \tau}{T} C_0 \cdot [1 - P_f(\tau)] \cdot \text{P}_\text{r}(\mathcal{H}^0), \tag{16}$$

$$R_1(\tau) = \frac{T - \tau}{T} C_1 \cdot [1 - P_d(\tau)] \cdot \text{P}_\text{r}(\mathcal{H}^1). \tag{17}$$

Finally, the total throughput in the SU network is given by

$$R(\tau) = R_0(\tau) + R_1(\tau). \tag{18}$$

For the case of the ED spectrum sensing, the throughput is given by eq. (19) [11], at the top of next page.

To simplify, we consider that the probability of the channel is occupied is low, i.e $\text{Pr}(\mathcal{H}^1) \leq 0.2$ and the second term of the throughput function in (19) becomes insignificant and can be simplified as

$$\widehat{R}(\tau) = B_0(\tau)\left(1 - Q\left(\sqrt{2\text{SNR}_p + 1} Q^{-1}(\overline{P_d}) + \right.\right. \\ \left.\left. + \sqrt{\tau f_s}\text{SNR}_p\right)\right) \text{P}_\text{r}(\mathcal{H}^0), \tag{20}$$

Finally, the simplified sensing-throughput optimization (STO) problem can be expressed as

$$\begin{aligned} \max_{\tau} \quad & \widehat{R}(\tau) \\ \text{s.t.} \quad & \text{(C.1.)} \qquad 0 \leq \tau \leq T \\ & \text{(C.2.)} \qquad P_d(\tau) \geq \overline{P_d} \end{aligned} \tag{21}$$

where $\overline{P_d} = 0.9$ is the probability of detection target according to the IEEE 802.22 WRAN. The convexity of the optimization problem (21) is demonstrated in the Appendix.

The optimization problem above can be interpreted as a sensing-throughput tradeoff whose objective is to identify the optimal sensing duration τ for each frame time in the MAC layer, such that the achievable throughput of the SU is guaranteed, while ensure the PU protection, that is related with the value of the P_d.

IV. Numerical Results

Table I depicts the main parameter values deployed in this section. The values of the throughput using such parameters are $C_0 = 6.6582$ and $C_1 = 6.6137$.

TABLE I
REFERENCE VALUES USED FOR SIMULATIONS.

Parameter	Value
$\text{Pr}(\mathcal{H}^0)$	[0.8, 0.5, 0.2]
$\text{Pr}(\mathcal{H}^1)$	[0.2, 0.5, 0.8]
SNR_s	20[dB]
SNR_p	-15[dB]
T	100[ms]
$\overline{P_d}$	0.9
f_s	6[MHz]
PU signal	QPSK

Using the simple but effective tool *fmincon* of *MATLAB Optimization Toolbox*, the STO problem was solved easily and the solver returns the optimal sensing time value equal to $\tau^* = 2.6$ [ms] for the three scenarios, i.e., for low, medium as well as high channel occupancy; the estimated optimal throughput $\widehat{R^*}$, original optimal throughput and the difference are given in Table II.

Since the number of samples N_s is related to the sensing time and the sample frequency and considering that the optimum sensing time for the three scenarios results same, then

$$N_s^* = \tau^* f_s = 15600 \quad \text{[samples]}. \tag{22}$$

$$R(\tau) = B_0(\tau)\left(1 - Q\left(\sqrt{2\text{SNR}_p + 1}Q^{-1}(\overline{P_d}) + \sqrt{\tau f_s}\text{SNR}_p\right)\right)\text{P}_\text{r}(\mathcal{H}^0) + \\ + B_1(\tau)\left(1 - Q\left(\frac{1}{\sqrt{2\text{SNR}_p + 1}}Q^{-1}(\overline{P_f}) - \sqrt{\tau f_s}\text{SNR}_p\right)\right)\text{P}_\text{r}(\mathcal{H}^1). \quad (19)$$

TABLE II
SIMPLIFIED, ORIGINAL AND DIFFERENCE OF THROUGHPUT.

$\Pr(\mathcal{H}^1)$	0.2	0.5	0.8
$\widehat{R}^*$ $\left[\frac{\text{bits}}{\text{s·Hz}}\right]$	5.1659	3.228	1.2815
R^* $\left[\frac{\text{bits}}{\text{s·Hz}}\right]$	5.295	3.550	1.807
ΔR^* %	**12.8**	**32.2**	**52.6**

In the sequel, instrumental numerical results are analysed aiming to corroborate the optimality of the solution.

A. Throughput vs. Sensing Time

The behavior of the throughput as a function of the sensing time, i.e. the objective function in (20), can be shown in Fig. 2. For the simulation results, $3 \cdot 10^4$ Monte Carlo simulation (MCS) trials were deployed and compared with the theoretical curve. One can infer that the throughput function has an unique maximum point, witch is the global optimum. Hence, one can conclude that the objective function is concave. Moreover, examining Fig. 2, one can infer by inspection that the maximum value of throughput is achieved in ≈ 2.55 [ms] for the three channel occupancy probability scenarios, in which is confirmed by the solution of the optimization problems.

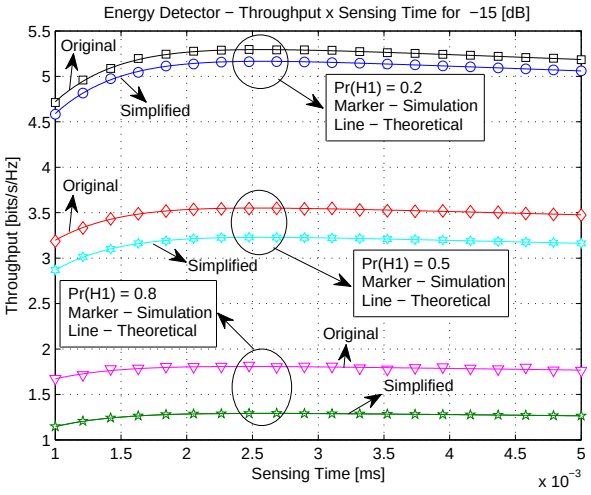

Fig. 2. Throughput *vs.* sensing time for $\text{SNR}_p = -15$[dB].

B. Probability of Detection vs. Threshold

In order to obtain the probability of detection *vs.* threshold of the energy detector operating under the optimum sensing time, a number of MCS realizations equal to $3 \cdot 10^4$ trials was chosen. Fig. 3 depicts the probability of detection *vs.* threshold adopting $\tau^* f_s = 15600$ samples. We have compared values in which the channel occupancy probability are low, medium, high and when the channel is completely occupied. Examining Fig. 3 one can conclude that the target probability of detection $\overline{P_d} = 0.9$ is obtained for different values of threshold that can be obtained using the equation (9).

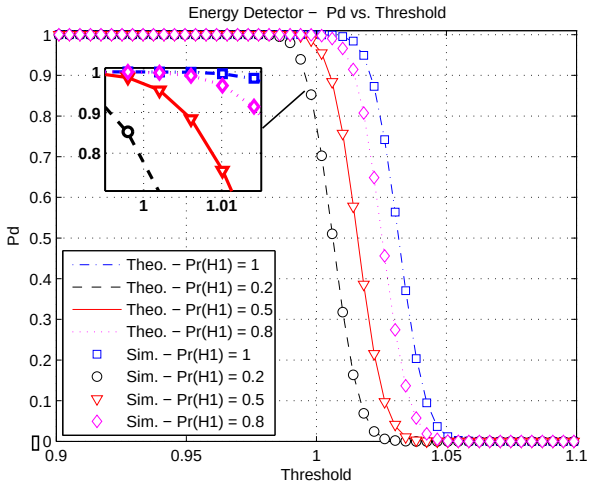

Fig. 3. Probability of detection *vs.* Threshold for $N_s = 15600$ samples.

C. Probability of Detection vs. Number of Samples

To obtain the figure of merit described by the probability of detection *vs.* N_s in the context of CRN equipped with ED, the same number of MCS trials ($3 \cdot 10^4$ trials) was chosen. As a consequence, Fig. 4 shows the probability of detection *vs.* N_s adopting value of the $\overline{P_d} = 0.9$ and the PU SNR value is $\text{SNR}_p = -15$ [dB]. Notice that in Fig 4, we compare values in that the probability of the channel is occupied are low, medium, high and when the channel is completely occupied; notice that a guaranteed 0.9 probability of detection is attained under the four scenarios when $N_s \geq 15600$ samples.

V. FINAL REMARKS

An optimization problem was formulated to deal with the sensing *vs.* throughput tradeoff (STO problem) in a CRN with one PU and one SU in a single-band spectrum sensing scheme. The equivalent and simplified optimization problem is convex but nonlinear in τ, and can be solved optimally using efficient solvers, such

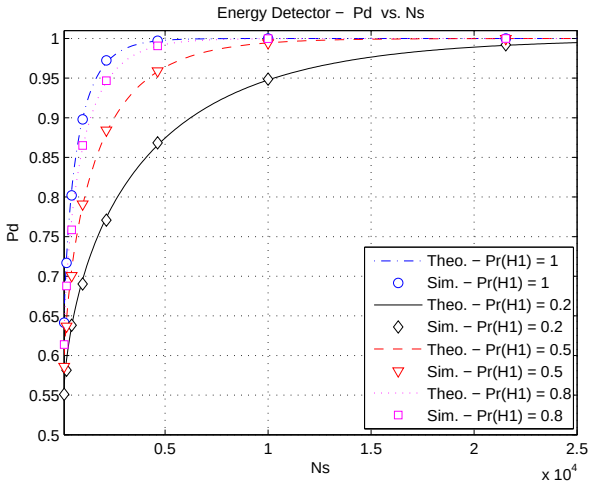

Fig. 4. Probability of Detection *vs.* N_s.

as *fmincon* tool of *MATLAB Optimization Toolbox*. The numerical solutions discussed in this paper confirm that the maximum is a global optimum and the objective function is a concave function.

Comparing the values of P_d with values of threshold one can see that different values of threshold implies in values of $P_d \geq 0.9$, which respects the constraints. Comparing values of P_d with values of N_s and values of sensing time, it is possible to conclude that for values of $N_s \geq 15600$ samples, implies in values of P_d above 0.9, with no violation of the constraints limits. Hence, we concluded that the obtained solution respect the constraint of the optimization problem, in addition to maximize the throughput of the SU.

APPENDIX

PROOF OF CONCAVITY

The convexity of the STO problem (21) is equivalent to demonstrate the concavity of the objective function $\widehat{R}(\tau)$ in (20), since the constraint set is convex, *i.e.* the constraint `(C.1.)` is a affine function in relation to τ and `(C.2.)` is a concave function regarding τ, as predicted by (6) and confirmed by numerical values of Fig. 4.

Clearly, the objective function (20) depends on the false alarm probability function that can be written as

$$\widehat{R}(\tau) = \frac{T-\tau}{T} C_0 \cdot [1 - P_f(\tau)] \cdot \mathrm{P_r}(\mathcal{H}^0). \qquad (23)$$

The proof can be done using the concept of composition of convex functions [12] that preserve the concavity of objective function (20). The values of C_0 and $\mathrm{P_r}(\mathcal{H}^0)$ are constants. The function $\frac{T-\tau}{T}$ is an affine function, i.e the function is concave. Then, it is necessary to prove that $[1 - P_f(\tau)]$ is concave.

In order to ensure that $[1 - P_f(\tau)]$ is concave, the false alarm probability function must be convex. Taking the first derivative of the false alarm probability function, eq. (5), we obtain:

$$\frac{dP_f(\tau)}{d\tau} = -\frac{\mathrm{SNR}_p\sqrt{f_s}}{2\sqrt{2\pi\tau}} e^{-0.5\left(\sqrt{2\mathrm{SNR}_p+1}Q^{-1}(\overline{P_d})+\mathrm{SNR}_p\sqrt{\tau f_s}\right)^2}.$$

Hence, assuming $\tau > 0$ implies that $\frac{dP_f(\tau)}{d\tau} < 0$, i.e $P_f(\tau)$ is convex in τ when subject to $P_f(\tau) \leq 0.5$.

Finally, ensuring that $\frac{dP_f(\tau)}{d\tau}$ is negative and increasing in τ, *i.e.* false alarm probability function is convex, it follows that $[1 - P_f(\tau)]$ is concave in τ. Hence, $\widehat{R}(\tau)$ is concave in τ. ■

REFERENCES

[1] FCC Spectrum Policy Task Force, "Report of the spectrum efficiency working group," http://transition.fcc.gov/sptf/reports.html, 2002.

[2] J. M. III and G. Q. M. Jr., "Cognitive radio: making software radios more personal," *IEEE Personal Commun.*, vol. 6, no. 4, pp. 13–18, 1999. [Online]. Available: http://dx.doi.org/10.1109/98.788210

[3] S. Haykin, "Cognitive radio: brain-empowered wireless communications," *Selected Areas in Communications, IEEE Journal on*, vol. 23, no. 2, pp. 201–220, Feb 2005.

[4] M. Cardenas-Juarez, U. Pineda-Rico, E. Stevens-Navarro, and M. Ghogho, "Sensing-throughput optimization for cognitive radio networks under outage constraints and hard decision fusion," in *Electronics, Communications and Computers (CONIELECOMP), 2015 International Conference on*, Feb 2015, pp. 80–86.

[5] S. Zhang, A. Hafid, H. Zhao, and S. Wang, "A cross-layer aware sensing-throughput tradeoff in cooperative sensing for cognitive radio networks," in *2015 IEEE International Conference on Communications (ICC)*, June 2015, pp. 7462–7467.

[6] Y. C. Liang, Y. Zeng, E. Peh, and A. T. Hoang, "Sensing-throughput tradeoff for cognitive radio networks," in *2007 IEEE International Conference on Communications*, June 2007, pp. 5330–5335.

[7] E. C. Y. Peh, Y. C. Liang, Y. L. Guan, and Y. Zeng, "Cooperative spectrum sensing in cognitive radio networks with weighted decision fusion schemes," *IEEE Transactions on Wireless Communications*, vol. 9, no. 12, pp. 3838–3847, December 2010.

[8] J. Jafarian and K. A. Hamdi, "Non-cooperative double-threshold sensing scheme: A sensing-throughput tradeoff," in *2013 IEEE Wireless Communications and Networking Conference (WCNC)*, April 2013, pp. 3376–3381.

[9] ——, "Sensing-throughput tradeoff in a non-cooperative double-threshold sensing scheme," in *Ultra Modern Telecommunications and Control Systems and Workshops (ICUMT), 2012 4th International Congress on*, Oct 2012, pp. 201–206.

[10] R. Fan and H. Jiang, "Optimal multi-channel cooperative sensing in cognitive radio networks," *IEEE Transactions on Wireless Communications*, vol. 9, no. 3, pp. 1128–1138, March 2010.

[11] Y.-C. Liang, Y. Zeng, E. Peh, and A. T. Hoang, "Sensing-throughput tradeoff for cognitive radio networks," *Wireless Communications, IEEE Transactions on*, vol. 7, no. 4, pp. 1326–1337, April 2008.

[12] S. Boyd and L. Vandenberghe, *Convex optimization*. Cambridge University Press, 2004.

A.3 Sensoriamento Espectral Cooperativo Distribuído baseado em Consenso

Título:	*Improved Weighted Average Consensus in Distributed Cooperative Spectrum Sensing Networks;*
Autores:	Aislan Gabriel Hernandes, Mário Lemes Proença Junior and Taufik Abrão;
Categoria:	*Full Paper*;
Publicação:	Aceito (2017);
Revista:	*Transactions on Emerging Telecommuncations Technologies.*

Resumo das Contribuições: A seção VI do artigo a seguir apresenta uma melhoria no modelo WAC, cujos pesos são calculados a partir da condição do canal AWGN/Rayleigh dos SUs vizinhos em conjunto com a condição do canal do SU em questão , i.e, o SU de interesse recebe informações do canal e da estimação do teste estatístico dos SUs vizinhos para realizar a técnica de consenso de forma distribuída. Com esta técnica obteve-se uma boa velocidade de convergência e bom desempenho em termos de ROC com a mesma complexidade computacional dos outros modelos de consenso, enquanto evita-se a necessidade de se ter uma central de fusão (FC) das informações relativas ao SS, reduzindo assim o consumo de energia em geral e melhorando a qualidade da informação trocada entre os SUs do sistema em relação às técnicas de sensoriamento espectral centralizadas.

Received: 4 June 2017 | Revised: 27 September 2017 | Accepted: 28 September 2017

DOI: 10.1002/ett.3259

RESEARCH ARTICLE

WILEY

Improved weighted average consensus in distributed cooperative spectrum sensing networks

Aislan Gabriel Hernandes[1] | Mario Lemes Proença Jr.[2] | Taufik Abrão[1]

[1]Department of Electrical Engineering, State University of Londrina, Londrina, Brazil

[2]Department of Computer Science, State University of Londrina, Londrina, Brazil

Correspondence
Taufik Abrão, Department of Electrical Engineering, State University of Londrina, Londrina-PR 86051-990, Brazil.
Email: taufik@uel.br

Funding information
Conselho Nacional de Desenvolvimento Científico e Tecnológico (CNPq) of Brazil, Grant/Award Number: 304066/2015-0 and 308348/2016-8; Coordenação de Aperfeiçoamento de Pessoal de Nível Superior (CAPES), Brazil; Universidade Estadual de Londrina (UEL), Paraná State Government, Brazil

Abstract

This work proposes a fully distributed improved weighted average consensus (IWAC) technique applied to a cooperative spectrum sensing (CSS) problem in cognitive radio systems. This method allows the secondary users to cooperate based on only local information exchange without a fusion centre. We have compared 4 rules of average consensus (AC) algorithms. The first rule is the simple AC without weights. The AC rule presents performance comparable to the traditional CSS techniques such as the equal gain combining rule, which is a soft combining centralised method. Another technique is the weighted AC (WAC) rule, using the weights based on the SUs' channel condition. This technique results in a performance similar to that of the maximum ratio combining with soft combining (centralised CSS). Two new AC rules are analysed, namely, WAC accuracy exchange (WAC-AE) and IWAC; the former relates the weights to the channel conditions of the SUs' neighbours, whereas the latter combines the conditions of WAC and WAC-AE in the same rule. All methods are compared with each other and with the hard combining centralised CSS. The WAC-AE results in a similar performance of the WAC technique but with fast convergence, whereas the IWAC can deliver suitable performance with small complexity increment. Moreover, the IWAC method results in a similar convergence rate than the WAC-AE method but slightly higher than the AC and WAC methods. Hence, the computational complexity of IWAC, WAC-AE, and WAC is proven to be very similar. The analyses are based on numerical Monte Carlo simulations, whereas the algorithm's convergence is evaluated for both fixed and dynamic mobile communication scenarios and under additive white Gaussian noise and Rayleigh channels.

1 | INTRODUCTION

Because of the growth of the wireless communication services, the available spectrum has become scarce. Measurements carried out by the Federal Communications Commission have demonstrated that the most of the allocated spectrum is not utilised.[1] This motivates the use of the cognitive radio (CR) that has humanlike characteristics, such as learning, adaptation, and cooperation,[2,3] which is able to increase spectrum efficiency considerably. In wireless regional area networks, the main objective is to maximise the spectrum utilisation of TV channels. The CR is the main technology in the wireless regional area network IEEE Standard 802.22,[4] which is applied in white space TV channels.

One of the tasks realised by the CR is the spectrum sensing, which can be performed by means of single-band or multiband channel techniques, the latter being accomplished in multiple channels wideband scenarios. This task can be carried out in 2 ways, either in a noncooperative manner, where secondary users sense independently the spectrum, or in a cooperative way, where the latter can be realised in a distributed or centralised way. In channel scenarios with shadowing and deep fading, the noncooperative techniques result in poor performance. In such channel conditions, cooperative spectrum sensing (CSS) techniques are used, which allow the exchange of information between the elements of the network; hence, channel severity can be partially surpassed because of the diversity gain obtained with the CSS techniques but with an increase in the complexity cost. In this sense, secondary users can be deployed as cooperative elements aiming at establishing a decision based on *hard combining* (AND, OR, and Majority) or *soft combining* rules, including equal gain combining (EGC) and maximal ratio combining (MRC) *rules*.

In the cooperative centralised mode, a fusion centre (FC) is deployed as the final decision maker for all secondary users. Moreover, relay nodes are widely applied in cooperative schemes employing the amplify-and-forward and decode-and-forward transmission protocols in a single-hop or multihop communication scheme. Usually, multihop communication increases energy efficiency compared with the single-hop schemes.

The performance of the centralised cooperative spectrum sense schemes operating under fading and additive white Gaussian noise (AWGN) channels is discussed in the work of Ibnkahla and Alkheir.[5] As well known, the hard combining presents degraded performance regarding soft combining rules. Among the hard combining rules, the more reliable performance is attained in most cases by the OR rule followed by the Majority and the AND rule, whereas among soft combining, the EGC always results in the worst performance than the MRC rule.

The term distributed (or decentralised) is defined as the way in which the decision is formed, implying in a local decision made by individual nodes. Thus, the term *distributed CSS* (DCSS) is defined as the final decision made from information exchanged between each node that previously made a local decision. There are some techniques in distributed/decentralised cooperative sensing such as belief propagation,[6] alternating direction method of multipliers,[7] and consensus algorithms (CA).[8-10]

Recently, the consensus techniques have become promising in distributed cooperative sensing that allows sensing without a proper FC receiver in a local one-hop neighbour communication. Communication is based on bidirectional links (full-duplex mode) and implies in a larger energy and spectrum efficiency and a smaller latency in the network. However, the major part of existing techniques in the literature results in performance similar to the EGC centralised cooperative sensing, which is called simply average consensus (AC). Zhang et al[8] proposed a novel consensus technique able to ensure a soft centralised cooperative sensing under the MRC rule. In the work of Ashrafi,[11] a binary consensus technique was developed to guarantee a superior performance to the quantised AC. Moreover, an AC technique applied to fixed and dynamic communication channels was discussed in the work of Li et al.[12] A distributed AC (DAC) was developed in the work of Teguig et al,[13] based on the goodness-of-fit test. This technique requires only the knowledge of the noise and using the Anderson-Darling test.[14] Furthermore, in the work of Vosoughi et al,[15] a trust-aware consensus was applied in the DCSS using gossip algorithm. In the work of Soatti et al,[16] a technique named *weighted AC accuracy exchange* (WAC-AE) was proposed to solve the localisation problem in networks equipped with several fixed nodes ensuring similar performance to the WAC and optimal ML but with fast convergence. Moreover, in the work of Nurellari et al,[17] a new consensus technique was applied in a quantised way, whereas in the work of Kailkhura et al,[18] a new consensus technique was proposed to deal with security in a cognitive network in a system with Byzantine attacks.

Against this background in the spectrum sensing methods, this paper proposes 2 new AC techniques for cooperative decentralised spectrum sensing purpose, namely, the WAC-AE and the *improved weighted AC* (IWAC). The IWAC method achieves the same performance of the WAC method, which is similar to the optimal MRC combining, but with a competitive performance-complexity trade-off. The WAC-AE is deployed in DCSS for the first time. The proposed IWAC method adopts similar conditions as that deployed in the WAC-AE and WAC rules. The advantage of IWAC lies on the lower number of iterations to achieve a target performance, which implies in a lower overall power consumption in the whole network. In summary, the following contributions of this paper are threefold:

- the proposition of new rules on AC for distributed spectrum sensing purpose in the CRN context, namely, IWAC and WAC-AE, which can achieve similar performance to the optimal centralised CSS with a small or similar number of iterations, depending on channel and system scenario,
- an analysis of convergence for the proposed consensus rules operating under fixed and dynamic network scenarios, and
- a comparative complexity analysis of the proposed IWAC and WAC-AE regarding other AC rules.

TABLE 1 Acronyms

3C	Cooperative consensus convergence
AC	Average consensus
ADMM	Alternating direction method of multipliers
AF	Amplify and forward
AWGN	Additive white Gaussian noise
BF	Belief propagation
CLT	Central limit theorem
CR	Cognitive radio
CSS	Cooperative spectrum sensing
DAC	Distributed average consensus
DCSS	Distributed cooperative spectrum sensing
DF	Decode and forward
ED	Energy detector
EGC	Equal gain combining
FC	Fusion centre
FCC	Federal communication commission
GoF	Goodness of fit
IWAC	Improved weighted average consensus
MCS	Monte Carlo simulation
MRC	Maximal ratio combining
NLOS	Non–line of sight
PU	Primary user
ROC	Receiver operating characteristic
SE	Spectral efficiency
SLEM	Second largest eigenvalues modulo
SS	Spectrum sensing
SNR	Signal-noise ratio
SU	Secondary user
WAC	Weighted average consensus
WAC-AE	Weighted average consensus accuracy exchange
WRAN	Wireless regional area network

The rest of this paper is organised as follows. The CR system model is presented in Section 2. The formulation of the centralised CSS and the fixed and dynamic channel communication model based on the graph theory are revisited in Section 3. In Section 4, the existing AC techniques applied to DCSS are explored, whereas a novel DAC rule is formulated in Section 4. Numerical results supporting our findings are analysed in Section 6. Concluding remarks are offered in Section 7. For reference and due to the large number of abbreviations deployed in this paper, a list of acronyms is summarised in Table 1.

2 | SYSTEM MODEL

We consider a cognitive wireless network with N SUs and 1 PU (single-band system). All SUs sense the spectrum and cooperate with each other to determine the final decision. We can define 2 stages in the process, namely, the sensing phase and the decision phase. In the sensing phase, each SU senses the spectrum. In this work, we adopt the energy detector (ED) because it requires lower design complexity and no prior information of the primary user (PU) but with suboptimal performance. For the ith SU, the received signal is defined as follows:

$$y_i(t) = \begin{cases} n_i(t) & , \mathcal{H}_0 \\ h_i s_i(t) + n_i(t) & , \mathcal{H}_1, \end{cases} \tag{1}$$

where $\mathcal{H}_0$ is the hypothesis that the channel is idle, $\mathcal{H}_1$ is the hypothesis that the channel is busy, $y_i(t)$ is the received signal by the ith SU, $s_i(t)$ is a binary phase-shift keying–modulated signal transmitted by the PU, $n_i(t)$ is the AWGN, and h_i is the amplitude channel gain that represents the multipath Rayleigh fading channel effect.

2.1 | Energy detector

Using the ED,[19] each SU calculates a decision statistic T_i over a detection interval of N_s samples. The statistic test of the ith SU can be written as

$$T_i = \sum_{t=0}^{N_s} |y_i(t)|^2. \tag{2}$$

Hence, it is compared with a predefined threshold λ, and the decision of each user is

$$T_i \underset{\mathcal{H}_0}{\overset{\mathcal{H}_1}{\gtrless}} \lambda. \tag{3}$$

The value $T_i \in \mathbb{R}^+$ under AWGN channels presents a statistical distribution given by[9]

$$T_i \sim \begin{cases} \chi^2_{2TW} & , \mathcal{H}_0 \\ \chi^2_{2TW}(2\gamma) & , \mathcal{H}_1, \end{cases}$$

where χ^2_{2TW} and $\chi^2_{2TW}(2\gamma)$ is the central and noncentral chi-square distributions with $2TW = 2N_s$ degrees of freedom and noncentrality parameter of 2γ.

Furthermore, under Rayleigh channels, the channel gain is random, and the distribution of the decision statistic becomes[9]

$$T_i \sim \begin{cases} \chi^2_{2TW} & , \mathcal{H}_0 \\ \chi^2_{2TW}(2\gamma) + \exp(2\overline{\gamma} + 2) & , \mathcal{H}_1, \end{cases}$$

where the exponential distribution $\exp(2\overline{\gamma} + 2)$ presents parameter $2\overline{\gamma} + 2$. The $\overline{\gamma}$ is the average signal-noise ratio (SNR), and γ is the instantaneous SNR.

Using the central limit theorem for a large number of samples, the ith statistic test T_i is asymptotically normally distributed with mean and variance given by[8]

$$\mathbb{E}(T_i) = \begin{cases} N_s\sigma_i^2 & , \mathcal{H}_0 \\ (N_s + \eta_i)\sigma_i^2 & , \mathcal{H}_1 \end{cases}$$

$$\text{var}(T_i) = \begin{cases} 2N_s\sigma_i^4 & , \mathcal{H}_0 \\ 2(N_s + 2\eta_i)\sigma_i^4 & , \mathcal{H}_1, \end{cases}$$

where σ_i^2 is the noise variance, and the ith SNR of the SUs is given by

$$\eta_i = \sum_{t=0}^{N_s} \frac{s_i^2 |h_i|^2}{\sigma_i^2}. \tag{4}$$

3 | COOPERATIVE SPECTRUM SENSING

Centralised versus distributed CSS strategies are revised in this section. Besides, dynamic communication channels are modelled with the aid of graph theory.

3.1 | Centralised CSS

Centralised CSS methods need an FC to operate. A cooperative network uses the SUs to sense the spectrum and an FC for the final decision.

In the FC, there are some ways to determine the final decision, including the hard combining, which can use a different decision rule such as the OR, Majority, and AND rules, and the soft combining way, which is based on EGC combining and MRC combining rules.

3.1.1 | Hard decision

In the hard combining spectrum sensing, N cooperative SUs are sensing the total spectrum cooperatively; the final decision is given by the following metric, called final statistical test T_f^{HD}:

$$T_f^{\mathrm{HD}} = \sum_{i=1}^{N} d_i, \tag{5}$$

where d_i is the decision of the ith SU and $d_i \in \{0, 1\}$, being $d_i = 0$ if PU is absent or $d_i = 1$ if the PU is present in the band. The performance is given in terms of probability of detection as follows[5]:

$$\mathrm{P}_d^{\mathrm{HD}} = \sum_{q=i}^{N} \binom{N}{q} \left[\prod_{\gamma=1}^{q} \mathrm{P}_d^{\gamma} \cdot \prod_{\beta=1}^{N-q} (1 - \mathrm{P}_d^{\beta}) \right]. \tag{6}$$

The *Or-And-Majority* rules allow to describe different ways to construct the threshold λ in a hard combining centralised CSS scheme; in summary, we have the following.

- *Or* rule: $\lambda = 1$. The rule *OR* ensures minimum interference to the PUs. The PU is considered present in a band if only a single PU sends one to FC in its decision, ie, if the statistic test of some SU adds one. It can be seen that the OR rule is very conservative for the SUs to access the licenced band. As such, the chance of causing interference to the PU is minimised.
- *And* rule: $\lambda = N$, where N means the number of collaborative nodes sensing the same subband. It is an aggressive rule, ensuring high rate of transmission to the SUs. The PU is considered present in the band if and only if all CRs' collaborative nodes are sensing the presence of PU in the band;
- *Majority* rule: $\lambda = \lceil \frac{N}{2} \rceil$. The PU is considered present in the band if the majority of SUs sends one to the FC. The function $\lceil \cdot \rceil$ is the ceil function.

3.1.2 | Soft decision

The statistic test of the ith SU is sent to the coordinator, ie, the FC, which collects all values of test statistics from all SUs. Then, the overall statistic test T_f^{SD} is calculated at the coordinator node as

$$T_f^{\mathrm{SD}} = \sum_{i=1}^{N} \rho_i T_i. \tag{7}$$

If all ρ_i is equal to each user, the cooperative technique has the EGC performance. If the values of ρ_i is proportional to SNR, then the performance is same to MRC.

As in the case of CSS and following the work of Zhang et al,[8] the final decision T_f is normally distributed with mean and variance given by

$$\mathbb{E}(T_f^{\mathrm{SD}}) = \begin{cases} \sum_{i=1}^{N} \rho_i N_s \sigma_i^2 & , \mathcal{H}_0 \\ \sum_{i=1}^{N} (N_s \sigma_i^2 (1 + \eta_i)) & , \mathcal{H}_1 \end{cases} \tag{8}$$

$$\mathrm{var}(T_f^{\mathrm{SD}}) = \begin{cases} \sum_{i=1}^{N} \rho_i^2 2 N_s \sigma_i^4 & , \mathcal{H}_0 \\ \sum_{i=1}^{N} \rho_i^2 (2 N_s \sigma_i^4 (1 + 2\eta_i)) & , \mathcal{H}_1. \end{cases} \tag{9}$$

As discussed in the work of Nurellari et al,[17] the performance of the centralised soft CSS can be evaluated for a given P_f as

$$\mathrm{P}_d^{\mathrm{C}} = Q\left(\frac{Q^{-1}(\mathrm{P}_f) \sqrt{\mathrm{var}\left(T_f^{\mathrm{SD}} \middle| \mathcal{H}_0\right)} - \mathbb{E}\left(T_f^{\mathrm{SD}} \middle| \mathcal{H}_1\right) + \mathbb{E}\left(T_f^{\mathrm{SD}} \middle| \mathcal{H}_0\right)}{\sqrt{\mathrm{var}\left(T_f^{\mathrm{SD}} \middle| \mathcal{H}_1\right)}} \right), \tag{10}$$

where $Q(\cdot)$ is the Gaussian Q-function.

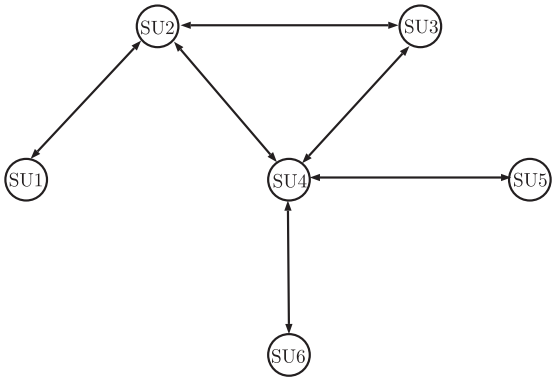

FIGURE 1 Decentralised cooperative scheme with 6 secondary users (SUs)[18]

3.2 | Fixed and dynamic DCSS networks based on graph theory

The fixed-node and mobile-node cooperative networks are modelled based on a graph theory description. We define the elements of the network as the vertices and the communication links as the graph edges.

3.2.1 | Graph theory results

To illustrate the graph theory-based description of a DCSS network, Figure 1 depicts an example of a DCSS network with 6 SUs keeping a bidirectional (full-duplex) one-hop communication. From the graph theory, this network presents 6 vertices (or nodes) and 6 edges.

In this paper, we will consider a decentralised network operating under fixed and mobile communication channels.

3.2.2 | Fixed communication channel

We consider that there are N SUs interconnected and sharing the same channel bandwidth and links. The network is modelled as a connected graph $\mathrm{G} = (\mathscr{V}, \mathscr{E})$, where $\mathscr{V} = \{1, 2, \dots, N\}$ is the vertices of the graph, ie, the SUs contained in the network, and $\mathscr{E} \subseteq \mathscr{V} \times \mathscr{V}$ is the edges, representing the channel links between the SUs. The set of neighbours for the ith SU is represented as $\mathscr{N}_i = \{j \in \mathscr{V} : (i,j) \in \mathscr{E}\}$, the cardinality (number of elements in the set) is represented as $\aleph_i$, and the maximum cardinality is represented as $\max(\aleph_i)$.

The symmetric adjacent matrix of the graph $\mathscr{G}$ is $\mathbf{G} = [g_{ij}]_{N\times N}$, where $g_{ij} = 1$ if $(i,j) \in \mathscr{E}$, ie, when the ith SU communicates with the jth SU and $g_{ij} = 0$ otherwise.

The Laplacian matrix of the graph $\mathscr{G}$ is defined as $\mathbf{L} = N - G$, where $\mathbf{N}$ is the maximum cardinality diagonal matrix of the graph defined as $\mathbf{N} = \mathrm{diag}(\aleph_1, \dots, \aleph_N)$. Thus, the Laplacian matrix $\mathbf{L} = [l_{ij}]_{N\times N}$ can be constructed as

$$l_{ij} = \begin{cases} \aleph_i & , \text{if} \quad i = j \\ -1 & , \text{if} \quad j \in \mathscr{N}_i \\ 0 & , \text{otherwise.} \end{cases} \tag{11}$$

To illustrate those definitions, the network presented in Figure 1, which will be analysed in Section 6.1.1, defines the following diagonal matrix with maximum cardinality:

$$\mathbf{N}_6 = \begin{bmatrix} 1 & 0 & 0 & 0 & 0 & 0 \\ 0 & 3 & 0 & 0 & 0 & 0 \\ 0 & 0 & 2 & 0 & 0 & 0 \\ 0 & 0 & 0 & 4 & 0 & 0 \\ 0 & 0 & 0 & 0 & 1 & 0 \\ 0 & 0 & 0 & 0 & 0 & 1 \end{bmatrix}, \tag{12}$$

and the adjacency matrix takes the form

$$\mathbf{G}_6 = \begin{bmatrix} 0 & 1 & 0 & 0 & 0 & 0 \\ 1 & 0 & 1 & 1 & 0 & 0 \\ 0 & 1 & 0 & 1 & 0 & 0 \\ 0 & 1 & 1 & 0 & 1 & 1 \\ 0 & 0 & 0 & 1 & 0 & 0 \\ 0 & 0 & 0 & 1 & 0 & 0 \end{bmatrix}. \tag{13}$$

Therefore, the Laplacian matrix for this network is given by

$$\mathbf{L}_6 = \begin{bmatrix} 1 & -1 & 0 & 0 & 0 & 0 \\ -1 & 3 & -1 & -1 & 0 & 0 \\ 0 & -1 & 2 & -1 & 0 & 0 \\ 0 & -1 & -1 & 4 & -1 & -1 \\ 0 & 0 & 0 & -1 & 1 & 0 \\ 0 & 0 & 0 & -1 & 0 & 1 \end{bmatrix}. \tag{14}$$

3.2.3 | Dynamic communication channel

Similarly to the static communication channel, in the dynamic channel case, the Laplacian matrix of the graph $\mathscr{G}(k)$ is defined as $\mathbf{L}(k) = \mathbf{N} - \mathbf{G}(k)$, where k is an integer that represents the time of network change, ie, the graph positions change according to the time integer intervals, $\mathbf{N}$ is the maximum cardinality diagonal matrix of the graph defined as $\mathbf{N} = \text{diag}(\aleph_1, \ldots, \aleph_N)$. Thus, the Laplacian matrix $\mathbf{L}(k) = [l_{ij}]_{N\times N}$ can be constructed similarly as Equation 11.

A better description of the dynamic channel can be made taking into account a probability of connection (in the neighbours' communication sense) that can be described by the a priori probability $\text{Pr}_{\text{connection}} \in [0, 1]$. The probability of link failure is $\text{Pr}_{\text{fail}} = 1 - \text{Pr}_{\text{connection}}$. When this probability is zero, the channel is fixed, otherwise the network presents some mobility. Hence, the structure of the Laplacian matrix is ready modified considering the *a priori* probability of connection as:

$$l_{pij} = \begin{cases} \sum_{j=1}^{N} \text{Pr}_{\text{connection}} & \text{, if} \quad i = j \\ -\text{Pr}_{\text{connection}} & \text{, if} \quad j \in \mathscr{N}_i \\ 0 & \text{, otherwise.} \end{cases} \tag{15}$$

4 | CONSENSUS-BASED DCSS

Existing distributed consensus-based fusion techniques only ensure EGC performance; such techniques are identified as average CA.[8] Therefore, the EGC performance is inferior regarding the centralised MRC combining (optimal combining) schemes. Based on this, new CAs have been proposed in the literature to ensure MRC performance. These algorithms are denominated weighted AC (WAC) techniques.[8] The performance of the WAC technique is close to that of the MRC centralised combining (soft combining). However, the WAC algorithm has slow convergence in the case of unbalanced SNR at different SUs, which are directly related to the weights design.

4.1 | Average consensus

In the AC method, the estimation of the ith SU energy is updated at the iteration time $k = 1, 2, \ldots$ according to the rule as follows[20]:

$$x_i(k+1) = x_i(k) + \alpha \sum_{j\in\mathscr{N}_i} \text{g}_{ij} \left(x_j(k) - x_i(k)\right), \tag{16}$$

where α is the iteration step size satisfying $0 < \alpha < (\max(\aleph_i))^{-1}$. The elements of the adjacent matrix g_{ij} define the network topology.

The initial statistic before the fusion at the iteration $k = 0$ is considered as $x_i(0) = T_i$.

For the AC method, the final convergence is obtained as follows[8]:

$$x_i(k) \to x^* = \frac{\sum_{i=1}^{N} x_i(0)}{N}, \qquad \text{when} \quad k \to \infty, \tag{17}$$

whereas the final decision is compared with a predefined threshold λ and has the form

$$\text{Decision} = \begin{cases} \mathcal{H}_0 & , x^* > \lambda \\ \mathcal{H}_1 & , \text{otherwise.} \end{cases} \tag{18}$$

In the compact vector-matrix form, the rule can be described as

$$\mathbf{x}(k+1) = \mathbf{P}_{\text{AC}}\mathbf{x}(k), \tag{19}$$

where $\mathbf{P}_{\text{AC}} = \mathbf{I} - \alpha(\mathbf{N} - \mathbf{G})$ is the Perron matrix and can be written also as $\mathbf{P}_{\text{AC}} = \mathbf{I} - \alpha\mathbf{L}_{\text{AC}}$. Here, the Laplacian matrix is $\mathbf{L}_{\text{AC}} = \mathbf{L}$, as defined in the last section. Hence, the performance regarding probability of detection, for a given fail probability at the ith SU, can be described in the same way of Equation 10 but, now, considering distributed soft CSS decisions.

Algorithm 1 describes a pseudocode of the AC method.

Algorithm 1 Average consensus

1: **Input:** α, K, $\mathbf{T}$
2: **for** $k = 0$ **to** $K - 1$ **do**
3: $\quad \mathbf{x}(0) = \mathbf{T}$
4: $\quad \mathbf{P}_{\text{AC}} = \mathbf{I} - \alpha\mathbf{L}_{\text{AC}}$
5: $\quad \mathbf{x}(k+1) = \mathbf{P}_{\text{AC}}\mathbf{x}(k)$
6: **end for**
7: **Output:** $\mathbf{x}$

4.2 | Weighted AC

The WAC rule can approach to soft combining performance (MRC). The WAC rule is given by,[8,10]

$$x_i(k+1) = x_i(k) + \frac{\alpha}{\omega_i}\sum_{j\in\mathcal{N}_i} g_{ij}(x_j(k) - x_i(k)), \tag{20}$$

where ω_i is the weighted ratio according to the channel condition of the ith SU and α is the iteration step size satisfying $0 < \alpha < (\max(\aleph_i))^{-1}$. The final convergence is obtained as[8]:

$$x_i(k) \to x^* = \frac{\sum_{i=1}^{N}\omega_i x_i(0)}{\sum_{i=1}^{N}\omega_i}, \qquad \text{when} \quad k \to \infty. \tag{21}$$

Moreover, when the values of ω_i is equal to all SUs, the final convergence is similar to EGC combining, ie, the same of the AC method.

In the WAC algorithm, the weights are related to the channel conditions of the ith SU. According to the work of Zhang et al,[8] *suboptimal weights* for the WAC spectrum sensing receiver operating under Rayleigh fading channels can be obtained as an estimative of the SNR state channel as follows:

$$\omega_i = \frac{1}{2\ell}\sum_{\wp=k-\ell}^{k}(T_{i,\wp} - 2N_s), \tag{22}$$

where ℓ is the length of the estimation window and $T_{i,\wp}$ is the $\wp$th measurement (statistic test) of the ith SU.

For the AWGN channel, the optimal weights are simply calculated solving an optimisation problem that maximises the *deflection coefficient*[8] as follows:

$$\omega_i = \frac{\eta_i}{\sigma_i^2}, \tag{23}$$

where η_i is defined in Equation 4.

Using the WAC in the compact form, the discrete consensus rule can be represented in the vector-matrix form as follows[8]:

$$\mathbf{x}(k+1) = \mathbf{P}_{\text{WAC}}\mathbf{x}(k), \tag{24}$$

where the Perron matrix can be written as $\mathbf{P}_{\text{WAC}} = \mathbf{I} - \alpha\Delta^{-1}\mathbf{L}_{\text{WAC}}$. The diagonal matrix $\Delta = \text{diag}(\omega_1, \ldots, \omega_N)$ is the weight diagonal matrix. Here, the Laplacian matrix $\mathbf{L}_{\text{WAC}} = \mathbf{L}$.

The performance can be obtained in the same way of Equation 10 but, now, considering distributed soft decisions. The pseudocode for the WAC algorithm is depicted in Algorithm 2.

Algorithm 2 Weighted average consensus

Input: α, K, $\mathbf{\Delta}$, $\mathbf{T}$
for $k = 0$ **to** $K - 1$ **do**
  $\mathbf{x}(0) = \mathbf{T}$
  $\mathbf{P}_{\text{WAC}} = \mathbf{I} - \alpha\mathbf{\Delta}^{-1}\mathbf{L}_{\text{WAC}}$
  $\mathbf{x}(k+1) = \mathbf{P}_{\text{WAC}}\mathbf{x}(k)$
end for
Output: $\mathbf{x}$

4.3 | WAC accuracy exchange

Recently, the WAC-AE has been proposed[16] and[18] in a different context treated herein, ie, respectively to solve the localisation problem in networks equipped with several fixed nodes and deal with security issues in a cognitive network. In the new context of DCSS, the WAC-AE rule to is given by

$$x_i(k+1) = x_i(k) + \alpha \sum_{j \in \mathcal{N}_i} \omega_j g_{ij} \left(x_j(k) - x_i(k) \right), \tag{25}$$

where ω_j is the weighted ratio according to the channel condition of the jth SUs. The convergence is guaranteed taking the step size among $0 < \alpha < (\max_i \sum_{j \in \mathcal{N}_i} \omega_j)^{-1}$. The associated final convergence is obtained as

$$x_i(k) \to x^* = \frac{\sum_{i=1}^{N} \omega_i x_i(0)}{\sum_{i=1}^{N} \omega_i}, \qquad \text{when} \quad k \to \infty. \tag{26}$$

In the WAC-AE algorithm, the weights are related to the channel conditions of the jth SUs neighbours. Adopting the *suboptimal weights* for Rayleigh channels results the following:

$$\omega_j = \frac{1}{2\ell} \sum_{\wp=k-\ell}^{k} (T_{j,\wp} - 2N_s), \tag{27}$$

where ℓ is the length of the estimation window and $T_{j,\wp}$ is the $\wp$th measurement (statistic test) of the jth SUs. Besides, for the AWGN channel, the optimal weights are simply calculated as in Equation 23.

In the compact form, the discrete WAC-AE consensus rule can be represented in the vector-matrix form as

$$\mathbf{x}(k+1) = \mathbf{P}_{\text{WAC-AE}}\mathbf{x}(k), \tag{28}$$

where the Perron matrix is $\mathbf{P}_{\text{WAC-AE}} = \mathbf{I} - \alpha\mathbf{L}_{\text{WAC-AE}}$. The modified Laplacian matrix $\mathbf{L}_{\text{WAC-AE}} = [l_{ij_{\text{WAC-AE}}}]_{N \times N}$ is constructed as

$$l_{ij_{\text{WAC-AE}}} = \begin{cases} \sum_{j \in \mathcal{N}_i} \omega_j & , \text{if} \quad i = j \\ -\omega_j & , \text{if } j \in \mathcal{N}_i \\ 0 & , \text{otherwise.} \end{cases} \tag{29}$$

The pseudocode of the WAC-AE is presented in Algorithm 3.

Algorithm 3 Weighted average consensus - accuracy exchange

Input: α, K, $\mathbf{\Delta}$, $\mathbf{T}$
for $k = 0$ **to** $K - 1$ **do**
  $\mathbf{x}(0) = \mathbf{T}$
  $\mathbf{P}_{\text{WAC-AE}} = \mathbf{I} - \alpha\mathbf{\Delta}^{-1}\mathbf{L}_{\text{WAC-AE}}$
  $\mathbf{x}(k+1) = \mathbf{P}_{\text{WAC-AE}}\mathbf{x}(k)$
end for
Output: $\mathbf{x}$

5 | IMPROVED WAC

In this section, we propose a new rule to WAC for a DCSS purpose. The new rule improves the WAC (IWAC) being described by the following updating equation:

$$x_i(k+1) = x_i(k) + \frac{\alpha}{\omega_i} \sum_{j \in \mathcal{N}_i} \omega_j g_{ij} \left[x_j(k) - x_i(k) \right], \tag{30}$$

where ω_j is the weighted ratio according to the channel condition of the jth SUs and ω_i is the weight according to the channel condition of the ith SU. The convergence is guaranteed taking the step size in the interval as follows:

$$0 < \alpha < \left(\max_i \sum_{j \in \mathcal{N}_i} \omega_j \right)^{-1}. \tag{31}$$

The final convergence to the IWAC method is obtained as

$$x_i(k) \to x^* = \frac{\sum_{i=1}^{N} \omega_i x_i(0)}{\sum_{i=1}^{N} \omega_i}, \qquad \text{when} \quad k \to \infty. \tag{32}$$

Moreover, we can adopt the same *suboptimal weights* of the WAC rule (22) for the distributed cooperative SSNs operating under Rayleigh fading channels as

$$\omega_\xi = \frac{1}{2\ell} \sum_{\wp=k-\ell}^{k} (T_{\xi,\wp} - 2N_s), \tag{33}$$

where ℓ is the length of the estimation window, $\xi \in (i,j)$, and $T_{\xi,\wp}$ is the $\wp$th measurement (statistic test) of SU. Again, for the AWGN channel, the weights are calculated as in Equation 23, ie, $\omega_\xi = \frac{\eta_\xi}{\sigma_\xi^2}$.

In the compact form, the discrete consensus rule can be represented in the vector-matrix form as

$$\mathbf{x}(k+1) = \mathbf{P}_{\text{IWAC}} \mathbf{x}(k), \tag{34}$$

where the modified Perron matrix now is defined as

$$\mathbf{P}_{\text{IWAC}} = \mathbf{I} - \alpha \Delta^{-1} \mathbf{L}_{\text{IWAC}}. \tag{35}$$

In the proposed IWAC spectrum sensing, the modified Laplacian matrix $\mathbf{L}_{\text{IWAC}} = [l_{ij_{\text{IWAC}}}]_{N \times N}$ is constructed as

$$l_{ij_{\text{IWAC}}} = \begin{cases} \sum_{j \in \mathcal{N}_i} \omega_j & , \text{if} \quad i = j \\ -\omega_j & , \text{if } j \in \mathcal{N}_i \\ 0 & , \text{otherwise.} \end{cases} \tag{36}$$

The matrix $\Delta = \text{diag}(\omega_1, \ldots, \omega_N)$ is the weight diagonal matrix. Notice that the *receiver operating characteristics* (ROC) performance for the IWAC spectrum sensor can be obtained in a same way of Equation 10 but taking into account distributed soft CSS decisions, as discussed in Section 6.4.1.

A pseudocode for the IWAC implementation considering static and dynamic channel environments is presented in Algorithm 4.

Algorithm 4 Improved weighted average consensus

1: **Input:** α, K, $\mathbf{\Delta}$, $\mathbf{T}$
2: **for** $k = 0$ **to** $K - 1$ **do**
3: $\quad \mathbf{x}(0) = \mathbf{T}$
4: $\quad \mathbf{P}_{\text{IWAC}} = \mathbf{I} - \alpha \mathbf{\Delta}^{-1} \mathbf{L}_{\text{IWAC}}$
5: $\quad \mathbf{x}(k+1) = \mathbf{P}_{\text{IWAC}} \mathbf{x}(k)$
6: **end for**
7: **Output:** $\mathbf{x}$

5.1 | Convergence analysis for the IWAC algorithm

In this section, the convergence analysis for the IWAC algorithm is developed taking into account both system scenarios, ie, static and dynamic SUs in the CR networks.

5.1.1 | Fixed networks

Using the IWAC in the compact form, the discrete consensus rule can be represented in the vector-matrix form by updating Equation 34, where the Perron matrix $\mathbf{P}_{\text{IWAC}}$ is given by Equation 35.

The IWAC rule convergence depends on the convergence of the infinite stochastic matrix product. Based on the Perron-Frobenius theorem,[8,21] we find the following:

$$\mathbf{P}_{\infty_{\text{IWAC}}} = \lim_{k\to\infty} \prod_{\ell=1}^{k} \mathbf{P}_{\ell_{\text{IWAC}}} = \frac{\mathbf{1}\omega^T}{\omega^T\mathbf{1}}, \tag{37}$$

where $\omega^T = [\omega_1 \omega_2 \ \dots \ \omega_N]$ and vector $\mathbf{1} = [11 \ \dots \ 1]^T$ has dimension $N \times 1$.

The proof can be obtained considering that the matrix $\mathbf{P}_{\text{IWAC}}$ is a primitive nonnegative matrix, ie, the kth power is positive for some natural number k with left and right eigenvectors $\mathbf{u}$ and $\mathbf{v}$, respectively, which satisfy $\mathbf{P}_{\text{IWAC}}\mathbf{v} = \mathbf{v}$ and $\mathbf{u}^T\mathbf{P}_{\text{IWAC}} = \mathbf{u}^T$. The Perron-Frobenius theorem ensures that $\lim_{k\to\infty} \prod_{\ell=1}^{k} \mathbf{P}_{\ell_{\text{IWAC}}} = \frac{\mathbf{v}\mathbf{u}^T}{\mathbf{v}^T\mathbf{u}}$.

Lemma 1. *Let $\mathcal{G}$ a connected graph with N vertices. The Perron matrix $\mathbf{P}_{\text{IWAC}}$ with $0 < \alpha < (\max_i \sum_{j\in\mathcal{N}_i} \omega_j)^{-1}$ has the following properties.*

- *The Perron matrix $\mathbf{P}_{\text{IWAC}}$ is a nonnegative matrix with left eigenvector ω and right eigenvector $\mathbf{1}$.*
- *All eigenvalues of Perron matrix $\mathbf{P}_{\text{IWAC}}$ are in a unit circle.*
- *The Perron matrix $\mathbf{P}_{\text{IWAC}}$ is a primitive matrix.*

Proof. The first property is based on that $\mathbf{P}_{\text{IWAC}}\mathbf{1} = \mathbf{1} - \alpha\Delta^{-1}\mathbf{L}_{\text{IWAC}}\mathbf{1} = \mathbf{1}$ and $\omega^T\mathbf{P}_{\text{IWAC}} = \omega^T - \alpha\omega^T\Delta^{-1}\mathbf{L}_{\text{IWAC}} = \omega^T$ that implies in a left eigenvector ω and a right eigenvector $\mathbf{1}$.

The second property is guaranteed by the Gershgorin theorem, and the third property is guaranteed by the step size α of the IWAC method. □

Theorem 1. *For the IWAC iterative process, the step size α satisfies the condition $0 < \alpha < (\max_i \sum_{j\in\mathcal{N}_i} \omega_j)^{-1}$, in which the elements ω_i and ω_j operating in a fixed communication network occur infinitely (infinite iterations, fixed values); hence, the iteration converges to*

$$\lim_{k\to\infty} x_i(k) = \frac{\sum_{i=1}^{N} \omega_i x_i(0)}{\sum_{i=1}^{N} \omega_i}. \tag{38}$$

Proof. The IWAC consensus method achieves asymptotically the convergence, and the Perron-Frobenius theorem ensures that the limit $\lim_{k\to\infty} \prod_{\ell=1}^{k} \mathbf{P}_{\ell_{\text{IWAC}}}$ exists for primitive matrices; then, we have

$$\begin{aligned} \mathbf{x}(k+1) &= \mathbf{P}_{\text{IWAC}}\mathbf{x}(k), \\ \mathbf{x}^* = \lim_{k\to\infty} \mathbf{x}(k+1) &= \lim_{k\to\infty} \prod_{\ell=1}^{k} \mathbf{P}_{\ell_{\text{IWAC}}}\mathbf{x}(0), \\ \mathbf{x}^* &= \frac{\mathbf{1}\omega^T}{\omega^T\mathbf{1}}\mathbf{x}(0), \\ \text{where} \quad x_i^* &= \frac{\sum_{i=1}^{N} \omega_i x_i(0)}{\sum_{i=1}^{N} \omega_i}. \end{aligned} \tag{39}$$

□

5.1.2 | Dynamic networks

For a network with N SUs, there are a finite number of possible graphs (for example, r graphs). We denote the set of possible graphs $\{\mathcal{G}_1, \dots, \mathcal{G}_r\}$, and there are a correspondent set of Perron matrices $\{\mathbf{P}^1_{\text{IWAC}}, \dots, \mathbf{P}^r_{\text{IWAC}}\}$. Considering that $1 \le s \le r$. The *WAC rule* is given by

$$\mathbf{x}(k+1) = \mathbf{P}^{s(k)}_{\text{IWAC}}\mathbf{x}(k). \tag{40}$$

The proof for the dynamic network follows that the IWAC consensus iteration is a paracontraction* process with fixed points building by the eigenspaces of the Perron matrices.

For the connected graph $\mathcal{G}(k)$ and the Perron matrix $\mathbf{P}_{\text{IWAC}}$, a nonnegative primitive matrix has ω and $\mathbf{1}$ as the left and right eigenvector, respectively. For a paracontracting matrix, we denote the subspace $\mathbb{H}(\mathbf{P}_{\text{IWAC}})$, which is an eigenspace associated with eigenvalue 1. The collection of graphs $\{\mathcal{G}_1, \dots, \mathcal{G}_r\}$ are connected and occurs infinitely; the Perron matrices satisfy $\cap_{z=1}^{r}\mathbb{H}(\mathbf{P}^{z}_{\text{IWAC}}) = \text{span}(\mathbf{1})$. From the properties of the paracontracting process, the subspace is fixed; then, the iterative process has a limit, which is guaranteed by the Perron-Frobenius theorem that ensures the asymptotic convergence.

Hence, the following theorem guarantees the convergence of the IWAC procedure operating under dynamic DCSS networks.

Theorem 2. *For the IWAC iterative process, the step size* α *satisfying* $0 < \alpha < (\max_i \sum_{j\in\mathcal{N}_i}\omega_j)^{-1}$ *, with weight elements* ω_i *and* ω_j *for a dynamic cooperative communication occurring infinitely (infinite iterations), the IWAC rule converges to*

$$x_i^* = \lim_{k\to\infty} x_i(k) = \frac{\sum_{i=1}^{N}\omega_i x_i(0)}{\sum_{i=1}^{N}\omega_i} \quad or \quad \boldsymbol{x}^* = \frac{\mathbf{1}\omega^T}{\omega^T\mathbf{1}}\boldsymbol{x}(0). \tag{41}$$

Proof. The proof is similar to the fixed network case, given that the Perron-Frobenius applies. Hence, the proof is omitted. □

It should be observed that the convergence of the fixed and dynamic communications results in the same final result. Numerical evidence corroborating this fact is presented in Section 6.

6 | NUMERICAL RESULTS

In this section, we have compared the performance of various spectrum sensors discussed in this work. We have considered 4 scenarios, all of them with 1 PU, ie, PU= 1. In Scenario A, the network is fixed, ie, the SUs are considered static in the same position during the entire DCSS process. The channel is considered only under an AWGN noise effect, where the SUs' SNRs are contained in a range of $[-10, 0]$ dB. The Monte Carlo simulations (MCSs) have been realised considering a network with 6 and 10 SUs. In Scenario B, we consider 10 and 20 SUs in the network in an AWGN channel with SNRs between $[-10, 0]$ dB. Now, the scenario is dynamic, ie, the SUs has mobility in the network. In Scenario C, the channel is Rayleigh with SNR $\in [-2, 5]$ dB. Furthermore, the SUs are fixed and the simulations consider 6 and 10 SUs. Finally, in Scenario D, the network is dynamic under a Rayleigh channel and SNR values between $[-2, 5]$ dB; 10 and 20 SUs have been considered in the simulations. In Rayleigh channels, we have considered the weights ω_i as a perfect estimation of the average SNRs in each node. The main system parameters for Scenarios A to D are summarised in Table 2.

Table 3 depicts the main adopted simulation parameters values. These values are adopted by all scenarios. For each MCS, 5000 realisations have been considered with 12 samples per decision and a fail probability communication between SUs in the dynamic channel as $\text{Pr}_{\text{fail}} = 0.4$.

6.1 | Network topology

In this work, we consider 3 different topologies to the cognitive network. The distributed network topology is based on graph theory. The application of graph theory in network context for consensus spectrum sensing purpose has been described in Section 3.2.

6.1.1 | Topology I - 6 SUs

This topology is based on the work of Kailkhura et al[18] and depicted previously in Figure 1. The 6 SUs cooperate with each other until the consensus convergence. 1 The associated adjacency matrix is defined in Equation 13.

*A paracontraction is a process where $||\mathbf{P}_{\text{IWAC}}\mathbf{x}|| \leq ||\mathbf{x}|| \iff \mathbf{P}_{\text{IWAC}}\mathbf{x} \neq \mathbf{x}$ is guaranteed.

TABLE 2 System scenarios considering PU = 1 user

Parameter	Adopted Values
Scenario **A**	
Channel	AWGN
Network type	Fixed, $Pr_{fail} = 0$
Secondary users	SU $\in \{6, 10\}$ users
Range of SNR	$SNR_{SU} \in \{0, -10\}$ [dB]
Scenario **B**	
Channel	AWGN
Network type	Dynamic, $Pr_{fail} = 0.4$
Secondary users	SU $\in \{10, 20\}$ users
Range of SNR	$SNR_{SU} \in \{0, -10\}$ [dB]
Scenario **C**	
Channel	Flat Rayleigh
Network type	Fixed, $Pr_{fail} = 0$
Secondary users	SU $\in \{6, 10\}$ users
Range of SNR	$SNR_{SU} \in \{-2, 5\}$ [dB]
Scenario **D**	
Channel	Flat Rayleigh
Network type	Dynamic, $Pr_{fail} = 0.4$
Secondary users	SU $\in \{10, 20\}$ users
Range of SNR	$SNR_{SU} \in \{-2, 5\}$ [dB]

Abbreviations: AWGN, additive white Gaussian noise; PU, primary user; SNR, signal-noise ratio; SU, secondary user.

TABLE 3 Reference values used in simulations

Parameter	Adopted Value
Samples	$N_s = 12$
MCS trials	5000
SUs	SU $\in \{6, 10, 20\}$
PUs	1
Pr_{fail}	0.4
SNR range	$SNR_{SU} \in \{-10, 5\}$ [dB]
Channels	AWGN, Rayleigh
Network	Fixed, dynamic

Abbreviations: AWGN, additive white Gaussian noise; MCS, Monte Carlo simulation; PU, primary user; SNR, signal-noise ratio; SU, secondary user.

6.1.2 | Topology II - 10 SUs

This topology is based on previous works.[8-10] The 10 SUs cooperate with each other until the consensus convergence. Figure 2 shows the network topology.

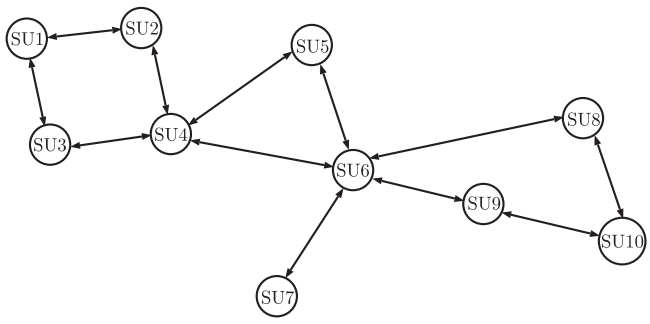

FIGURE 2 Decentralised cooperative scheme with 10 secondary users (SUs)[8]

As a consequence, the adjacent matrix in Equation 42 defines the network topology represented by the graph of Figure 2.

$$\mathbf{G}_{10} = \begin{bmatrix} 0 & 1 & 1 & 0 & 0 & 0 & 0 & 0 & 0 & 0 \\ 1 & 0 & 0 & 1 & 0 & 0 & 0 & 0 & 0 & 0 \\ 1 & 0 & 0 & 1 & 0 & 0 & 0 & 0 & 0 & 0 \\ 0 & 1 & 1 & 0 & 1 & 1 & 0 & 0 & 0 & 0 \\ 0 & 0 & 0 & 1 & 0 & 1 & 0 & 0 & 0 & 0 \\ 0 & 0 & 0 & 1 & 1 & 0 & 1 & 1 & 1 & 0 \\ 0 & 0 & 0 & 0 & 0 & 1 & 0 & 0 & 0 & 0 \\ 0 & 0 & 0 & 0 & 0 & 1 & 0 & 0 & 0 & 1 \\ 0 & 0 & 0 & 0 & 0 & 1 & 0 & 0 & 0 & 1 \\ 0 & 0 & 0 & 0 & 0 & 0 & 0 & 1 & 1 & 0 \end{bmatrix} \tag{42}$$

6.1.3 | Topology III – 20 SUs

We create a new topology to characterise the performance of the DCSS methods in larger networks. The 20 SUs cooperate with each other until the CSS consensus achieves convergence. Figure 3 depicts the graph for the network topology, and the adjacent matrix $\mathbf{G}_{20}$ is straightforwardly defined in a similar way of the $\mathbf{G}_{10}$ in *Topology II*.

6.2 | Parameter values and scenarios

The 2 main parameters analysed in this work are the numerical *cooperative consensus convergence* and ROC. The goal of the numerical convergence analysis is to determine and compare the number of iterations needed for each consensus spectrum sensing technique that achieves practical convergence. The parameter considered herein is the level of energy of each ED in decibel. The cooperative consensus convergence is given when the energy difference ΔE among all the SUs' output energy detected is $\Delta E \leq 1$ dB. The ROC analysis is the main figure of merit of analysis in the SS methods. The ROC is the relation of the probability of detection against the probability of false alarm.

6.3 | Convergence

In this section, we consider the numerical convergence as a figure of merit for analysis of the 4 consensus-based distributed spectrum sensing methods. The consensus methods are numerically compared considering the different scenarios aiming

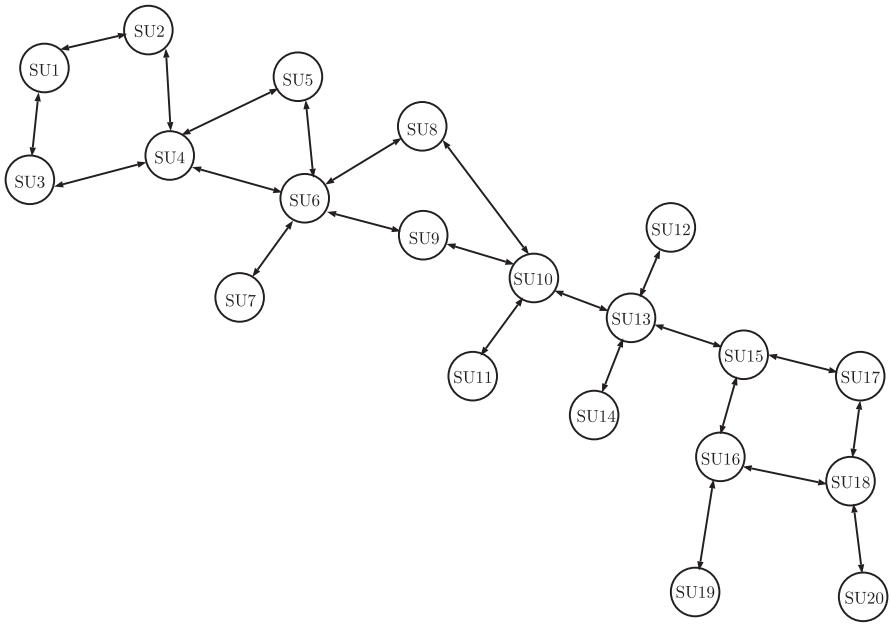

FIGURE 3 Decentralised cooperative scheme with 20 secondary users (SUs)

TABLE 4 The number of iterations for the DCSS method to achieve convergence under $\Delta E \leq 1$ [dB]

Scenario	#SUs	AC	WAC	WAC-AE	IWAC
A-AWGN	**6**	4	15	5	15
(Fixed)	10	4	6	9	10
B-AWGN	10	4	6	9	10
(Mobile)	20	22	25	30	31
C-Rayleigh	6	15	19	35	34
(Fixed)	10	19	11	18	27
D-Rayleigh	10	19	11	18	27
(Mobile)	20	42	48	>50	>50

Abbreviations: AC, average consensus; AWGN, additive white Gaussian noise; DCSS, distributed cooperative spectrum sensing; IWAC, improved weighted average consensus; SU, secondary user; WAC, weighted average consensus; WAC-AE, weighted average consensus accuracy exchange.

at demonstrating the effectiveness of the spectrum sensing methods. The results regarding the number of iterations for convergence are synthesised in Table 4.

For Scenario A, the network with 10 SUs needs a less average number of iterations to reach the convergence criterion $\Delta E \leq 1$ [dB], compared with the network with 6 SUs, due to the higher availability of connections among the SU neighbours. On average, the AC method needs less number of iterations than the WAC, WAC-AE, and IWAC methods to achieve convergence in almost all scenarios, including AWGN × Rayleigh, fixed × mobile channels, and a low-medium × a high number of cooperative SUs.

In most cases, the IWAC method requires a higher number of iterations to achieve ΔE-based convergence, whereas the WAC-AE method operating under dynamic/mobile channels needs approximately the same number of iterations compared with the IWAC method yet higher than AC and WAC methods. Moreover, as expected, in the Rayleigh channel scenarios, all methods require a higher number of iterations to achieve convergence due to the channel characteristics. Notice that, in the analysed numerical simulations, we have averaged on 500 channel realisations; the Rayleigh channel coefficients and SU localisation (reflecting different SNRs_{SU}) have been taken randomly and deployed to characterise the spectrum sensing detectors' convergence.

Figure 4 depicts convergence behaviour for the 4 AC detectors in the case of 10 SUs operating under dynamic AWGN channels, whereas Figure 5 reveals the convergence trend for the case of 10 cooperative SUs in a fixed network under Rayleigh channels.

6.4 | Receiver operating characteristic

The global ROC for the various spectrum sensing methods is numerically compared considering different scenarios (A, B, C, and D) aiming at demonstrating the effectiveness of the proposed cooperative IWAC method under both AWGN and non-line-of-sight–Rayleigh channels. Indeed, Figure 6 depicts the ROC for several classical methods and the proposed IWAC and WAC-AE DCSS methods, considering 6, 10, and 20 SUs, AWGN Channel, fixed and dynamic Networks.

For the 6 SUs, the WAC and the proposed WAC-AE methods have similar performance and can be compared with that of the MRC rule, which represents the optimum centralised SS performance. The proposed IWAC method presents a slight degradation compared with the WAC and WAC-AE methods but keeps better performance compared with the AC method, which has similar performance with the EGC rule. On the other hand, the classical hard combining rules result in poor performance compared with the soft combining rule. Among all classical rules, the OR rule has the best performance whereas the AND rule presents the worse performance. A similar conclusion can be obtained for 10 and 20 SUs (see Figures 6B, 6C, and 6D). Moreover, the mobility of network does not affect substantially the ROC performance of all spectrum sensing techniques operating under AWGN channels.

The ROC behaviour for the 9 spectrum sensing rules operating under Rayleigh channels and 6, 10, and 20 fixed and dynamic SUs is depicted in Figure 7. Again, for 6 SUs, the IWAC, WAC-AE, and WAC methods demonstrate similar performance when compared with the optimum performance (MRC rule). The AC method has similar performance to the EGC rule, and for this scenario, it results in a similar performance of the MRC and WAC methods. Interestingly, one can conclude that, in severe Rayleigh fading channels scenarios, the OR rule results in a

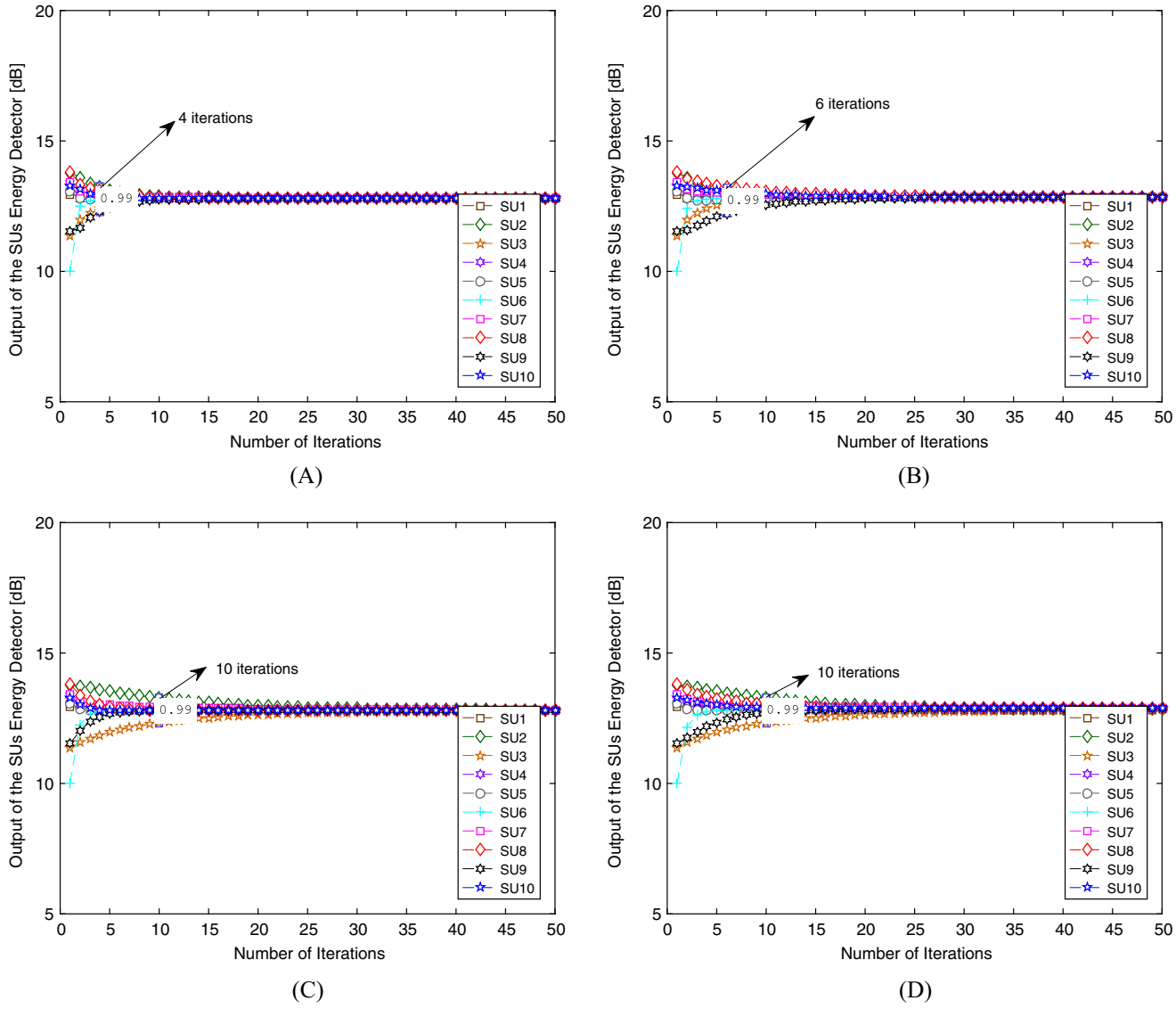

FIGURE 4 Convergence for the different decentralised cooperative spectrum sensing under AC rules considering 10 secondary users (SUs) and dynamic additive white Gaussian noise channel. A, AC; B, WAC; C, WAC-AE; D, Proposed IWAC. AC, average consensus; IWAC, improved weighted average consensus; WAC, weighted average consensus; WAC-AE, weighted average consensus accuracy exchange

suitable performance whereas the AND rule performances has worse. A similar conclusion can be obtained for a different number of cooperative SUs. Finally, the mobility of network does not affect the ROC performance substantially. Note that the suitable ROC performance achieved for all rules, except the AND rule, under Rayleigh channels could be attained because of a higher range of $\mathrm{SNR}_{\mathrm{SU}} \in \{-2, 5\}$ [dB] when compared with the SNR range adopted in AWGN scenarios.

6.4.1 | Analytical versus simulated ROC

Figure 8 demonstrates the local (distributed) ROC for the proposed IWAC-DCSS method considering only Scenario A (6 and 10 SUs in an AWGN fixed channel). The analytical expression for the ROC of each SU inspired in Equation 10, but considering the local decision, is compared with the numerical MCS results. In the analytical performance considering a fail probability at the ith SU, P_f^i can be described adapting Equation 10 to the distributed IWAC soft CSS decision as follows:

$$\mathrm{P}_d^i = Q\left(\frac{Q^{-1}\left(\mathrm{P}_f^i\right)\sqrt{\mathrm{var}(x_i|\mathcal{H}_0)} - \mathbb{E}(x_i|\mathcal{H}_1) + \mathbb{E}(x_i|\mathcal{H}_0)}{\sqrt{\mathrm{var}(x_i|\mathcal{H}_1)}}\right), \tag{43}$$

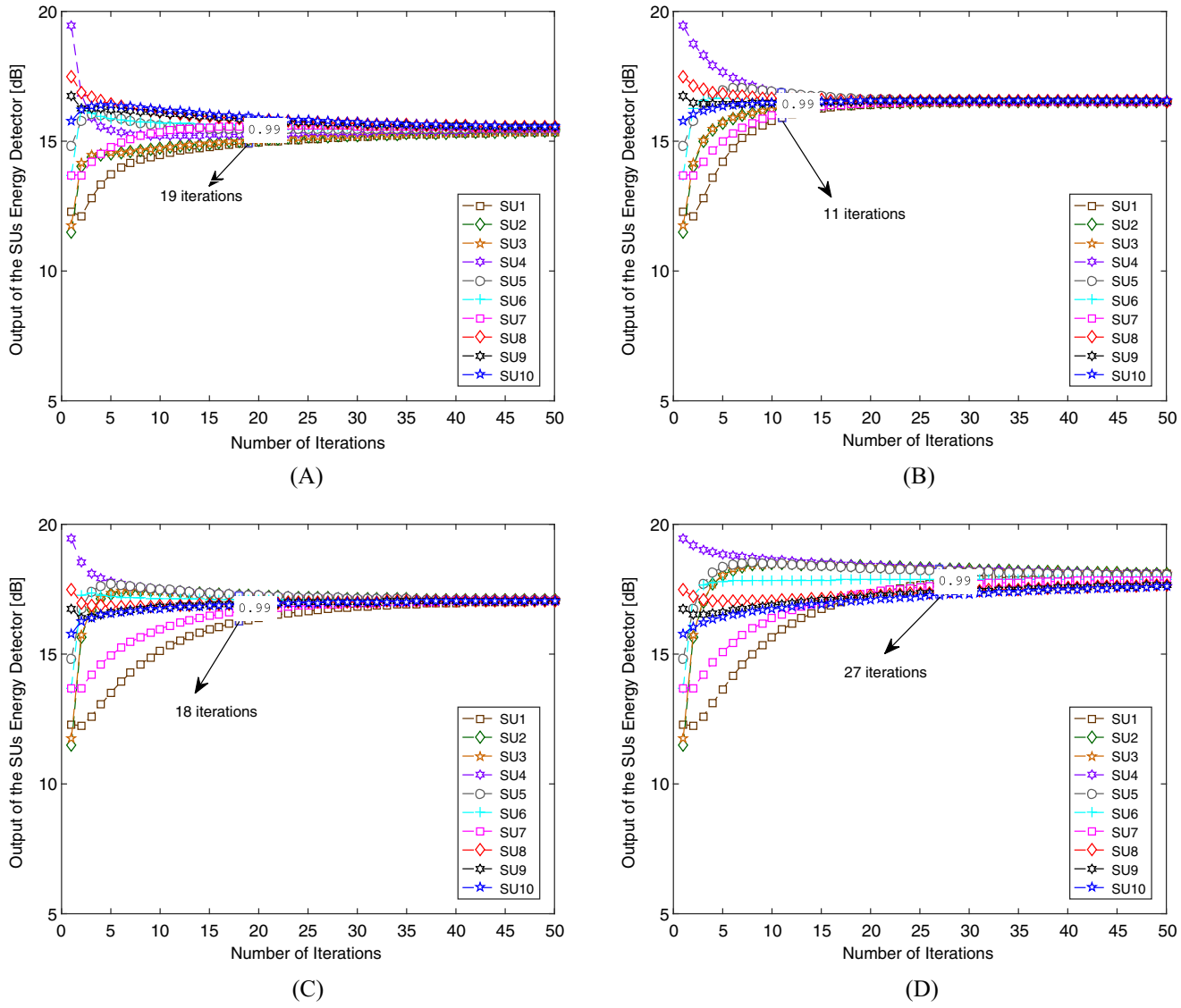

FIGURE 5 Convergence for the different decentralised cooperative spectrum sensing rules considering 10 secondary users (SUs) under fixed Rayleigh channel. A, AC; B, WAC; C, WAC-AE; D, Proposed IWAC. AC, average consensus; IWAC, improved weighted average consensus; WAC, weighted average consensus; WAC-AE, weighted average consensus accuracy exchange

where

$$\mathbb{E}(x_i|\mathcal{H}_{0,1}) = \begin{cases} \left(\prod_{\ell=1}^{k} \mathbf{P}_{\ell_{\text{IWAC}}} \mathbb{E}(\mathbf{x}(0)|\mathcal{H}_0)\right)_i & ,\mathcal{H}_0 \\ \left(\prod_{\ell=1}^{k} \mathbf{P}_{\ell_{\text{IWAC}}} \mathbb{E}(\mathbf{x}(0)|\mathcal{H}_1)\right)_i & ,\mathcal{H}_1 \end{cases} \tag{44}$$

$$\text{var}(x_i|\mathcal{H}_{0,1}) = \begin{cases} \left(\prod_{\ell=1}^{k} \mathbf{P}_{\ell_{\text{IWAC}}} \text{cov}(\mathbf{x}(0)|\mathcal{H}_0) \prod_{\ell=1}^{k} \mathbf{P}_{\ell_{\text{IWAC}}}\right)_{ii} & ,\mathcal{H}_0 \\ \left(\prod_{\ell=1}^{k} \mathbf{P}_{\ell_{\text{IWAC}}} \text{cov}(\mathbf{x}(0)|\mathcal{H}_1) \prod_{\ell=1}^{k} \mathbf{P}_{\ell_{\text{IWAC}}}\right)_{ii} & ,\mathcal{H}_1, \end{cases} \tag{45}$$

where $\text{cov}(\mathbf{x}) = \mathbb{E}[(\mathbf{x} - \mathbb{E}(\mathbf{x}))(\mathbf{x} - \mathbb{E}(\mathbf{x}))^T]$ is the covariance matrix of the vector $\mathbf{x}$.

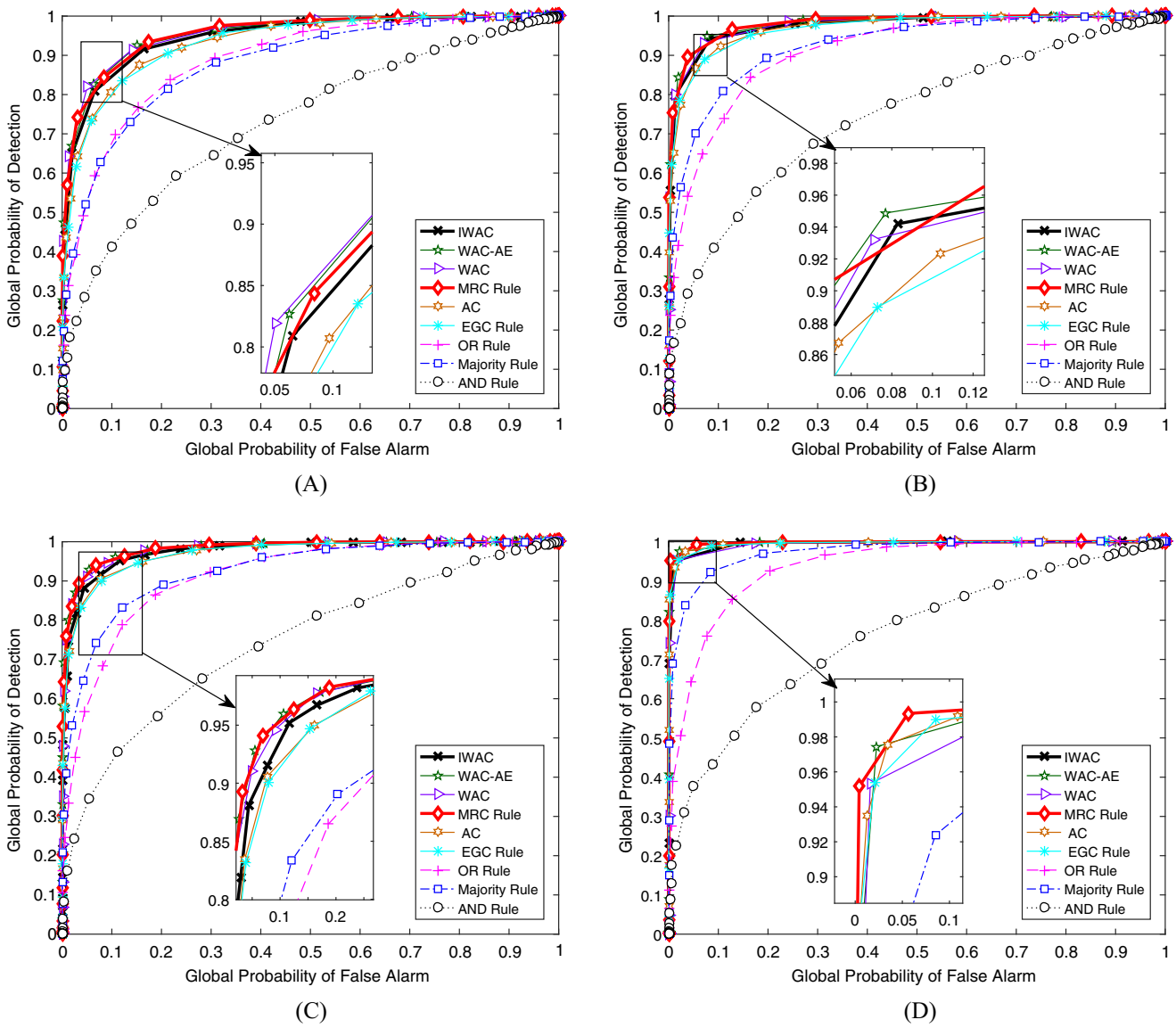

FIGURE 6 Global receiver operating characteristic for several decentralised cooperative spectrum sensing methods operating with 6, 10, and 20 secondary users (SUs) for fixed and dynamic networks in **additive white Gaussian noise channels**. A, **Fixed** network, 6 SUs; B, **Fixed** network, 10 SUs; C, **Mobile** network, 10 SUs; D, **Mobile** network, 20 SUs. AC, average consensus; EGC, equal gain combining; IWAC, improved weighted average consensus; MRC, maximal ratio combining; WAC, weighted average consensus; WAC-AE, weighted average consensus accuracy exchange

Indeed, for Scenario A, Figure 8 demonstrates a suitable fitting among the Monte Carlo simulated results and the analytical expression, evidencing that the set of Equations 43 to 45 is a valid analytical description to characterise the IWAC ROC performance.

6.5 | Computational complexity and average convergence time for DAC techniques

The *average convergence time* for the AC methods was established in the work of Benezit et al,[22] considering a large number of nodes n (or number of SUs) in the network as

$$\mathcal{T}_{\mathrm{AC}}(n) = \mathcal{O}\left(\frac{\log(n)}{1-\rho_2(\mathbb{E}[\mathbf{P}^T\mathbf{P}])}\right), \quad (\text{large } n),$$

where ρ_2 is the second largest eigenvalue modulo (SLEM), the associated Perron matrix is $\mathbf{P}$, and n is the number of nodes in the network (number of SUs). When $\rho_2(\mathbb{E}[\mathbf{P}^T\mathbf{P}]) \to 1$, it implies that the number of secondary users in the network

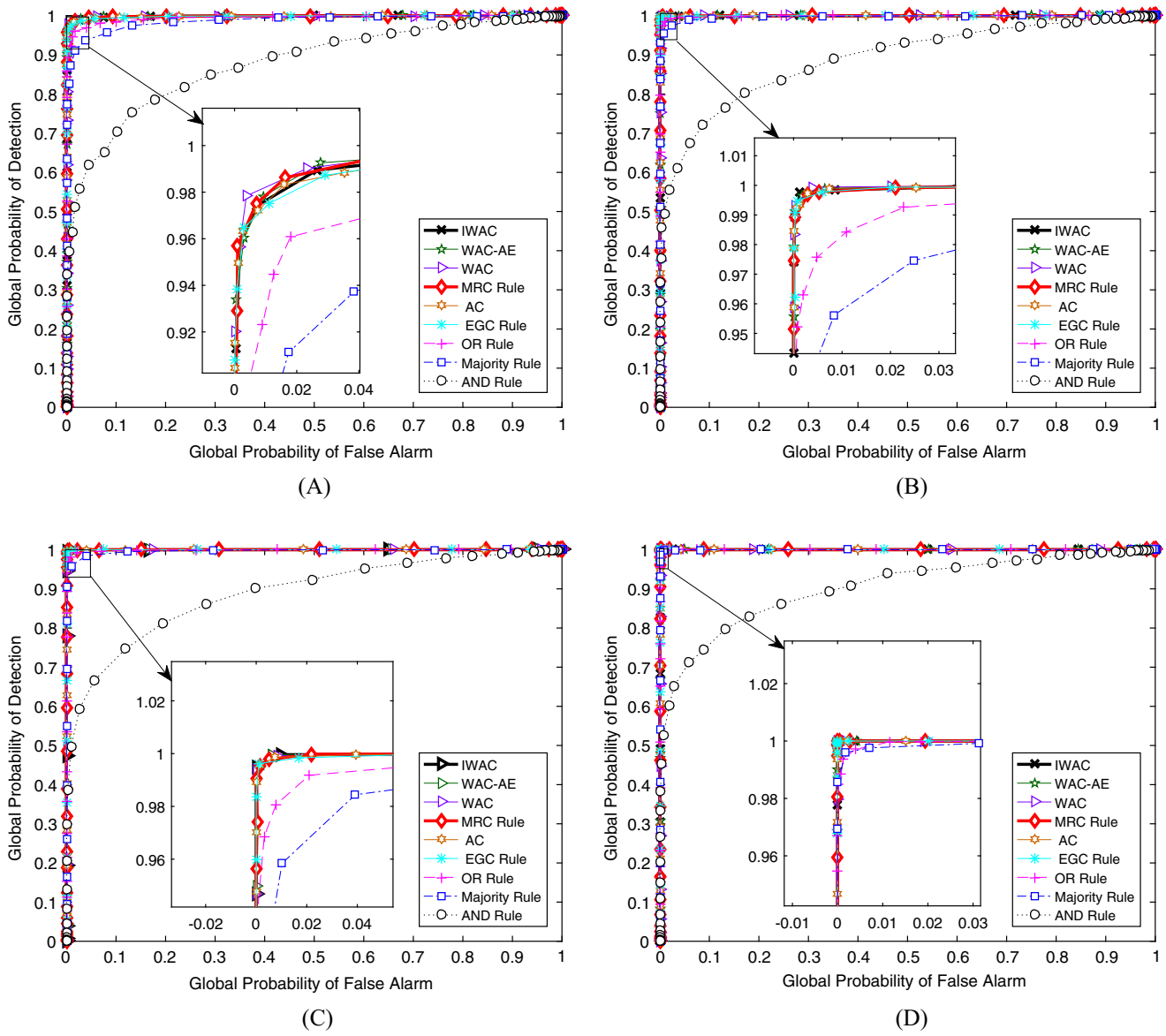

FIGURE 7 Global receiver operating characteristic for several decentralised cooperative spectrum sensing methods operating with 6, 10, and 20 secondary users (SUs) for fixed and dynamic networks operating under **Rayleigh channels**. A, **Fixed** network, 6 SUs; B, **Fixed** network, 10 SUs; C, **Mobile** network, 10 SUs; D, **Mobile** network, 20 SUs. AC, average consensus; EGC, equal gain combining; IWAC, improved weighted average consensus; MRC, maximal ratio combining; WAC, weighted average consensus; WAC-AE, weighted average consensus accuracy exchange

tends to infinity, ie, $n \to \infty$. In this way, the *average convergence time* allows us to verify the dependence of the number of iterations for convergence regarding the size of the network and the AC rule chosen. In other words, the higher the value of $\rho_2(\mathbb{E}(\mathbf{P}^T\mathbf{P}))$, the more time is required to the consensus rule to achieve convergence.

The AC complexity analysis based on SLEM values associated to the Perron matrices for each AC rule analysed in this work confirms the tendency found in our numerical results of Section 6.3, corroborating our findings that the AC rule achieves reduced convergence time among the analysed rules, followed by our proposed WAC-AE and IWAC rules, and finally by the WAC rule. In fact, in our paper, we consider a low number of nodes in the network. Hence, a more appropriate expression correlating the SLEM (ρ_2) and average convergence time is as follows[23]:

$$\widetilde{\tau}_{\text{AC}} = \frac{1}{\ln\left(\frac{1}{\rho_2(\mathbb{E}[\mathbf{P}])}\right)} \qquad \text{(small or medium } n\text{)},$$

where $\ln(\cdot)$ is the natural logarithm.

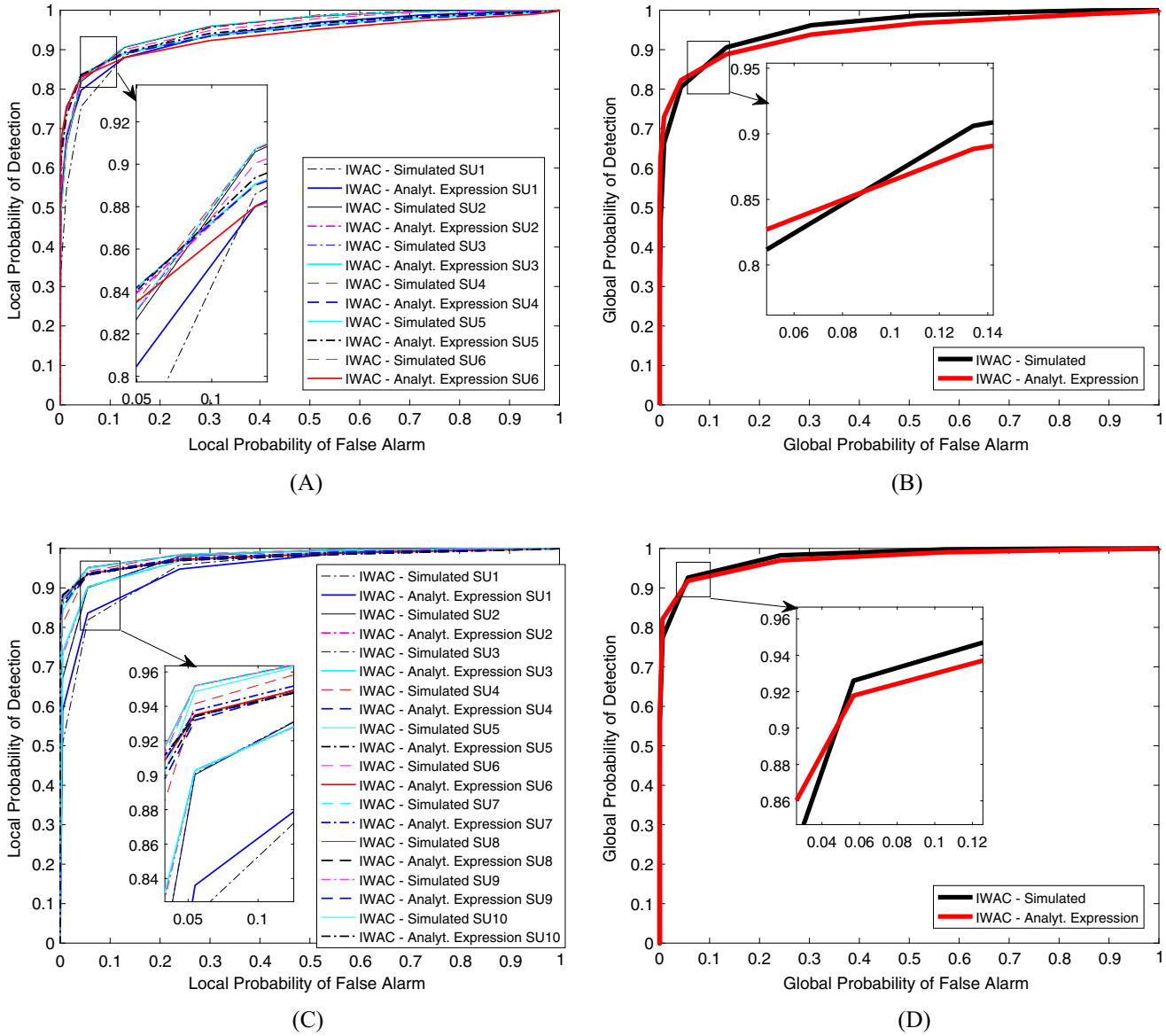

FIGURE 8 Local and global receiver operating characteristic for 6 and 10 secondary users (SUs) under additive white Gaussian noise channel Scenario A. A, **Fixed** network, 6 SUs; B, **Fixed** network, 6 SUs; C, **Fixed** network, 10 SUs; D, **Fixed** network, 10 SUs. IWAC, improved weighted average consensus

TABLE 5 Computational complexity for DAC algorithms

AC Rule Algorithm	Consensus Method	Asymptotic Complexity
1	**AC**	$\mathcal{O}(KN)$
2	**WAC**	$\mathcal{O}(KN^2)$
3	**WAC-AE**	$\mathcal{O}(KN^2)$
4	**IWAC**	$\mathcal{O}(KN^2)$

Abbreviations: AC, average consensus; IWAC, improved weighted average consensus; WAC, weighted average consensus; WAC-AE, weighted average consensus accuracy exchange.

The asymptotic expressions for the computational complexity of the analysed AC rules have been determined from the AC pseudocodes (Section 4) and depicted in Table 5. As expected, the AC has the lower computational complexity among all AC distributed SS methods. The methods WAC, WAC-AE, and IWAC distributed consensus methods present same computational complexity order, resulting in a quadratic dependence with the number of SUs N and a linear dependence with the number of iterations K.

7 | CONCLUSIONS

In this paper, we have proposed and analysed 2 new decentralised average consensus-based spectrum sensing schemes, namely, IWAC and WAC-AE, and have compared their performance and complexity with 2 other conventional CSS decentralised consensus-based methods (AC and WAC), as well as other traditional centralised CSS under hard and soft combining rules. The performance comparison is made regarding the ROC and numerical *versus* analytical convergence. The proposed IWAC method results in a similar convergence rate to that of the WAC-AE method.

Regarding the ROC analysis, the WAC and WAC-AE methods demonstrate similar performance, which is comparable with that of the centralised MRC rule. Moreover, the AC method and EGC have also similar performance, which results worse than the MRC performance. Indeed, the proposed decentralised IWAC method has demonstrated an ROC performance in between the centralised MRC and EGC rules.

The weighted DCSS methods discussed herein result in a similar computational complexity cost, being asymptotically equal to the product of the squared number of cooperative SUs and the number of iterations, ie, N^2K. Another way to evaluate the complexity of the AC rules is the *average convergence time* based on the SLEM, which is dependent on the associated Perron matrix $\mathbf{P}$ and the number of SUs n. The AC complexity analysis based on SLEM has confirmed the tendency found in our numerical simulation results, corroborating our conclusion that the AC rule achieves reduced convergence time among the analysed rules followed by our proposed WAC-AE and IWAC rules and, finally, by the WAC rule. In summary, the IWAC method results in a similar convergence rate than the WAC-AE method but slightly higher than the AC and WAC methods.

ACKNOWLEDGEMENTS

This work was supported in part by the Conselho Nacional de Desenvolvimento Científico e Tecnológico (CNPq) of Brazil under grants 304066/2015-0 and 308348/2016-8, through the scholarship by Coordenação de Aperfeiçoamento de Pessoal de Nível Superior (CAPES), Brazil, and by the Universidade Estadual de Londrina (UEL)-Paraná State Government (UEL).

ORCID

Taufik Abrão http://orcid.org/0000-0001-8678-2805

REFERENCES

1. FCC Spectrum Policy Task Force. Report of the spectrum efficiency working group; 2002. https://transition.fcc.gov/sptf/reports.html
2. Mitola III J, Maguire Jr GQ. Cognitive radio: making software radios more personal. *IEEE Pers Commun*. 1999;6(4):13-18. https://doi.org/10.1109/98.788210
3. Haykin S. Cognitive radio: brain-empowered wireless communications. *IEEE J Sel Areas Commun*. 2005;23(2):201-220.
4. Stevenson CR, Chouinard G, Lei Z, Hu E, Shellhammer SJ, Caldwell W. IEEE 802.22: the first cognitive radio wireless regional area network standard. *Comm Mag*. 2009;47(1):130-138. https://doi.org/10.1109/MCOM.2009.4752688
5. Ibnkahla M, Alkheir AA. *Cooperative Cognitive Radio Networks: The Complete Spectrum*. Boca Raton, FL, USA: CRC Press Inc; 2014.
6. Wu R. Distributed spectrum sensing using belief propagation framework. Paper presented at: 2014 IEEE International Inter-Disciplinary Conference on Cognitive Methods in Situation Awareness and Decision Support (CogSIMA); March 2014; San Antonio, TX, USA.
7. Ding G, Wang J, Wu Q, et al. Robust spectrum sensing with crowd sensors. *IEEE Trans Commun*. 2014;62(9):3129-3143.
8. Zhang W, Guo Y, Liu H, Chen Y, Wang Z, Mitola III J. Distributed consensus-based weight design for cooperative spectrum sensing. *IEEE Trans Parallel and Distrib Syst*. 2015;26(1):54-64.
9. Li Z, Yu FR, Huang M. A distributed consensus-based cooperative spectrum-sensing scheme in cognitive radios. *IEEE Trans Veh Technol*. 2010;59(1):383-393.
10. Zhang W, Wang Z, Guo Y, Liu H, Chen Y, Mitola III J. Distributed cooperative spectrum sensing based on weighted average consensus. Paper presented at: 2011 IEEE Global Telecommunications Conference (GLOBECOM); December 2011; Kathmandu, Nepal.

11. Ashrafi S, Malmirchegini M, Mostofi Y. Binary consensus for cooperative spectrum sensing in cognitive radio networks. Paper presented at: 2011 IEEE Global Telecommunications Conference (GLOBECOM); December 2011; Kathmandu, Nepal.
12. Li Z, Yu FR, Huang M. A cooperative spectrum sensing consensus scheme in cognitive radios. Paper presented at: IEEE INFOCOM 2009; April 2009; Rio de Janeiro, Brazil.
13. Teguig D, Scheers B, Nir VL, Horlin F. Consensus algorithms for distributed spectrum sensing based on goodness of fit test in cognitive radio networks. Paper presented at: 2015 International Conference on Military Communications and Information Systems (ICMCIS); May 2015; Cracow, Poland.
14. Anderson TW, Darling DA. Asymptotic theory of certain goodness of fit criteria based on stochastic processes. *Ann Math Stat*. 1952;23:193-212.
15. Vosoughi A, Cavallaro JR, Marshall A. Trust-aware consensus-inspired distributed cooperative spectrum sensing for cognitive radio ad hoc networks. *IEEE Trans Cogn Commun and Netw*. 2016;2(1):24-37.
16. Soatti G, Nicoli M, Savazzi S, Spagnolini U. Consensus-based algorithms for distributed network-state estimation and localization. *IEEE Trans Signal and Info Process over Netw*. 2016;99:1-1.
17. Nurellari E, McLernon D, Ghogho M. Distributed two-step quantized fusion rules via consensus algorithm for distributed detection in wireless sensor networks. *IEEE Trans Signal and Info Process over Netw*. 2016;2(3):321-335.
18. Kailkhura B, Brahma S, Varshney PK. Data falsification attacks on consensus-based detection systems. *IEEE Trans Signal and Info Process over Netw*. 2017;3(1):145-158.
19. Urkowitz H. Energy detection of unknown deterministic signals. *Proc IEEE*. 1967;55(4):523-531.
20. Yu FR, Huang M, Tang H. Biologically inspired consensus-based spectrum sensing in mobile ad hoc networks with cognitive radios. *IEEE Network*. 2010;24(3):26-30.
21. Horn RA, Johnson CR, eds. *Matrix Analysis*. New York, NY, USA: Cambridge University Press; 1986.
22. Benezit F, Dimakis AG, Thiran P, Vetterli M. Order-optimal consensus through randomized path averaging. *IEEE Trans Inf Theory*. 2010;56:5150-5167.
23. Boyd S, Ghosh A, Prabhakar B, Shah D. Randomized gossip algorithms. *IEEE/ACM Trans Netw*. 2006;14:2508-2530.

How to cite this article: Hernandes AG, Proença Jr ML, Abrão T. Improved weighted average consensus in distributed cooperative spectrum sensing networks. *Trans Emerging Tel Tech*. 2017;e3259. https://doi.org/10.1002/ett.3259

Referências

ASHRAFI, S.; MALMIRCHEGINI, M.; MOSTOFI, Y. Binary consensus for cooperative spectrum sensing in cognitive radio networks. In: . Houston, TX, USA: Global Telecommunications Conference (GLOBECOM 2011), 2011 IEEE, 2011. p. 1–6.

BHARGAVI, D.; MURTHY, C. Performance comparison of energy, matched-filter and cyclostationarity-based spectrum sensing. In: . Marrakech, Morocco: Signal Processing Advances in Wireless Communications (SPAWC), 2010 IEEE Eleventh International Workshop on, 2010. p. 1–5.

DHOPE, T.; SIMUNIC, D. On the performance of AoA estimation algorithms in cognitive radio networks. In: . Mumbai, India: Communication, Information Computing Technology (ICCICT), 2012 International Conference on, 2012. p. 1–5.

DOHLER, M.; LI, Y. *Cooperative communications : hardware, channel & PHY*. Chichester, West Sussex, U.K., Hoboken, NJ: Wiley, 2010.

FCC Spectrum Policy Task Force. *Report of the spectrum efficiency working group*. Washington, D.C., USA: FCC, 2002.

HATTAB, G.; IBNKAHLA, M. Multiband spectrum access: Great promises for future cognitive radio networks. Proceedings of the IEEE, USA, v. 102, n. 3, p. 282–306, March 2014.

HAYKIN, S. Cognitive radio: brain-empowered wireless communications. Selected Areas in Communications, IEEE Journal on, USA, v. 23, n. 2, p. 201–220, February 2005.

HONGNING, L.; XIANJUN, L.; LEILEI, X. Analysis of distributed consensus-based spectrum sensing algorithm in cognitive radio networks. In: . China: Computational Intelligence and Security (CIS), 2014 Tenth International Conference on, 2014. p. 593–597.

HOSSAIN DUSIT NIYATO, Z. H. E. *Dynamic Spectrum Access and Management in Cognitive Radio Networks*. 1. ed. The Edinburgh Building, Cambridge CB2 8RU, UK: Cambridge University Press, 2009.

IBNKAHLA, M. *Cooperative cognitive radio networks : the complete spectrum cycle*. USA: CRC Press, 2014.

LI, Z.; YU, F. R.; HUANG, M. A cooperative spectrum sensing consensus scheme in cognitive radios. In: . Rio de Janeiro, Brazil: INFOCOM 2009, IEEE, 2009. p. 2546–2550.

LI, Z.; YU, F. R.; HUANG, M. A distributed consensus-based cooperative spectrum-sensing scheme in cognitive radios. IEEE Transactions on Vehicular Technology, USA, v. 59, n. 1, p. 383–393, January 2010.

LIANG, Y. C.; ZENG, Y.; PEH, E.; HOANG, A. T. Sensing-throughput tradeoff for cognitive radio networks. In: . Glasgow, Scotland: 2007 IEEE International Conference on Communications, 2007. p. 5330–5335.

LIANG, Y.-C.; ZENG, Y.; PEH, E.; HOANG, A. T. Sensing-throughput tradeoff for cognitive radio networks. Wireless Communications, IEEE Transactions on, USA, v. 7, n. 4, p. 1326–1337, April 2008.

MITOLA, J.; MAGUIRE G.Q., J. Cognitive radio: making software radios more personal. Personal Communications, IEEE, USA, v. 6, n. 4, p. 13–18, August 1999.

PEH, E. C. Y.; LIANG, Y. C.; GUAN, Y. L. Optimization of cooperative sensing in cognitive radio networks: A sensing-throughput tradeoff view. In: . Dresden, Germany: 2009 IEEE International Conference on Communications, 2009. p. 1–5.

ROY, R.; PAULRAJ, A.; KAILATH, T. Direction-of-arrival estimation by subspace rotation methods - ESPRIT. In: . Tokyo, Japan: Acoustics, Speech, and Signal Processing, IEEE International Conference on ICASSP '86., 1986. v. 11, p. 2495–2498.

SCHMIDT, R. Multiple emitter location and signal parameter estimation. Antennas and Propagation, IEEE Transactions on, USA, v. 34, n. 3, p. 276–280, March 1986.

SULEIMAN, W.; PESAVENTO, M.; ZOUBIR, A. M. Decentralized cooperative detection based on averaging consensus. In: . Rio de Janeiro, Brazil: 2016 IEEE Sensor Array and Multichannel Signal Processing Workshop (SAM), 2016. p. 1–5.

SUTTON, P. D.; NOLAN, K. E.; DOYLE, L. E. Cyclostationary signatures in practical cognitive radio applications. *IEEE Journal on Selected Areas in Communications*, v. 26, n. 1, p. 13–24, January 2008. ISSN 0733-8716.

TEGUIG, D.; SCHEERS, B.; NIR, V. L.; HORLIN, F. Consensus algorithms for distributed spectrum sensing based on goodness of fit test in cognitive radio networks. In: . Cracow, Poland: Military Communications and Information Systems (ICMCIS), 2015 International Conference on, 2015. p. 1–5.

TIAN, Z.; GIANNAKIS, G. A wavelet approach to wideband spectrum sensing for cognitive radios. In: . Mykonos Island, Greece: 2006 1st International Conference on Cognitive Radio Oriented Wireless Networks and Communications, 2006. p. 1–5.

TIAN, Z.; GIANNAKIS, G. B. Compressed sensing for wideband cognitive radios. In: . Honolulu, HI, USA: 2007 IEEE International Conference on Acoustics, Speech and Signal Processing - ICASSP '07, 2007. v. 4, p. IV–1357–IV–1360.

VOSOUGHI, A.; CAVALLARO, J. R.; MARSHALL, A. Trust-aware consensus-inspired distributed cooperative spectrum sensing for cognitive radio ad hoc networks. IEEE Transactions on Cognitive Communications and Networking, USA, v. 2, n. 1, p. 24–37, March 2016.

WEI, J.; HAIXI, C.; ZHEN, Y. Distributed cooperative spectrum sensing based on consensus among reliable secondary users. In: . Nanjing, China: Wireless Communications Signal Processing (WCSP), 2015 International Conference on, 2015. p. 1–6.

WYGLINSKI MAZIAR NEKOVEE, T. H. A. M. *Cognitive Radio Communications and Networks: Principles and Practice*. Amsterda: Elsevier, 2009.

YAN, Q.; LI, M.; JIANG, T.; LOU, W.; HOU, Y. T. Vulnerability and protection for distributed consensus-based spectrum sensing in cognitive radio networks. In: . Orlando, FL, USA: INFOCOM, 2012 Proceedings IEEE, 2012. p. 900–908.

YU, F. R.; HUANG, M.; TANG, H. Biologically inspired consensus-based spectrum sensing in mobile ad hoc networks with cognitive radios. IEEE Network, USA, v. 24, n. 3, p. 26–30, May 2010.

YUCEK, T.; ARSLAN, H. A survey of spectrum sensing algorithms for cognitive radio applications. Communications Surveys Tutorials, IEEE, USA, v. 11, n. 1, p. 116–130, First 2009.

ZENG, Y.; LIANG, Y.-C. Eigenvalue-based spectrum sensing algorithms for cognitive radio. Communications, IEEE Transactions on, USA, v. 57, n. 6, p. 1784–1793, June 2009.

ZENG, Y.; LIANG, Y.-C. Spectrum-sensing algorithms for cognitive radio based on statistical covariances. Vehicular Technology, IEEE Transactions on, USA, v. 58, n. 4, p. 1804–1815, May 2009.

ZHANG, W.; GUO, Y.; LIU, H.; CHEN, Y. .; WANG, Z.; III, J. M. Distributed consensus-based weight design for cooperative spectrum sensing. IEEE Transactions on Parallel and Distributed Systems, USA, v. 26, n. 1, p. 54–64, January 2015.

ZHANG, Y.; ZHENG, J.; CHEN, H.-H. *Cognitive Radio Networks: Architectures, Protocols, and Standards*. USA: CRC Press, 2010.

ZHENG, S.; YANG, X.; LOU, C. Distributed consensus algorithms for decision fusion based cooperative spectrum sensing in cognitive radio. In: . Hangzhou, China: Communications and Information Technologies (ISCIT), 2011 11th International Symposium on, 2011. p. 217–221.